Titre: Title:	Gas phase hydrodynamics of bubble columns
Auteur: Author:	Caroline Louise Hyndman
Date:	1995
Type:	Mémoire ou thèse / Dissertation or Thesis
Référence: Citation:	Hyndman, C. L. (1995). Gas phase hydrodynamics of bubble columns [Thèse de doctorat, École Polytechnique de Montréal]. PolyPublie. https://publications.polymtl.ca/32151/

UNIVERSITÉ DE MONTRÉAL

GAS PHASE HYDRODYNAMICS OF BUBBLE COLUMNS

CAROLINE LOUISE HYNDMAN
DÉPARTEMENT DE GÉNIE CHIMIQUE
ÉCOLE POLYTECHNIQUE DE MONTRÉAL

THÈSE PRÉSENTÉE EN VUE DE L'OBTENTION
DU DIPLÔME DE PHILOSOPHIAE DOCTOR (Ph.D.)
(GÉNIE CHIMIQUE)
AOÛT 1995

UNIVERSITÉ DE MONTRÉAL

ÉCOLE POLYTECHNIQUE DE MONTRÉAL

Cette thèse intitulée:

GAS PHASE HYDRODYNAMICS OF BUBBLE COLUMNS

présentée par: HYNDMAN Caroline Louise
en vue de l'obtention du diplôme de: Philosophiae Doctor
a été dûment acceptée par le jury d'examen constitué de:

M. CARREAU, Pierre, Ph.D., président
M. GUY Christophe, Ph.D., membre et directeur de recherche
M. CHAOUKI Jamal, Ph.D., membre
M. FAN Liang-Shih, Ph.D., membre

DÉDICACE

À Alexander et à Louise.

ACKNOWLEDGEMENTS

First, I would like to thank my supervisor, Professor Christophe Guy, for his guidance and continuous support. This experience would not have been possible without the persuasion of Professor Claude Chavarie, who convinced me to do my doctorate at the École Polytechnique. Professor Jamal Chaouki provided the NaI scintillation detectors for residence time distribution (RTD) experiments. Dr. Greg Kennedy and Jean St-Pierre were very helpful, consulting on matters relating to radioactive isotopes and their use in RTD studies. They irradiated innumerable argon samples. The research associates in rheology, François St-Louis, Paul-André Lavoie and Luc Parent, were generous with their time though none of those experiments were retained for the thesis. I would also like to thank the department and its professors for their open door policy which created an excellent atmosphere for learning and research. Richard Caron assisted with dynamic gas disengagement experiments and our research collaboration has been a most enjoyable experience. I would also like to thank the members of my jury, and especially Professor Liang-Shih Fan of Ohio State University, for taking the time to critique this thesis.

On a more personal note, I thank all the members of the Department of Chemical Engineering, students and staff alike, for respecting my decision not to practice their english with them. Becoming fluent in french has been one of the more satisfying

personal projects I have undertaken. The friendly atmosphere in the department made my stay at the École Polytechnique a particularly enjoyable one. Specifically, I would like to mention a few people who really made a difference: Isabelle, Gordon, Nathalie, Michel, José, Larin, Daniel, Faïçal, Josée and David. The encouragement of Philippe, in no small part, helped me finish this thesis. My family and friends supported me through the highs and lows during this project. I owe them a debt of gratitude.

RÉSUMÉ

D'une construction relativement simple, les colonnes à bulles sont des contacteurs gaz-liquide (diphasiques) ou gaz-liquide-solide (triphasiques) aux multiples applications comme réacteurs chimiques, fermenteurs et absorbeurs. Sous leur forme la plus simple, elles sont constituées d'une colonne verticale munie, à sa base, d'un distributeur à gaz. L'énergie nécessaire à l'agitation de la phase liquide est uniquement due à l'injection d'une phase gazeuse. Bien que le mélange de la phase liquide ait été largement étudié (mais n'est toujours pas complètement compris), la phase gazeuse, quant à elle, a été un sujet d'étude relativement négligé. L'hydrodynamique de cette dernière peut affecter le taux de conversion lorsque le transfert de masse est limitant. Elle peut aussi affecter la sélectivité du produit désiré.

Cette thèse est une étude fondamentale de l'hydrodynamique de la phase gazeuse dans les colonnes à bulles. Elle a pour objectifs de modéliser l'écoulement de la phase gazeuse et la structure du taux de vide. Des expériences de distribution de temps de séjour (DTS) avec de l'argon radioactif ont été utilisées pour analyser l'écoulement de la phase gazeuse. La structure du taux de vide a été evaluée expérimentalement en utilisant la technique de désengagement dynamique du gaz (DDG). Toutes les expériences ont été effectuées avec un système air-eau à pression atmosphérique dans une colonne à bulles ayant un diamètre de 0.2 m. Le taux de vide global a été aussi

mesuré.

Le modèle de dispersion axiale est souvent utilisé dans la littérature pour décrire l'écoulement de la phase gazeuse dans les colonnes à bulles. Bien que ce modèle décrive bien les signaux-réponses du traceur, il sous-estime la vitesse moyenne du gaz et ce surtout à des vitesses superficielles élevées. Des tests basés sur les moments statistiques des signaux-réponses ont été developpés pour distinguer un écoulement dispersif d'un écoulement convectif. Ces tests montrent que l'écoulement est convectif au lieu de dispersif. Un modèle purement convectif est proposé. Il est capable à la fois de bien décrire les signaux-réponses du traceur et la vitesse moyenne du gaz. Bien que dans la littérature des modèles de dispersion axiale avec des modifications de type convectif (par ex.: modèles à deux populations de bulles) aient été proposés, cette thèse présente le premier modèle purement convectif pour les colonnes à bulles gaz-liquide. Ce modèle permet le calcul de la distribution des vitesses des bulles. Ses paramètres sont corrélées avec la vitesse superficielle du gaz sur une plage de 0.037 à 0.095 m/s.

La structure du taux de vide diffère largement selon le régime d'écoulement. Dans le régime homogène on observe de petites bulles de taille uniforme. À l'opposé, le régime hétérogène est composé d'une variété de tailles de bulles. En utilisant des données de taux de vide global et des fluctuations de pression, la transition entre les

deux régimes d'écoulement peut-être déterminer. Ces deux méthodes donnent le même point de transition. Les données de DDG ont été comparées avec des valeurs calculées à partir des distributions des vitesse des bulles du modèle convectif. La courbe de désengagement théorique décrit bien les données expérimentales au point de transition. On conclut de cette analyse que le taux de vide dans le régime turbulent-baratté est composé d'une superposition des grosses bulles sur une distribution des vitesses des bulles au point de transition. Un modèle théorique basé sur la théorie cinétique est proposé pour décrire la structure du taux de vide dans les deux régimes d'écoulement. Il décrit l'évolution de la distribution des vitesses des bulles avec l'accroissement du taux de vide. Une singularité dans la distribution, en forme d'une fonction delta-Dirac, apparaît au point de transition pour décrire la vitesse des grosses bulles. En régime à bulles, le modèle permet le calcul du taux de vide global, et en régime turbulent-baratté, la fraction du taux de vide en grosses bulles. Les calculs du modèle cinétique sont en bon accord avec les données du taux de vide global et les données de DDG.

ABSTRACT

Bubble columns are gas-liquid or gas-slurry contactors of simple construction which may be used as chemical reactors, fermenters, strippers and absorbers. In their simplest form they consist of a vertical vessel with a gas sparger in the bottom. The gas phase provides the energy and momentum for mixing the liquid phase. While the liquid phase mixing has been extensively studied (though still not fully understood), the gas phase behaviour has been a relatively neglected subject area. Gas phase hydrodynamics in bubble column reactors can affect product conversion if mass transfer is the limiting step. The selectivity of a desired product may also be affected by the gas phase behaviour.

This thesis is a fundamental study of gas phase hydrodynamics in bubble columns. The objectives of the study are to model the gas phase flow and the gas hold-up structure. Gas phase flow was analyzed using residence time distribution (RTD) of a radioactive argon tracer. Gas hold-up structure was evaluated experimentally using the dynamic gas disengagement (DGD) technique. An air-water system was used for experiments which were conducted at atmospheric pressure in a 0.2 m diameter column. Overall gas hold-up was also measured.

The axial dispersion model has been widely used in the literature as a model for gas

phase flow. While the model fits tracer response curves well, it under estimates the average gas velocity particularly at higher superficial gas velocities. Tests based on tracer response curve moments are developed to distinguish dispersive from convective behaviour. These tests show that the gas phase flow is convective rather than dispersive in nature. A fully convective model is proposed: the model is capable of matching tracer response curves and average gas velocity. While there have been convective-type modifications made to the axial dispersion model (two-bubble-group models), this is the first report of a convective model for gas-liquid bubble columns. The model allows calculation of bubble velocity distributions. A log-normal form for the bubble velocity distribution is assumed and its parameters are correlated to superficial gas velocities ranging from 0.037 to 0.095 m/s.

Gas hold-up structure is strongly dependent upon the flow regime. In the homogeneous flow regime gas hold-up consists of small, uniformly-sized bubbles, while heterogeneous regime gas hold-up is composed of a wider range of bubble sizes. The transition point between the two flow regimes is determined using overall gas hold-up data and pressure fluctuation data. The two methods give the same result. DGD data is analyzed using the theoretical disengagement profiles from convective model bubble velocity distributions. Theoretical disengagement curves match experimental data at the transition point. In the churn turbulent regime, the gas hold-up is found to be composed of large bubbles superimposed upon a transition point

bubble velocity distribution. A theoretical model based on kinetic theory is proposed to describe gas hold-up structure in both flow regimes. The model describes the evolution of the bubble velocity distribution with increasing gas hold-up; a singularity appears in the distribution at the transition point. The velocity of the large bubbles is described by a Dirac function. In the bubbly flow regime, overall gas hold-up is calculated using the model, and in the churn turbulent flow regime, the fraction of gas hold-up in the form of large, fast bubbles is determined. Kinetic model calculations are in good agreement with overall hold-up and DGD data.

CONDENSÉ EN FRANÇAIS

D'une construction relativement simple, les colonnes à bulles sont des contacteurs gaz-liquide (diphasiques) ou gaz-liquide-solide (triphasiques) aux multiples applications comme réacteurs chimiques, fermenteurs et absorbeurs. Sous leur forme la plus simple, elles sont constituées d'une colonne verticale munie, à sa base, d'un distributeur à gaz. L'énergie nécessaire à l'agitation de la phase liquide est uniquement due à l'injection d'une phase gazeuse. Bien que le mélange de la phase liquide ait été largement étudié (mais n'est toujours pas complètement compris), la phase gazeuse, quant à elle, a été un sujet d'étude relativement négligé. L'hydrodynamique de cette dernière peut affecter le taux de conversion lorsque le transfert de masse est limitant. Elle peut aussi affecter la sélectivité du produit désiré.

Cette thèse est une étude fondamentale de l'hydrodynamique de la phase gazeuse dans les colonnes à bulles. Elle a deux objectifs:

1. Modéliser l'écoulement de la phase gazeuse dans les colonnes à bulles et plus spécifiquement sur la base de données expérimentales obtenues de façon non-intrusive: évaluer la pertinence du modèle de dispersion axiale et ce surtout dans le régime turbulent-baratté où sa validité a déjà été mise en question, proposer un modèle approprié du point de vue phénoménologique.

2. Modéliser la structure du taux de vide dans les colonnes à bulles pour le régime turbulent-baratté et le régime à bulles: élaborer un modèle phénoménologique compatible avec le modèle proposé dans le cadre de l'objectif précédent, évaluer ce modèle en utilisant des données expérimentales.

La colonne à bulles utilisée pour l'étude a un diamètre de 0.2 m et une hauteur de 1.9 m. Toutes les expériences ont été effectuées avec un système air-eau à pression atmosphérique. La phase liquide était en mode cuvée. L'étude hydrodynamique a compris deux types d'expériences. Pour évaluer l'écoulement de la phase gazeuse, des expériences de distribution de temps de séjour (DTS) ont été effectuées. Un traceur radioactif (Ar^{41} produit dans le réacteur Slowpoke de l'École Polytechnique) injecté dans la ligne d'alimentation de la phase gazeuse était détecté à quatre niveaux par des détecteurs à scintillation (NaI). Cette technique ne perturbe pas l'écoulement. Dans un deuxième temps la technique de désengagement dynamique de la phase gazeuse a servi à caractériser la structure du taux de vide dans la colonne. Elle consiste à fermer l'alimentation du gaz rapidement (avec une électrovanne) et à suivre l'évolution de la pression en haut de la colonne dans le temps (avec un transmetteur de pression). Pour les deux types d'expériences, les sondes de pressions permettent de calculer le taux de vide global.

Puisque le modèle de dispersion axiale est souvent utilisé pour décrire l'écoulement de la phase gazeuse dans les colonnes à bulles, nos résultats de DTS ont d'abord été analysés avec ce modèle. Les expériences de DTS consistent en la mesure du taux de radioactivité contenu dans un volume de contrôle du réacteur. L'analyse des résultats de DTS comprend la comparaison de deux signaux-réponses provenant des détecteurs localisés un en amont et l'autre en aval de l'écoulement de la phase gazeuse. Deux signaux-réponses peuvent alors décrire l'écoulement de la phase gazeuse à l'aide d'un modèle. Bien que le modèle de dispersion axiale décrive bien les signaux-réponses du traceur, il sous-estime la vitesse moyenne du gaz. De plus avec des tests basés sur les moments statistiques des signaux-réponses obtenus à plus de deux niveaux, nos résultats semblent indiquer qu'un modèle convectif est plus approprié que le modèle de dispersion axiale.

Un modèle purement convectif est présenté. Il est basé sur une distribution de vitesse et ressemble à une superposition de nombreux écoulements piston. Une distribution log-normale de la vitesse absolue a été choisi:

$$f(w) = \frac{1}{\beta w\sqrt{2\pi}}\exp[-\frac{(\ln w-\alpha)^2}{2\beta^2}]$$

Ce modèle est capable à la fois de bien décrire les signaux-réponses du traceur et la vitesse moyenne du gaz. Bien que dans la littérature des modèles de dispersion axiale

avec des modifications de type convectif (par ex.: modèles à deux populations de bulles) aient été proposés, cette thèse présente le premier modèle purement convectif pour les colonnes à bulles gaz-liquide. Le modèle est recommandé pour décrire l'écoulement de la phase gazeuse dans le régime turbulent-baratté et a été validé avec des données obtenues à partir de la transition entre les deux régimes d'écoulement. Il permet le calcul de la distribution volumique des vitesses des bulles à partir des données de DTS seulement. Des corrélations pour la moyenne et l'écart-type de la distribution de vitesses des bulles ont été proposées.

$$\overline{w} = 2.5\, U_g^{0.69}$$

$$\sigma_w = 2.1\, U_g^{0.91}$$

La moyenne ($\overline{w}$) et l'écart-type (σ_w) de la distribution log-normale sont bien évidemment des fonctions des paramètres α et β. Elles sont basées sur des expériences de DTS de 0.037 à 0.095 m/s, soit dans le régime turbulent-baratté.

La structure du taux de vide diffère largement selon le régime d'écoulement. Dans le régime à bulles on observe de petites bulles de taille uniforme. À l'opposé, dans le régime turbulent-baratté, il existe une population très hétérogène de bulles: petites bulles et grosses bulles. Pour modéliser l'hydrodynamique de la phase gazeuse il est nécessaire dans un premier temps de démarquer la transition entre les deux régimes

d'écoulement. En régime turbulent-baratté, il faut connaître, pour une vitesse superficielle de gaz donnée, non seulement le taux de vide global mais aussi la contribution de chaque population de bulles à ce taux de vide. Avec de simples mesures de taux de vide on a pu distinguer les deux régimes d'écoulement. La vitesse interstitielle moyenne du gaz (U_g/ϵ_g) reste invariante dans le régime à bulles tandis que elle augmente avec la vitesse superficielle du gaz (U_g) en régime turbulent-baratté. La transition entre les deux régimes est mise en évidence par le début de l'accroissement de la valeur de U_g/ϵ_g. Pour notre colonne la transition apparaît à 0.038 m/s. Ce point a été confirmé par le suivi des fluctuations de pression (mesurées en haut de la colonne). La contribution de chaque population de bulles au taux de vide global a été déterminée expérimentalement avec la technique de désengagement dynamique du gaz (DDG). Les profils de DDG comprennent deux phases en régime turbulent-baratté. Durant la phase I les grosses bulles rapides sortent de la colonne; durant la phase II les petites bulles lentes (une première partie est sortie durant la phase I) continuent à quitter la colonne. Les données montrent que la contribution de petites bulles au taux de vide reste constant en régime turbulent-baratté et égale au taux de vide à la transition pour un système air-eau. La vitesse des grosse bulles dans le régime turbulent baratté est fonction de la vitesse superficielle. Sur la base des conditions à la transition (U_{tran} et ϵ_{tran}) et du taux de vide global, la vitesse moyenne des grosses bulles peut-être calculée. Bien que nos essais n'aient porté que sur une colonne de 0.2 m de diamètre, la comparaison de nos résultats avec ceux publiés semble indiquer

que l'effet du diamètre de la colonne sur la vitesse des grosses bulles n'est observable seulement que pour des colonnes ayant des diamètres plus petits que 0.2 m.

Du modèle convectif présenté précédemment, des profils de désengagement de la phase gazeuse peuvent-être calculés. Ces estimations supposent qu'il n'y a pas de décélération de la circulation du liquide durant une expérience de DDG. Au point de transition, la courbe théorique, calculée à partir du modèle convectif et des corrélations présentées ci-dessus, décrit bien le désengagement. Pour le régime turbulent-baratté, les profils expérimentaux sont bien décrits par le modèle convectif durant la phase I. La phase II peut-être décrite par un désengagement théorique basé sur les conditions au point de transition. Cette analyse conduit logiquement à l'utilisation d'un modèle conceptuel simplifié pour décrire la structure du taux de vide. Le modèle est basé sur la théorie cinétique qui décrit l'interaction des bulles. À partir d'une distribution volumique des vitesses des bulles idéale, f^o, qui existerait pour une condition opératoire donnée en absence des interactions bulle-bulle, le modèle détermine la distribution volumique des vitesses de bulles réelle. Pour le cas stationnaire avec le taux de vide également réparti dans la colonne le modèle devient:

$$f(v) = \frac{f^o(v)}{1 + \frac{a}{a^o}(\bar{v} - v)\epsilon_o} + b\epsilon_o\delta(1 + \frac{a}{a^o}(\bar{v} - v)\epsilon_o)$$

La distribution réelle est une fonction de f^o, du taux de vide en régime permanent (ϵ_o) et de la vitesse moyenne ($\bar{v}$). Le deuxième terme dans l'équation décrit par une

fonction delta-Dirac n'apparaît qu'en régime turbulent-baratté. b représente la fraction du taux de vide en grosses bulles. Le développement du modèle dans le régime à bulles montre que la constante a/a° est le rapport de la vitesse moyenne sur la variance de la distribution de vitesse. Avec deux équations pour le premier et le deuxième moment de la distribution et f^o/ϵ_o (la distribution idéale normalisée), le modèle décrit bien le taux de vide global en fonction de la vitesse superficielle du gaz. Une singularité apparaît lorsque le dénominateur du modèle s'annule. Une fonction d'accommodation pour le régime à bulles est définie:

$$\Omega = 1 + \frac{\bar{v}}{\sigma^2}(\bar{v} - v_{max})\epsilon_o$$

Elle diminue vers zéro à la transition. v_{max} est la dernière classe de bulles dans la distribution f(v) (ou $f^o(v)$). Dans le régime turbulent-baratté la constante a/a° est déterminée à partir de la condition de singularité. En normalisant, l'aire sous la distribution à un, la fraction b des grosses bulles est déterminée.

$$b = 1 - (u_{bL} - \bar{v}) \int_0^{v_{max}} \frac{(f^o(v)/\epsilon_o)}{u_{bL} - v} dv$$

Sur la base de la connaissance de la valeur moyenne de la vitesse des grosses bulles (u_{bL}), de la distribution idéale f^o/ϵ_o et du taux de vide à la transition, la contribution des grosses bulles au taux de vide peut-être déterminée. b diminue vers zéro à la

transition. L'évolution de b avec la vitesse moyenne du gaz décrit bien les résultats expérimentaux de DDG. Pour les calculs dans les deux régimes d'écoulement, on détermine la distribution idéale normalisée à partir d'une distribution expérimentale dans le régime à bulles. À cette fin nous avons utilisé les corrélations proposées ci-dessus juste à la transition. Le point de transition décrit par b est à une vitesse superficielle de gaz plus élevée que celui calculé à partir de Ω. Peut-être que les deux points indiquent les limites du régime transitoire. Le modèle cinétique, bien qu'il soit simplifié, décrit bien la structure du taux de vide à travers les régimes à bulles et turbulent-baratté. Il suggère l'existence d'une régime transitoire graduel entre les deux.

TABLE OF CONTENTS

LIST OF TABLES

LIST FIGURES

LIST OF APPENDICES

CHAPTER II NOMENCLATURE

a	pre-exponential constant for Equation 2.1, counts
A	transfer function for axial dispersion model, s^{-1}
b	constant for Equation 2.1
c	normalized tracer concentration
C	tracer concentration
D_{ax}	axial dispersion coefficient, m^2/s
D_c	column diameter, m
E	RTD curve
f	volume distribution of bubble velocity w, s/m
F	cumulative RTD curve
g	weighted volume distribution of bubble velocity w (Equations 2.7 and 2.22), s/m
h	height of the detector window, m
H	height of gas-liquid mixture, m
L	distance between measurement points, m
L_{jk}	height between detector centres k and j, m
n	normalized counts
N	argon decays measured by a scintillation detector in a 0.05 s time interval, counts

Pe	Peclet number, U_gL/ϵ_gD_{ax}
t	time since irradiated argon first measured at detector 1, s
t_p	time for irradiated argon gas to pass before a detector window, s
U_g	superficial gas velocity, m/s
V_{jk}	mean velocity as calculated directly from tracer response curves j and k, m/s
w	gas velocity in convective model, m/s
$\bar{w}$	mean gas velocity, first moment of the velocity distribution, m/s

Greek letters

α	parameter of log-normal velocity distribution, e^{α} has units of m/s
β	parameter of log-normal velocity distribution
ϵ_g	gas hold-up
ϵ_{rms}	root-mean-square-error (Equations 2.5 and 2.10)
μ	mean or first moment of a tracer response signal, s
σ^2	variance or second central moment of a tracer response signal, s^2
τ	average gas phase residence time, ϵ_gL/U_g, s

Subscripts

calc	model calculation

conc concentration

cv control volume

expt experimental value

i point at which experimental tracer response is compared to predicted one; for convective model, calculation point for bubble velocity distribution as well as predicted response curve (varies from 1 to 128)

j detector number 1, 2, 3 or 5 (upstream)

k detector number 2, 3, 4 or 5 (downstream)

min minimum value

max maximum value

opt optimized value

Superscripts

c cumulative value; integral from minimum to calculation point i

CHAPTER III NOMENCLATURE

f	volume distribution of bubble velocity w, s/m
g	weighted volume distribution of bubble velocity w (Equation 3.2), s/m
h_{win}	detector window height, 0.1 m
L_{1k}	length from detector centre k to 1, m
n	normalized counts
t	time (t=0 when the detector 1 signal rises above baseline), s
t_{pass}	time for irradiated argon gas to pass before a detector window, s
U_g	superficial gas velocity, m/s
w	gas velocity, m/s
$\bar{w}$	mean gas velocity, m/s

greek

α	velocity distribution parameter, e^{α} has units of m/s
β	velocity distribution parameter
ϵ_g	gas hold-up
ϵ	objective function (Equation 3.5)
σ_w	standard deviation of bubble velocity distribution, m/s

subscripts

i	calculation points for bubble velocity distribution, predicted response curve or points at which experimental tracer response is compared to predicted one (1 to 128)
k	detector 2, 3, 4 or 5 (downstream)
min	minimum value
max	maximum value

superscripts

c	cumulative value; integral from minimum to calculation point i
calc	model calculation
expt	experimental value

CHAPTER IV NOMENCLATURE

a	hindrance parameter in kinetic model, m^{-1}
a^o	relaxation parameter in kinetic model, s^{-1}
b	volume fraction of gas hold-up rising at velocity u_{bL}
D_c	column diameter, m
f	volume distribution of absolute bubbles rise velocities w or velocity v, s/m
g	acceleration due to gravity, m^2/s
h	equivalent height of clear liquid above pressure transducer connection point, m
h_{PT}	height of pressure transducer connection point centre above the distributor, m
$h_{PT,l}$	height of the back of the small bubble front above the distributor i.e. height of clear liquid at t_{corr}, m
H_{nac}	total height of clear liquid in the column, m
P	pressure measured by the pressure transducer connected to the column wall a few centimetres below the non-aerated liquid height (referenced to pressure tap location), Pa
P_d	pressure measured in the chamber below the perforated plate distributor, Pa
t	time since solenoid valve closed for a DGD experiment (negative values represent the conditions in the column before closing the solenoid valve); time for Equation 4.16, s

u_b absolute bubble velocity, m/s

U superficial gas velocity, m/s

v gas velocity in kinetic model, m/s

$\bar{v}$ mean gas velocity for kinetic model, first moment of the velocity distribution, m/s

w gas velocity in convective model (Hyndman and Guy, 1995a), m/s

$\bar{w}$ mean gas velocity for convective model, first moment of the velocity distribution, m/s

x fraction of normalized gas hold-up remaining in the column at time t, ϵ/ϵ_o

z position, m

Greek letters

α parameter of log-normal velocity distribution, e^{α} is the mode of the distribution and has units of m/s

β parameter indicating skewness of log-normal velocity distribution

Δw_m width of bubble velocity histogram interval $w_{i+1} - w_i$, m/s

ϵ instantaneous gas hold-up below h_{PT} at time t in the reactor

ρ liquid density at operating temperature, kg/m^3

$\sigma_{\epsilon o}$ standard deviation of instantaneously measured gas hold-up fluctuations (due to pressure fluctuations) during steady-state operation

σ^2 variance or second central moment of the velocity distribution, m^2/s^2

Ω accomodation function as defined in Equation 4.22

Subscripts

clear clear liquid in the bottom of the column from which bubbles have already disengaged

corr corrected value; gas hold-up referenced to the height within the column containing the gas liquid mixture

expt experimental value

i calculation point for bubble velocity distribution in convective model

I first phase of a disengagement experiment in the churn turbulent regime (large bubble evacuation)

II second phase of a disengagement experiment in the churn turbulent regime (continued disengagement of small bubbles)

L large bubble

m midpoint for bubble velocity histogram interval

min minimum value

max maximum value

nae value for non-aerated liquid

O average value at steady-state or value at time when solenoid valve is closed for DGD experiments (t = 0)

s small bubble

tran value at the transition from bubbly to churn turbulent flow

Superscript

o ideal flow with no bubble-bubble interactions

CHAPTER I

INTRODUCTION

1.1 Introduction

In its simplest form, the bubble column reactor consists of a column without internals and a gas sparger in the bottom. Common modifications to the basic design may include an internal heat exchanger, draft-tube (air-lift) and multiple stages in the form of plates. Bubble columns may be used as chemical reactors, fermenters, strippers and absorbers. They may be operated as gas-liquid or gas-liquid-solid (gas-slurry) contactors. A well-known application of the slurry bubble column reactor is the Fischer-Tropsch synthesis. At low gas superficial velocities, the application in the mineral processing industry is the flotation column. While the gas phase may be either reactive or inert (or in the case of absorbers the phase to which or from which a product must be transferred) in all cases the gas phase provides the energy and momentum for mixing the liquid or slurry.

In large diameter columns, two main flow regimes for bubble columns are generally known to exist. At low superficial velocity, bubble columns operate in the homogeneous or bubbly flow regime; at high superficial gas velocity the heterogeneous or churn turbulent regime prevails. Slugging is also observed at high

superficial gas velocities but only in smaller diameter laboratory columns. In industrial applications, the churn turbulent flow regime is advantageous both from a mass and heat transfer perspective. For exothermic reactions, overall mixing is essential to ensure that reactors do not develop hot spots which can lead to undesired side reactions or reactor failure. Furthermore, for economic reasons, high gas throughputs may be desired. In the domain of reactor engineering, bubble column reactor models are often used as a starting point for the understanding of reactors with more complex geometry. The bubble column represents a limiting case (no solids hold-up) for three-phase fluidized bed reactors. The knowledge base which has been acquired in this basic operating unit provides a stepping stone upon which understanding of more complex gas-liquid and gas-liquid-solid systems are based. Krishna et al. (1993) have exploited the cross-fertilization which may take place when concepts in gas-solid fluidization are used to understand hydrodynamic behaviour of bubble columns. Thus, the concept of minimum bubbling velocity in gas-solid fluidization corresponds to the transition from the bubbly to the churn turbulent flow regime. An understanding of the hydrodynamics of bubble columns, these elementary building blocks of gas-liquid reactors, represents a fundamental tool which can be applied to other more complex reactor configurations.

Despite their simple construction, bubble column reactors exhibit complex hydrodynamic behaviour. Depending on the application, a model of varying

complexity may be required. For example, if a reaction is limited by kinetics, hydrodynamics do not affect the conversion in the reactor and a simple plug flow model may be adequate. For a fundamental understanding of the complex hydrodynamics, a relatively simple model which accurately describes the phenomena is best. In the long term, industry benefits from a fundamental understanding of the hydrodynamic phenomena by having to rely less on intangibles and the art of process design in order to understand why a particular unit may under-perform or outperform design expectations. In academic and industrial research projects, the bubble column has been for many years the basic unit operation used to gain a fundamental understanding of phenomena occurring in more complex process equipment.

The gas phase hydrodynamics have previously been relatively neglected because gas phase hydrodynamics become important in calculating reaction conversion when mass-transfer is limiting. This neglect may have been due in part to experimental difficulties and in part to the fact that bubble column reactors are typically used for slow reactions which are not mass transfer limited (Deckwer and Schumpe, 1993). Nevertheless, for fast reactions where mass transfer is limiting or in the case of absorbers and strippers where the design is based upon mass transfer, gas phase mixing can be an important factor in design and scale-up of bubble columns. Deckwer and Schumpe (1993) have noted an urgent need for better hydrodynamic models for the gas phase. Description of the gas phase behaviour in these columns has evolved

from a plug flow model to the axial dispersion model. Hydrodynamic models assuming bimodal residence time distribution of the gas phase have been proposed for the churn turbulent regime. Researchers have also noted that single-bubble-class and bimodal axial dispersion models can predict different product selectivities (Modak et al., 1994). Local measurements of gas hold-up and of bubble velocity and size (Chabot and de Lasa, 1994; Yao et al., 1991) and global measurements such as dynamic gas disengagement (Patel et al., 1989) have allowed insight to gas phase hydrodynamics. The complex flow structures of the liquid phase (Chen et al., 1995; Devanathan et al., 1990; Franz et al., 1984) play an important role in understanding bubble column hydrodynamics. Gas phase behaviour is obviously interrelated to the liquid flow structure.

Gas phase flow in bubble columns is much more complex than the axial dispersion model implies. Yet the simplicity of its application and its familiarity have made this model enduringly popular for scale-up purposes. The emphasis of this study is to examine gas phase behaviour using a phenomenological-based approach. The aim is to gain a more fundamental understanding of gas phase hydrodynamics through a combination of experiments and modelling.

1.2 Objectives

1. Model the gas phase flow in bubble columns. Determine the applicability of the axial dispersion model for the gas phase in bubble columns, particularly in the churn turbulent regime where its use is being questioned. Examine the literature and adapt a model or propose a new model with a basis in the observed phenomena for gas phase flow. Test the models with preferably non-intrusive data.

2. Model the gas hold-up structure in bubble columns over the bubbly and churn turbulent regimes. Develop a phenomenological model, compatible with the gas phase flow model in objective (1) and assess it using with experimental data.

1.3 Thesis Structure

This thesis is structured in the form of articles: two already accepted for publication in scientific journals, and a manuscript. In addition to the three articles which each comprise one chapter, are a general introduction, conclusions, recommendations and four appendices. The content of each section or chapter is described below:

• Chapter I consists of a general introduction to the gas phase hydrodynamics of bubble columns. The objectives of the present study are outlined.

• In Chapter II, the publication "Gas Phase Hydrodynamics in Bubble Columns: A Convective Phenomenon" is presented. This article will appear in the August 1995 edition of the Canadian Journal of Chemical Engineering. Gas phase residence time distribution (RTD) data are analyzed using the axial dispersion and a proposed convective model.

• Chapter III consists of a publication entitled "Gas Phase Hydrodynamics in Bubble Columns" published in Chemical Engineering Research and Design in April 1995. The convective model proposed in Chapter II is used to analyze gas phase RTD data and calculate absolute bubble velocity distributions for an air-water system. Correlations for the bubble velocity distribution parameters are developed.

• Chapter IV is a manuscript entitled "Understanding Gas Phase Hydrodynamics in Bubble Columns: A Convective Model Based on Kinetic Theory". A kinetic model for gas phase hydrodynamics which describes both the bubbly and churn turbulent flow regimes is developed and compared to gas hold-up and dynamic gas disengagement data.

• Chapter V is a brief discussion about issues relevant to the three articles (Chapters II, III and IV).

• Conclusions and Recommendations

• Three appendices which give more detail on experimental procedures and data analysis: gas phase residence time distribution, gas hold-up and dynamic gas disengagement. The fourth appendix has a complete derivation of the equation for the kinetic model in Chapter IV.

CHAPTER II

GAS PHASE FLOW IN BUBBLE COLUMNS:

A CONVECTIVE PHENOMENON

Reference: HYNDMAN, C.L. and C. GUY (1995), "Gas Phase Flow in Bubble Columns: A Convective Phenomenon", Canadian Journal of Chemical Engineering **73**, 426-434.

Keywords: bubble columns, hydrodynamics, convective, axial dispersion, residence time distribution

2.1 Abstracts

2.1.1 Abstract

The axial dispersion model has been commonly used to describe gas phase flow in bubble columns. Scatter in dispersion coefficients reported to date may be a result of the misuse of the axial dispersion model when a convective model would be more appropriate. Using simple tests with radioactive tracer response curve moments, convective and dispersive behaviours are differentiated. A convective model is presented. The model fits both tracer response curves and mean gas velocity well in both the bubbly and churn turbulent flow regimes, and may be used as a technique to calculate bubble rise velocity distributions.

2.1.2 Resumé

Le modèle de dispersion axiale est souvent utilisé pour décrire l'écoulement de la phase gazeuse dans les colonnes à bulles. Cependant, la grande variabilité des valeurs rapportés du coefficient de dispersion semble indiquer que ce modèle n'est pas adéquat et qu'un modèle de type convectif serait plus approprié. Des tests expérimentaux simples, basés sur l'utilisation d'un traceur radioactif, sont proposés pour distinguer les deux modèles. Un modèle convectif est présenté. Le modèle décrit

les signaux-réponses du traceur et la vitesse moyenne du gaz à la fois dans le régime à bulles et le régime turbulent-baratté. Ce modèle peut être utilisé pour calculer la distribution de vitesses des bulles.

2.2 Introduction

The simplest model to describe gas phase behaviour is a plug flow model. When hydrodynamics of the gas phase in gas-liquid contactors deviates from a plug flow model, an obvious choice for a hydrodynamic model has been the axial dispersion model. This model assumes an average gas velocity and an axial dispersion coefficient to account for the deviation from the average flow velocity. In the work done to date a large scatter in the dispersion coefficients reported (Deckwer and Schumpe, 1993) shows that the model is perhaps over simplified. Joshi (1982) correlated dispersion coefficients obtained from six different sources and different experimental methods based on the principle that "dispersion" is mainly a result of a distribution of bubble velocities. He argued that there are two causes for the bubble velocity distribution which are superimposed one upon the other. First, the liquid circulation pattern (Chen et al., 1994; Franz et al., 1984; Hills, 1974; Ueyama and Miyauchi, 1979) both accelerates and hinders rising bubbles. This gives rise to the radial gas hold-up profile observed by Hills (1974) and numerous other workers since. Second, a bubble size distribution also exists which implies that there exists a distribution of terminal bubble rise velocities. Therefore, both the influence of a bubble size distribution and liquid circulation within the column, give rise to a bubble velocity distribution for the gas phase. Even in the churn turbulent regime where bubble coalescence and break-up are known to occur, "dispersion" is mainly due to a bubble rise velocity distribution since

dispersion coefficients may be better correlated (Joshi, 1982) using this principle. Thus, a convective model may be a more appropriate description of gas phase behaviour.

Convective type modifications have been made to the axial dispersion model by assuming two average bubble rise velocities and an axial dispersion coefficient for each velocity. In their two-bubble group model Kawagoe et al. (1989) (H/D_c = 12.6 with D_c = 0.159 m, and H/D_c = 6.90 with D_c = 0.290 m) assume there are two average bubble velocities, one attributed to the core or upflow region of the bubble column where higher rise velocities tend to occur, and another in the annulus or downflow region where lower bubble rise velocities occur. Bubbles from one group are assumed not to interact with those from the other group. Shetty et al. (1992) (H/D_c = 18.0 with D_c = 0.15 m, and H/D_c = 10.8 with D_c = 0.25 m) also assume no interaction between large and small bubbles, but large bubbles are assumed to rise in plug flow. Modak et al. (1993) have presented a modified two-bubble-class model in which a cross-mixing coefficient accounts for interaction between the large and small bubble phases; the large bubble phase is assumed to have a negligible axial dispersion coefficient. (Their model is verified using the data from Kawagoe et al., 1989).

Whether the axial dispersion model or these modified models are used, a Fickian

dispersion coefficient is being used to explain a large part of the "mixing" phenomena seen in residence time distribution curves for the gas phase. A fundamental assumption in the axial dispersion models is that the dispersion coefficient is constant over the length of the column. Levenspiel and Fitzgerald (1983) argued that the axial dispersion model could be misused to represent a convective flow. If, for example, only two measurements are used for imperfect pulse data analysis, convective and dispersive phenomena cannot be distinguished. In this paper, we present a convective model to describe gas phase behaviour and discuss both the axial dispersion and convective models with respect to results obtained using tracer response (residence time distribution, RTD) data.

2.3 Experimental method for residence time distribution experiments

2.3.1 Equipment

An acrylic bubble column having an inside diameter of 0.2 m and a height of 1.9 m has been used for the residence time distribution experiments (refer to Figure 2.1). The distributor is a perforated plate with 69, 1-mm diameter orifices arranged in a square pattern. Orifice spacing is 20.5 mm centre to centre. Experiments are conducted in semi-batch mode with a water level of 1.4 m. An air-argon-water system is used for all experiments. Two rotameters are used to control gas flow: one is used to control filtered process air from a central supply system, while the other simultaneously allows gas from a pressurized gas cylinder to be fed to the bubble column. A mercury filled manometer is used to measure the pressure at the rotameters. Two vented gage pressure transmitters (Lucas Schaevitz, Pennsauken, NJ, P3061 100"WG and 20"WG) connected near the bottom and top of the column allow sensitive measurement of the gas hold-up. A gas phase tracer is introduced to the gas line via a septum using a syringe. Effluent gases are collected overhead and sent to a fume hood.

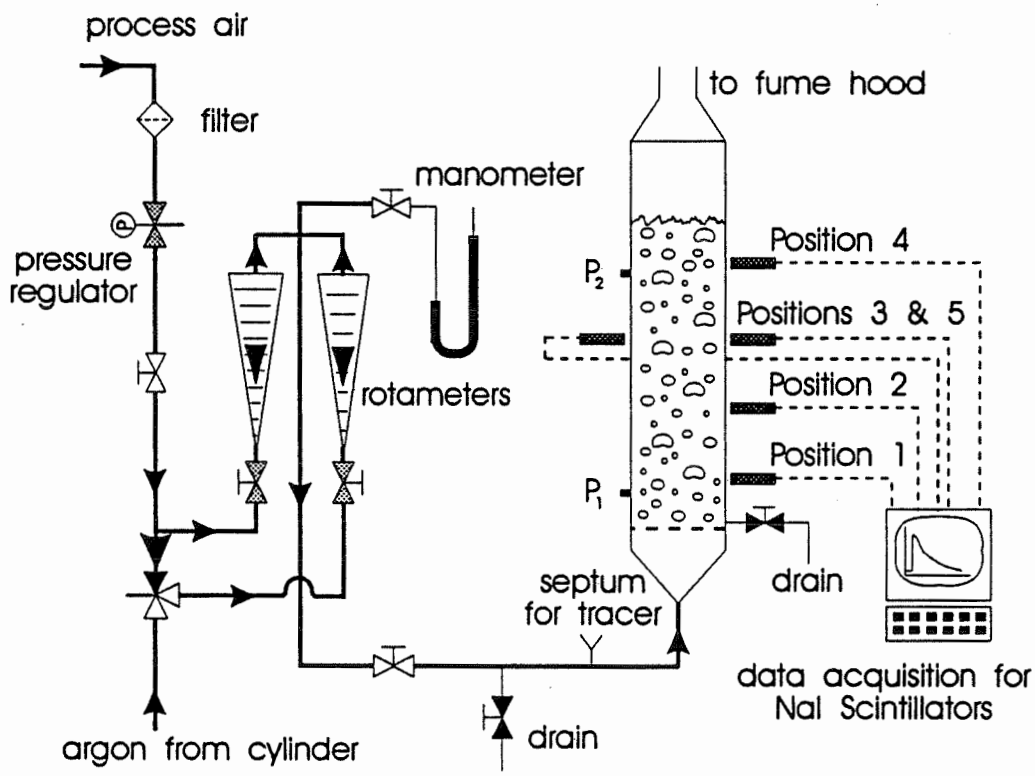

Figure 2.1: Experimental set-up.

2.3.2 Experimental procedure

Residence time distributions are measured using radioactive argon gas as tracer which is detected at four different axial positions outside the column. (Detectors are numbered from the bottom up; a fifth detector is placed opposite detector 3). Argon gas is irradiated in a Slowpoke nuclear reactor immediately prior to each experiment. The tracer samples are introduced to the bubble column via the septum (see Figure 2.1). NaI scintillation detectors (EG&G ORTEC, Oakville, ON) measure gamma radiation released by the radioactive argon gas as it decays ($t_{0.5}$ = 1.8 h). All detectors are surrounded by lead bricks having identical geometry to create identical detector windows. A detector window is the reactor volume seen by a detector. Lead bricks ensure that tracer is detected only at the height at which a detector is placed. Gamma rays detected in each 0.05 s interval by each of the five detectors are counted by the data acquisition system and recorded. Only those gamma rays corresponding to the energy peak associated with argon decay are counted. Gamma rays which interact with the gas-liquid dispersion, the reactor structure or the lead bricks before being measured by a detector have lower energies, and are not included in the counts. All bubbles located in a detector window containing tracer are seen by the detectors, however, there is a decreasing relationship between tracer distance from the detector and measured signal intensity. Lead shielding surrounding the detectors is arranged so that average counts per volume on radial shells are equivalent to those measured

in a cylinder at the centre of the column. Because the radial profile of gas hold-up is approximately axisymmetric (see for example Hills, 1974; Yao et al., 1991) the tracer response curve will give an accurate measurement for the control volume. The symmetry and even distribution of tracer across the column was verified experimentally by comparing signals from detectors placed on opposite sides of the column at the same height (see positions 3 and 5 in Figure 2.1). Because for all experiments tracer response curves at the two positions are very similar, the tracer must be evenly distributed. Data acquisition continues for a period of 180 s, by which time the signals were found to return to a baseline level. Because argon dissolves in water, it is fed simultaneously with air in a fixed ratio. Passage of the radioactive argon tracer into water which is already saturated in argon can occur only as a result of absorption associated with the dynamic nature of the absorption-desorption equilibrium. Three factors, the proportion of marked to unmarked argon in the gas feed, the ratio of gaseous to dissolved argon molecules and the kinetics of absorption/desorption with respect to the convective flow, render the loss of tracer into the liquid phase negligible. A fixed ratio of air/argon (3.3:1.0) is used so as to eliminate gas density as a variable in experiments. Superficial gas velocities of 0.037 and 0.094 m/s are examined.

2.3.3 Data treatment

Detector signals are filtered with a low pass filter to eliminate high frequency noise associated with the probabilistic nature of radiation counts. Time zero was taken to be when the signal from the first detector increases above the baseline signal. The baseline signal, which is due to background radiation in the atmosphere, is removed. A typical tracer response curve is shown in Figure 2.2. The secondary peak appears on all the response curves. Secondary peaks are due to the radioactive gas collection system and do not represent any phenomena occuring in the bubble column. As a result, the secondary peaks are removed from the response curves using an exponential fit for the descending part of each curve (see Figure 2.2).

$$N = a\exp(t-b) \tag{2.1}$$

Ascending portions are not modified. The gas collection system was eventually modified and new experimental runs indicate that no effect on data interpretation was introduced by either the gas collection system or the signal treatment procedure.[1] Finally, the response curves are resampled at 0.1 s to reduce the amount of data and are normalized with respect to their area.

Detector response, measured in counts per discrete time interval, represents the

---

1. See Appendix I for an example of a new experimental run.

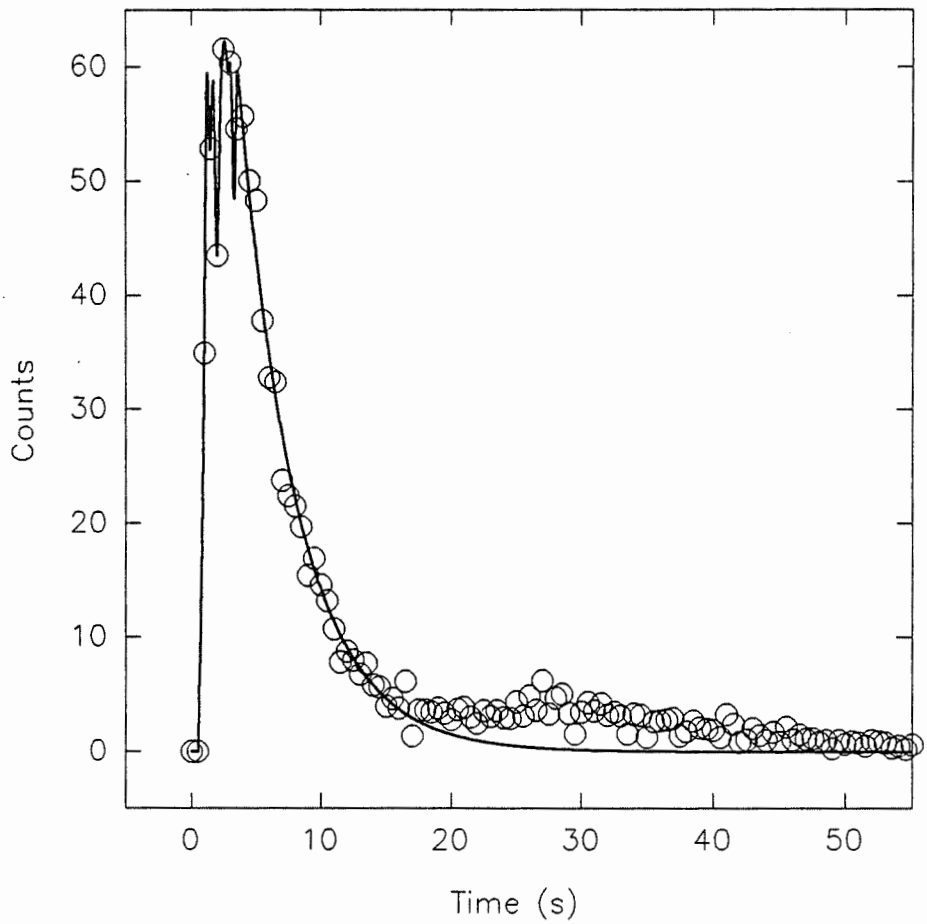

Figure 2.2: Typical tracer response curve (O, 1/5 of data points are shown for clarity) and exponential fit for descent (——); U_g = 0.094 m/s and ϵ_g = 0.18; response at detector 5.

number of irradiated argon molecules which decay per time interval in the reactor volume seen by a detector (window). The counts depend on the tracer concentration as well as the amount of time (t_p) the tracer takes to move past the window created by the lead bricks which surround each detector:

$$N \propto C\, t_p = \frac{C\, h}{w} \qquad (2.2)$$

where $N \equiv$ *detector counts and* $w \equiv$ *gas velocity.*

h is the same for all detectors. If all of the tracer spends the same amount of time in the detector windows, comparison of a downstream with an upstream detector response curve cancels out the effect of t_p. Thus, counts represent tracer concentration directly. Conversely if a bubble velocity distribution exists, the effect of t_p on tracer response curves must not be neglected.

2.4 Hydrodynamic models

2.4.1 Axial dispersion model

The transfer function for tracer concentration with open-open boundary conditions for the axial dispersion model is a function of the Peclet number and the average gas phase residence time (τ) (Wakao and Kaguei, 1982).

$$A(t) = \sqrt{\frac{Pe\ \tau}{4\pi t^3}}\ \exp[\frac{Pe\ (\tau-t)^2}{4\tau t}] \tag{2.3}$$

Tracer concentration at a downstream location ($c_k(t)$) is calculated by convoluting the concentration at the first detector ($c_1(t)$) and the transfer function for the model.

$$c_k = \int_0^t c_1(t)A(t-\eta)d\eta \tag{2.4}$$

Calculated tracer concentration ($c_k(t)$) is fitted to the experimental data by optimizing Pe and τ. The root-mean-square-error between calculated and experimental response curves is used as the objective function.

$$\varepsilon_{rms} = \sqrt{\frac{\Sigma (c_{i,calc} - c_{i,expt})^2}{\Sigma (c_{i,expt})^2}} \tag{2.5}$$

A box-complex algorithm (Kuester and Mize, 1973) is used for the optimization

procedure.

2.4.2 Convective model

The model has been adapted from one outlined by Aufderheide and Vogelpohl (1986) for dispersed phase flow in a liquid-liquid system. The model is used to determine the bubble rise velocity distribution and not the bubble size distribution as was the case for the above mentioned liquid-liquid system. The bubble velocity distribution is the combination of the distributions for liquid and relative bubble velocities.

The calculation procedure for the model is as follows. A form for the velocity distribution must be assumed. As suggested by experimental data reported by Fan (1989) for the bubbly and coalesced flow regimes of three-phase flow, a log-normal bubble rise velocity distribution is assumed. The volume distribution function of bubbles having a velocity w has the following form.

$$f(w) = \frac{1}{\beta w\sqrt{2\pi}}\exp[-\frac{(\ln w-\alpha)^2}{2\beta^2}] \qquad (2.6)$$

The mode of this distribution is e^{α} and β is an indication of its skewness. Parameters α and β are chosen and the distribution is discretized between the cutoff points w_{min} and w_{max}. Spreading of tracer response curves is caused by a distribution in bubble rise velocities. Bubbles containing tracer having higher rise velocities pass the second,

third and fourth detectors sooner than those with slower velocities. The effect of the detection control volume on the tracer response curve is accounted for by defining time $t_{p,i}$ as the time required for bubbles rising at velocity w_i to move through a detector window. The bubble velocity distribution is thus corrected by weighting it with $t_{p,i}$.

$$g(w_i) = \frac{f(w_i)\ t_{p,i}}{\int_{w_{min}}^{w_{max}} f(w)\ t_p dw} \tag{2.7}$$

Area under the weighted velocity distribution corresponding to the slowest rise velocities is matched with the tracer which passes in front of the detectors last. The inverted cumulative velocity distribution ($1-g^c$) is matched to the first cumulative tracer concentration response curve in order to link velocities w_i with arrival times at the first detector (t_i).

$$1 - g^c(w_i) = n_1^c(t_i) \tag{2.8}$$

If the parameters chosen for the log-normal distribution are correct then the other tracer response curves will be predicted accurately. Cumulative concentration curves for detectors 2 and above are calculated as follows.

$$n^c_{k,calc}(t_i') = n^c_1(t_i)$$
$$where \quad t_i' = t_i + \frac{L_{1k}}{w_i} \tag{2.9}$$

Log-normal velocity distribution parameters (α and β) are optimized using a downhill simplex method (Press et al., 1989) with an objective function consisting of the root-mean-square-error between the calculated and experimental response curves.

$$\varepsilon_{rms} = \sqrt{\frac{\sum (t_{ik,calc} - t_{ik,expt})^2}{\sum (t_{ik,expt})^2}} \tag{2.10}$$

To evaluate the average bubble velocity distribution in the column only the fit (ϵ_{rms}) at detector 4 is used as a criterion for goodness of fit because the times for bubbles to travel between detectors 1 and 4 are longer, and the accuracy of calculations is thus greater. Calculated tracer response curves were also produced for detectors 2, 3 and 5 to determine the validity of the model throughout the column.

2.4.3 Discrimination between dispersive and convective phenomena

As mentioned in the introduction, dispersive and convective phenomena may be confounded when RTD data consists of concentration measurements at only two axial positions along the column. Levenspiel and Fitzgerald (1983) developed a test which could be used to differentiate dispersive from convective phenomena. When a two-point measurement system is used, the difference in variance between a downstream and upstream tracer response curve is proportional to the axial distance between measurement points whether the deviations from plug flow are large or small (Levenspiel, 1972). The dimensionless variance for a two point measurement can be expressed as a function of the Peclet number.

$$\frac{\sigma_k^2 - \sigma_j^2}{\tau_{jk}^2} = \frac{2}{Pe} = \frac{2\epsilon_g D_{ax}}{U_g L_{jk}} \tag{2.11}$$

Substituting the average residence time between the two detectors, $\tau_{jk} = L_{jk}\epsilon_g/U_g$, Levenspiel and Fitzgerald (1983) showed that the change in the variance of the two signals is proportional to the distance between the detectors.

$$\Delta\sigma_{jk}^2 = \sigma_k^2 - \sigma_j^2 = 2(\frac{\epsilon_g}{U_g})^3 D_{ax} L_{jk} \propto L_{jk} \tag{2.12}$$

Levenspiel and Fitzgerald (1983) also presented a test for a Gaussian-convective model. In their model, the residence times of the fluid elements are assumed to follow

a Gaussian distribution. In this case the change in standard deviation between two signals is proportional to the distance between measurement points.

$$\Delta\sigma_{jk} = \sigma_k - \sigma_j \propto L_{jk} \tag{2.13}$$

To distinguish between dispersive and convective phenomena, these tests (Equations 2.12 and 2.13) require a minimum of three measurement points along the column.

The experimental procedure used in this investigation measures radioactive decay counts over a control volume in the bubble column. As mentioned previously decay counts are a function both of tracer concentration and time t_p for the tracer to move past the window. While this may seem unnecessarily complicated when compared to other methods which are capable of directly measuring concentration, the advantage is that the radioactive tracer technique is capable of discriminating between dispersive and convective phenomena with only two measurement points. (This is true for any technique which measures over a volume.)

The mean velocity of the gas phase in a bubble column is known to be U_g/ϵ_g. Since U_g is calculated using rotameter data and ϵ_g is calculated from pressure tap data, U_g/ϵ_g is independent of any calculations from RTD data. If t_p is the same for all marked bubbles, the mean velocity of the tracer between heights j and k along the column can be calculated using the method of moments.

$$V_{jk} = \frac{L_{jk}}{\mu_k - \mu_j} \tag{2.14}$$

V_{14}, which is the average tracer velocity in the column, should be equal to U_g/ϵ_g if the axial dispersion model accurately describes the gas phase hydrodynamics.

For gas phase flow which is described by a convective model with a bubble rise velocity distribution, the t_p of bubbles also has a distribution. Slow bubbles spend a relatively long time in the measurement control volume as compared to fast rising bubbles. As a consequence the tracer response signal is skewed in favour of slow bubbles. V_{14} thus under predicts the mean gas velocity (U_g/ϵ_g) for a convective gas phase flow.

While the calculation of V_{14} can confirm that the axial dispersion model is inappropriate, it cannot positively confirm that a convective model is appropriate. Here we present the development of a simple test using moments of tracer response curves to determine whether the phenomena is convective.

The convective model presented in the previous section assumes a log-normal velocity distribution. Since the cumulative RTD curve (F(t)) represents all the marked bubbles which leave the column in less than time t and have a rise velocity greater than w, we know that F(t) is numerically equivalent to the fraction of bubbles having a bubble

rise velocity greater than w.

$$F_{conc}(t) = \int_{w}^{\infty} f(\eta)d\eta \tag{2.15}$$

Using Leibnitz's rule we find

$$E_{conc}(t) = \frac{f(w)\,w^2}{L} \tag{2.16}$$

A RTD is properly expressed as a function of time rather than velocity and is found by replacing w with L/t.

$$E_{conc}(t) = \frac{1}{\sqrt{2\pi}\,\beta t}\exp[-\frac{(\ln t - \ln L + \alpha)^2}{2\beta^2}] \tag{2.17}$$

This is an approximate transfer function as in reality the bubble rise velocity distribution should have an upper limit where as the log-normal distribution has an infinite upper limit. The similarity of this transfer function to one developed by Molerus and Kurtin (1986a) should be noted. They developed a three-parameter model, suggested as an alternative to the axial dispersion model, for gas phase residence time distribution in the churn turbulent regime.

The mean and variance of $E_{conc}(t)$ are functions of the log-normal velocity distribution parameters as well as the distance between measurement points.

$$\mu_{conc} = L \exp(\frac{\beta^2}{2} - \alpha) \tag{2.18}$$

$$\frac{\sigma^2_{conc}}{\mu^2_{conc}} = \exp(\beta^2) - 1 \tag{2.19}$$

Dimensionless variance (Equation 2.19) is a constant. μ_{conc} is also equal to the average gas phase residence time ($\tau = \epsilon_g L/U_g$). By substituting τ into Equation 2.19, we find that the standard deviation is directly proportional to the distance between detectors.

$$\Delta\sigma_{jk} = \sigma_k - \sigma_j = [\exp(\beta^2) - 1]^{0.5} \frac{\epsilon_g}{U_g} L_{jk} \propto L_{jk} \tag{2.20}$$

Alternatively, by combining Equations 2.18 and 2.19 we may calculate the following proportionality.

$$\frac{\mu_k^2}{[\mu_k^2 + \sigma_k^2]^{0.5}} - \frac{\mu_j^2}{[\mu_j^2 + \sigma_j^2]^{0.5}} = \exp(-\alpha)\ L_{jk} \propto L_{jk} \tag{2.21}$$

When the experimental technique involves a measurement over a control volume, the RTD must be modified to account for t_p.

$$E_{cv}(t) = \frac{g(w)w^2}{L}$$

$$\text{where} \quad g(w) = \frac{f(w)}{w\int_0^{\infty}\frac{f(w)}{w}dw} \tag{2.22}$$

The RTD for the control volume differs from $E_{conc}(t)$ by the area under f(w)/w versus w.

$$E_{cv}(t) = \frac{1}{\sqrt{2\pi}\,\beta t}\exp(\alpha-\frac{\beta^2}{2})\ \exp[-\frac{(\ln t-\ln L+\alpha)^2}{2\beta^2}] \tag{2.23}$$

The first and second central moments of $E_{cv}(t)$ are also a function of the log-normal velocity distribution parameters and the distance between measurement points.

$$\mu_{cv} = L\ \exp(\frac{3\beta^2}{2} - \alpha) \tag{2.24}$$

$$\frac{\sigma_{cv}^2}{\mu_{cv}^2} = \exp(\beta^2) - 1 \tag{2.25}$$

Dimensionless variance for the control volume case is the same constant (see Equation 2.19). Since μ_{cv} does not equal the average gas phase residence time, the following test must be used for a control volume.

$$\frac{\mu_k^4}{[\mu_k^2+\sigma_k^2]^{1.5}} - \frac{\mu_j^4}{[\mu_j^2+\sigma_j^2]^{1.5}} = \exp(-\alpha)\ L_{jk} \propto L_{jk} \tag{2.26}$$

Equations 2.12, 2.14 and 2.26 are used to distinguish dispersive from convective behaviour in the gas phase flow when the data involves a control volume technique.

2.5 Results and discussion

Experiments at two superficial velocities, three in the bubbly regime and another three in the churn turbulent regime are used to demonstrate the capabilities of a convective model for gas phase flow in a bubble column. Gas hold-up as function of superficial velocity is presented in Figure 2.3 for RTD experiments at low and high superficial velocities. Also presented on Figure 2.3 are hold-up measurements done with the same air/argon ratio as used in RTD experiments (a volumetric ratio of 3.3:1.0) and with air only as the feed gas. These results show that the replacement of a part of the gas flow with argon (necessary for the tracer experiments) does not affect gas hold-up in the column.

2.5.1 Axial dispersion model

Optimization of the Peclet number and the average residence time gives a good fit to experimental tracer response curves at detector 4 (Figure 2.4). Only the response at detector 4 was fitted. The responses at detectors 2, 3 and 5 (Figure 2.5), predicted assuming a constant axial dispersion coefficient and mean gas velocity, also fit well with experimental curves. The dispersion coefficient and gas velocity are calculated using the optimal values for Pe and τ respectively. In Table 2.1 the axial dispersion coefficients calculated using Equations 2.3 to 2.5 and the optimization procedure are

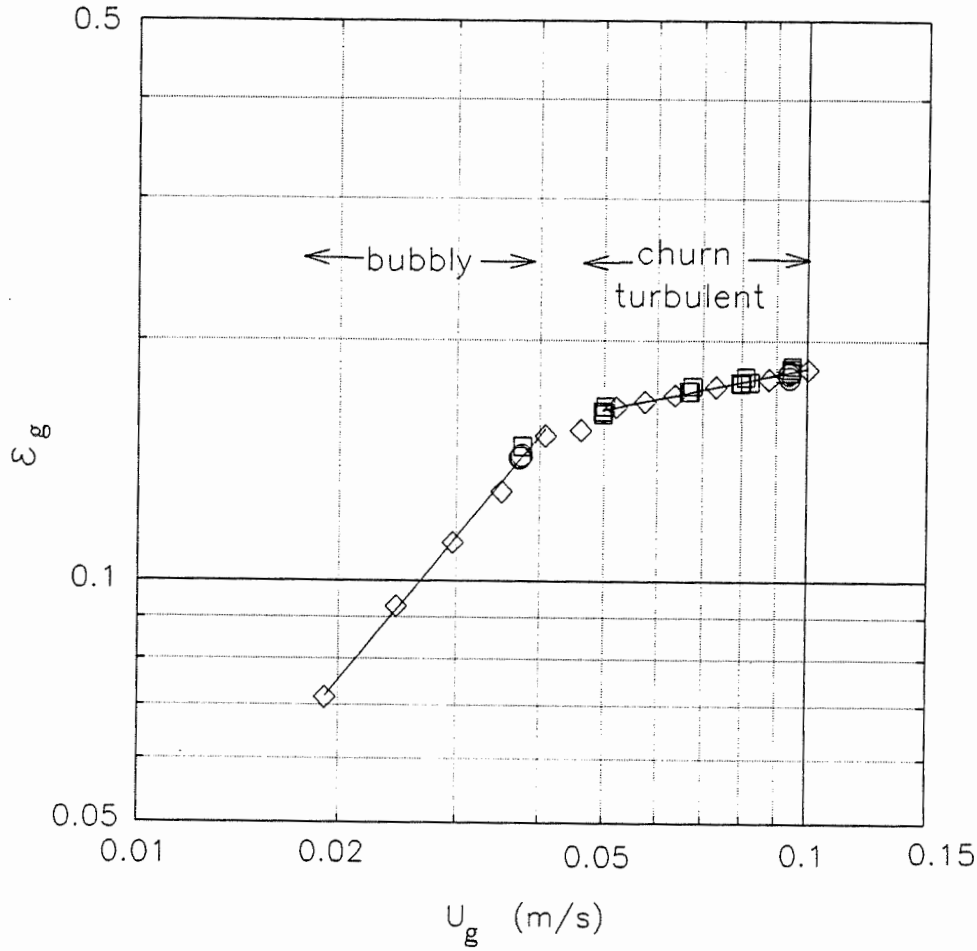

Figure 2.3: Gas hold-up versus superficial velocity (m/s) (RTD experiments ○, hold-up experiments with a fixed air/argon ratio□ and air only ◇).

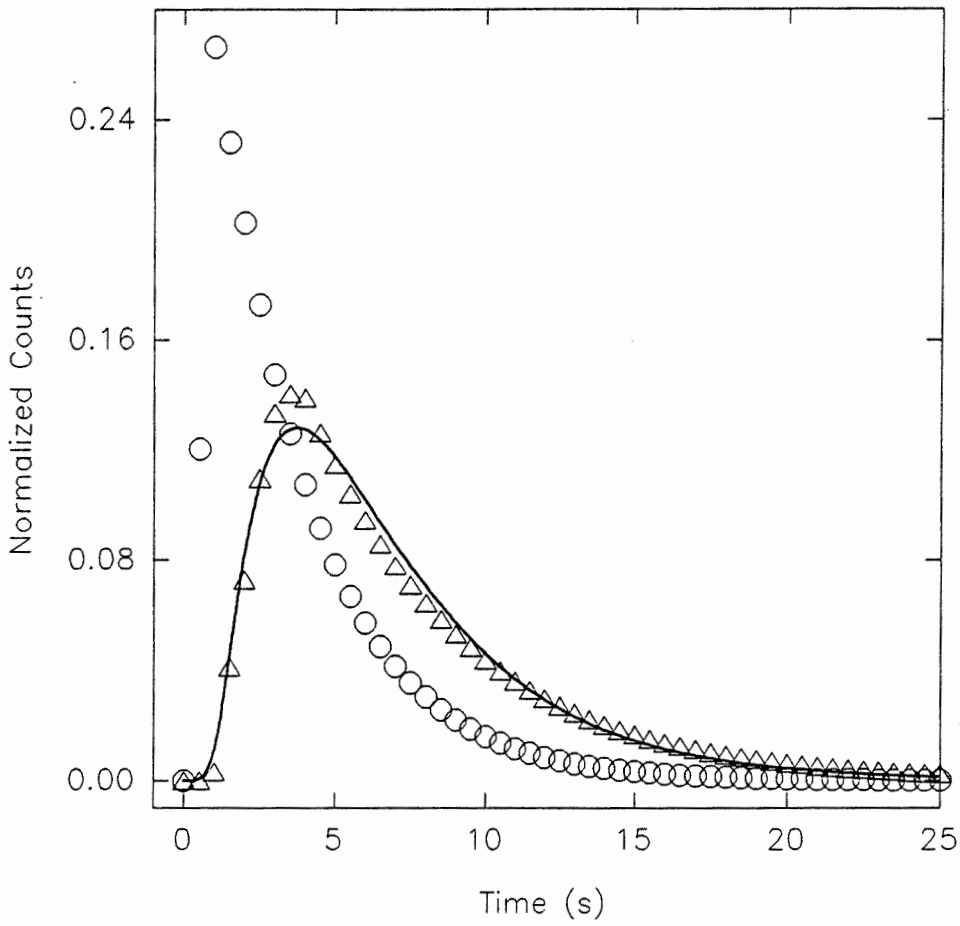

Figure 2.4: Axial dispersion model tracer response curve prediction versus experiment for U_g = 0.094 m/s; Response at detector 1 (data O); Response at detector 4 (data Δ ; prediction ——); 1/5 of data points are shown for clarity in this figure and Figures 2.5 to 2.7.

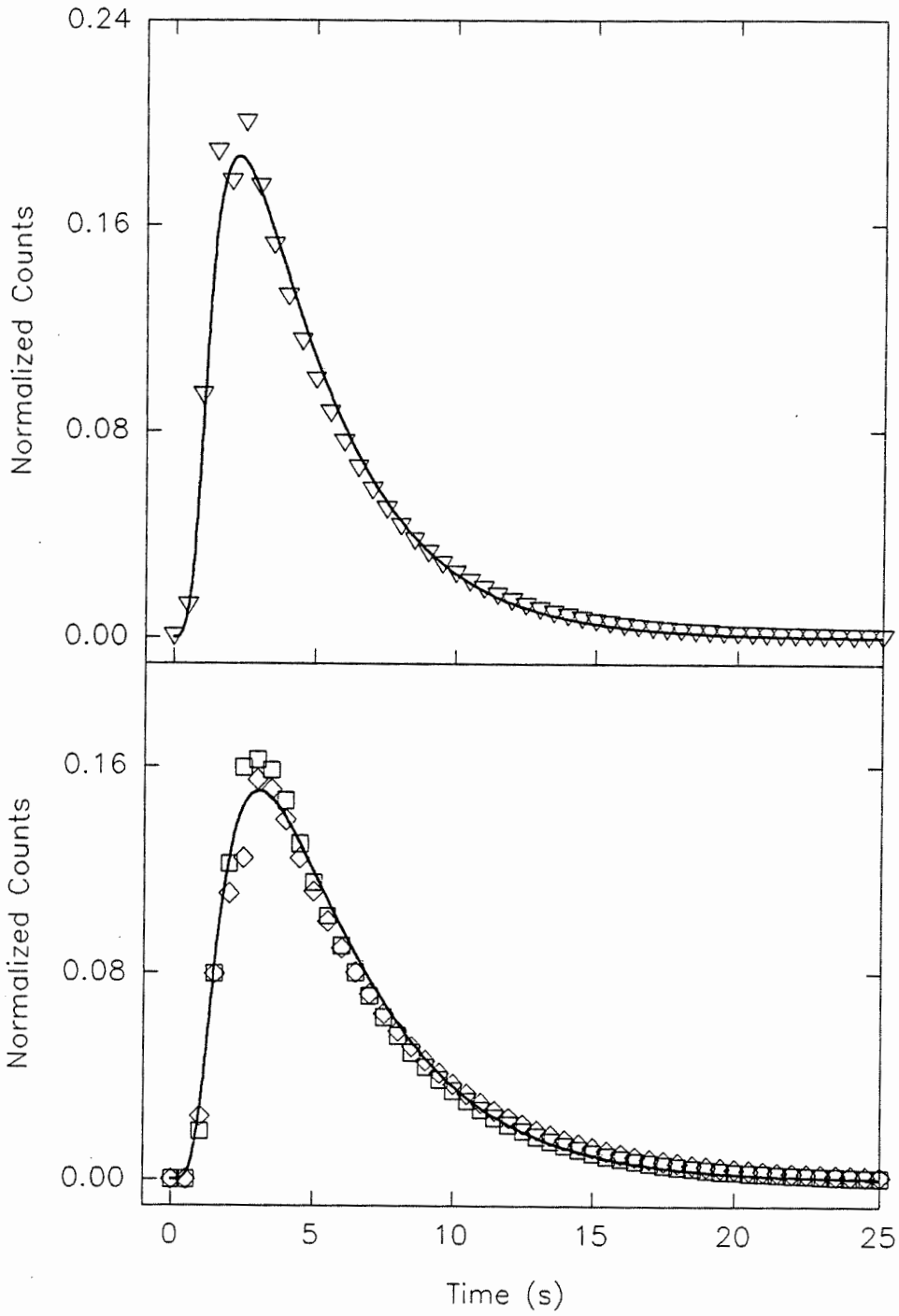

Figure 2.5: Axial dispersion model tracer response curve predictions versus experiment (not fitted) for U_g = 0.094 m/s; Response at detectors 2 (data ▽), 3 (data□) and 5 (data ◇), (predictions ——).

presented. In Table 2.2 the axial dispersion coeficients are compared to values calculated by correlations or data presented in the literature. In general, the values

Table 2.1

Axial dispersion model : dispersion coefficients and mean gas velocities.

Flow Regime	$U_g \pm 0.001$ (m/s)	D_{ax} (m^2/s)	$V_{14,opt}$ (m/s)	V_{14} moments (m/s)	$U_g/\epsilon_g \pm 0.01$ (m/s)
Churn	0.094	0.33	0.36	0.32	0.52
turbulent	0.094	0.46	0.27	0.27	0.52
	0.094	0.34	0.36	0.33	0.52
Bubbly	0.037	0.12	0.21	0.18	0.26
	0.038	0.12	0.22	0.18	0.26
	0.037	0.095	0.22	0.18	0.26

presented here are typical of those in the literature. Also presented in Table 2.1 are V_{14} calculated using the optimization procedure mentioned above ($V_{14,opt} = L_{14}/\tau_{opt}$) and V_{14} calculated from first moments of the tracer response signals (Equation 2.14). As is the case with D_{ax}, V_{14} calculated from repeated experiments in both the churn turbulent and bubbly flow regimes has acceptable repeatability. Both methods of calculation for V_{14} give similar results and both differ substantially from the average gas velocity. The large difference between V_{14} and U_g/ϵ_g indicates that the axial dispersion model does not correctly describe the behaviour of the gas phase. Because of the nature of the radioactive tracer technique, slowly rising marked bubbles are

Table 2.2

Comparison of axial dispersion coefficients with the literature.

Reference	Model	U_g/ϵ_g (m/s)	D_{ax} (m^2/s) D_c=0.2 m
This work	Axial Dispersion	0.52	0.33-0.46
		0.26	0.095-0.12
Field & Davidson (1980) H/D_c=5.91 with D_c=3.2 m their Equation (23)	Axial Dispersion	0.52	0.66
		0.26	0.056
Joshi (1982) correlation of data from six sources their Equation (12)	Axial Dispersion	0.52	0.22
		0.26	0.044
Kawagoe et al. (1989) H/D_c=12.6 with D_c=0.159 m H/D_c=6.90 with D_c=0.290 m their Equations (7) (8) & (11)	Two-Bubble-Group (equivalent value for Single-Bubble-Group)	0.52	0.17
		0.26	0.02
Modak et al. (1993) data from Kawagoe et al. (1989)	Modified Two-Bubble-Class (equivalent value)	0.50	0.39
Shetty et al. (1992) H/D_c=18.0 with D_c=0.15 m H/D_c=10.8 with D_c=0.25 m their Figure 8 (approximate ranges encompassing both D_c)	Axial Dispersion with mass transfer to fully backmixed liquid	U_g=0.094	0.18-0.37
		U_g=0.038	0.11-0.17

"counted" more than marked bubbles which rise quickly. This explains why, in both bubbly and churn turbulent flow regimes, V_{14} is systematically lower than the values for mean gas velocity (U_g/ϵ_g). The difference between V_{14} and U_g/ϵ_g is greater at the higher superficial velocity, and therefore, using the axial dispersion model to describe

gas phase flow in the churn turbulent regime is a poor approximation to reality.

The change in variance of tracer response signals (Equation 2.12) is presented in Table 2.3. The test developed by Levenspiel and Fitzgerald (1983) appears to

Table 2.3

Axial dispersion model test (Equation (2.12)).

Flow Regime	$U_g \pm 0.001$ (m/s)	detectors 1-2 (s^2/m)	$\Delta\sigma_{1k}^2/L_{1k}$ 1-3 (s^2/m)	1-5 (s^2/m)	1-4 (s^2/m)
Churn	0.094	7.6	9.8	14	15
turbulent	0.094	16	14	14	14
	0.094	3.4	8.1	12	14
Average		$11 \pm 32\%$	$(13 \pm 18\%$	without	1-2)
Bubbly	0.037	59	37	39	39
	0.038	29	43	50	47
	0.037	49	39	52	42
Average		$44 \pm 18\%$	$(43 \pm 12\%$	without	1-2)

eliminate the axial dispersion model because of the substantial variability in the test parameter. More variation is seen in the test parameters calculated between detectors 1 and 2, however these results are more prone to error because of the short distance involved. Thus, despite a good fit of tracer response signals and axial dispersion coefficients which match those in the literature, the axial dispersion model may be

invalidated in both flow regimes on the basis of V_{14} not corresponding to U_g/ϵ_g (Table 2.1) and on the test parameter (Table 2.3) which shows a large variability.

2.5.2 Convective model

The first moments ($\overline{w}$) of the bubble velocity distributions as calculated using the convective model (Equations 2.6 to 2.10 and an optimization procedure) are compared to U_g/ϵ_g in Table 2.4. Unlike the axial dispersion model (V_{14}), the mean gas velocity is well predicted by the convective model. Results for the convective model test parameter using moments (Equation 2.26) are presented in Table 2.5. The parameter

Table 2.4

Predicted mean gas velocities from convective model.

Flow Regime	$U_g \pm 0.001$ (m/s)	$U_g/\epsilon_g \pm 0.01$ (m/s)	$\bar{w}$ (m/s)
Churn	0.094	0.52	0.53
turbulent	0.094	0.52	0.48
	0.094	0.52	0.49
Bubbly	0.037	0.26	0.27
	0.038	0.26	0.26
	0.037	0.26	0.26

appears to confirm that the convective model is better suited to describe gas phase behaviour in a bubble column as its variability is small.

Table 2.5

Convective model test (Equation (2.26)).

Flow Regime	$U_g \pm 0.001$ (m/s)	detectors 1-2 (s/m)	$\Delta f(\mu^2,\sigma^2)/L_{1k}$ 1-3 (s/m)	1-5 (s/m)	1-4 (s/m)
Churn	0.094	2.1	2.1	2.2	2.0
turbulent	0.094	2.4	2.2	2.2	2.2
	0.094	2.1	2.1	2.0	2.0
Average		$2.1 \pm 5\%$	($2.1 \pm 4\%$	without	1-2)
Bubbly	0.037	3.7	3.8	3.6	3.9
	0.038	2.8	3.3	3.8	3.7
	0.037	3.9	3.6	3.7	3.9
Average		$3.6 \pm 9\%$	($3.7 \pm 5\%$	without	1-2)

For the same experiment as shown for the axial dispersion model, predicted and experimental tracer response curves are presented in Figures 2.6 and 2.7. Despite not being fitted, responses at detectors 2, 3 and 5, are well predicted by the proposed convective model at both superficial velocities. Response curves predicted by the convective model are not smooth (especially at the peaks) because they result from derivatives of the predicted cumulative response curves. Corresponding bubble velocity distributions for three experiments in the bubbly and three in the churn

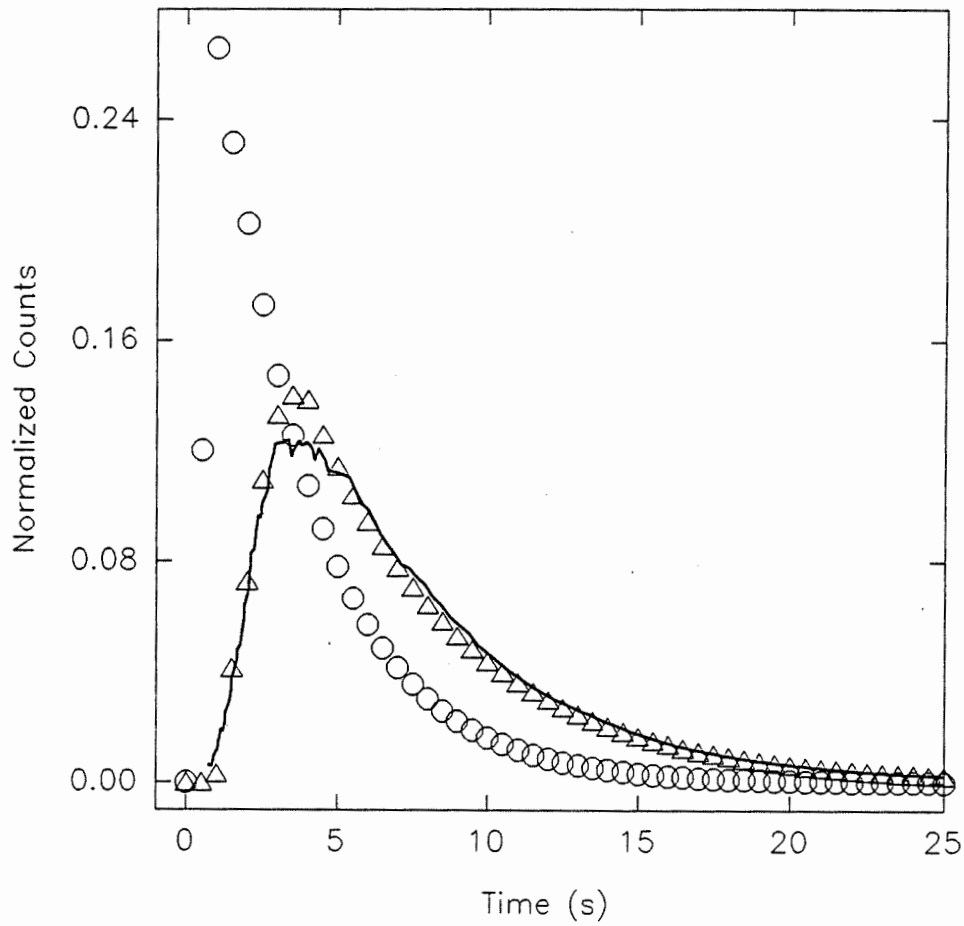

Figure 2.6: Convective model tracer response curve prediction versus experiment for U_g = 0.094 m/s; Response at detector 1 (data O); Response at detector 4 (data Δ ; prediction ——).

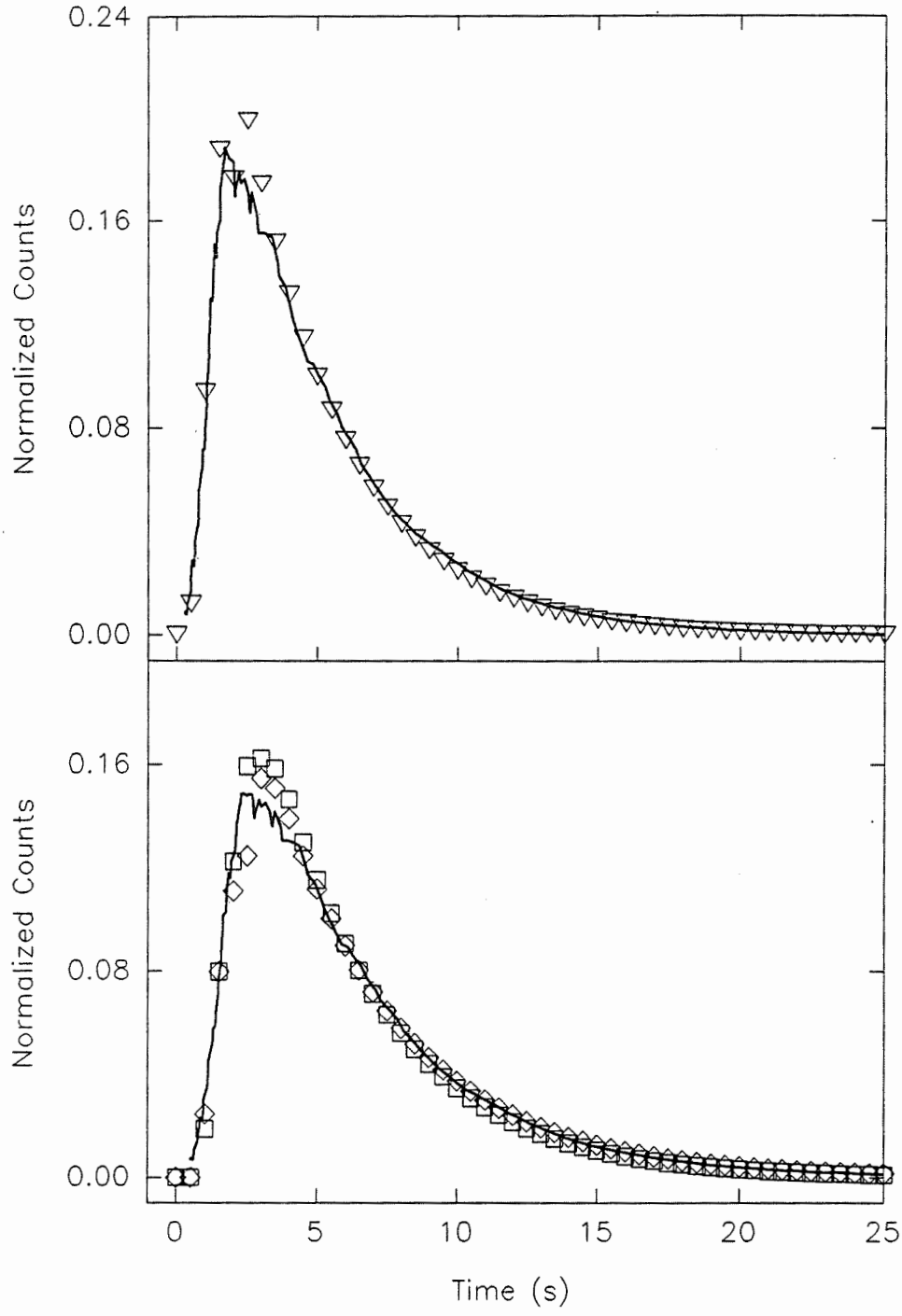

Figure 2.7: Convective model tracer response curve predictions versus experiment (not fitted) for U_g = 0.094 m/s; Response at detectors 2 (data ▽), 3 (data□) and 5 (data ◇), (predictions ——).

turbulent flow regime are presented in Figure 2.8. As would be expected, the distributions are narrower in the bubbly flow regime than in the churn turbulent flow regime. Further, good repeatability is seen in bubble velocity distribution parameters determined using the model (see Table 2.6).

Table 2.6

Parameters for log-normal bubble velocity distributions.

Flow Regime	$U_g \pm 0.001$ (m/s)	$ß_{opt}$	α_{opt} ($e^{\alpha} \equiv$ m/s)	α_{14} Equation (2.26) ($e^{\alpha} \equiv$ m/s)
Churn	0.094	0.51	-0.75	-0.69
turbulent	0.094	0.55	-0.87	-0.79
	0.094	0.45	-0.81	-0.69
Bubbly	0.037	0.43	-1.4	-1.4
	0.038	0.44	-1.4	-1.3
	0.037	0.43	-1.4	-1.4

The parameter α of the log-normal velocity distribution may be calculated using the test parameter presented in Table 2.5 (Equation 2.26). As shown in Table 2.6, these values correspond well with the optimized value of α calculated using the convective model. Equation 2.26 thus provides a shortcut method of calculating the mode of the bubble velocity distribution using moments of tracer response curves.

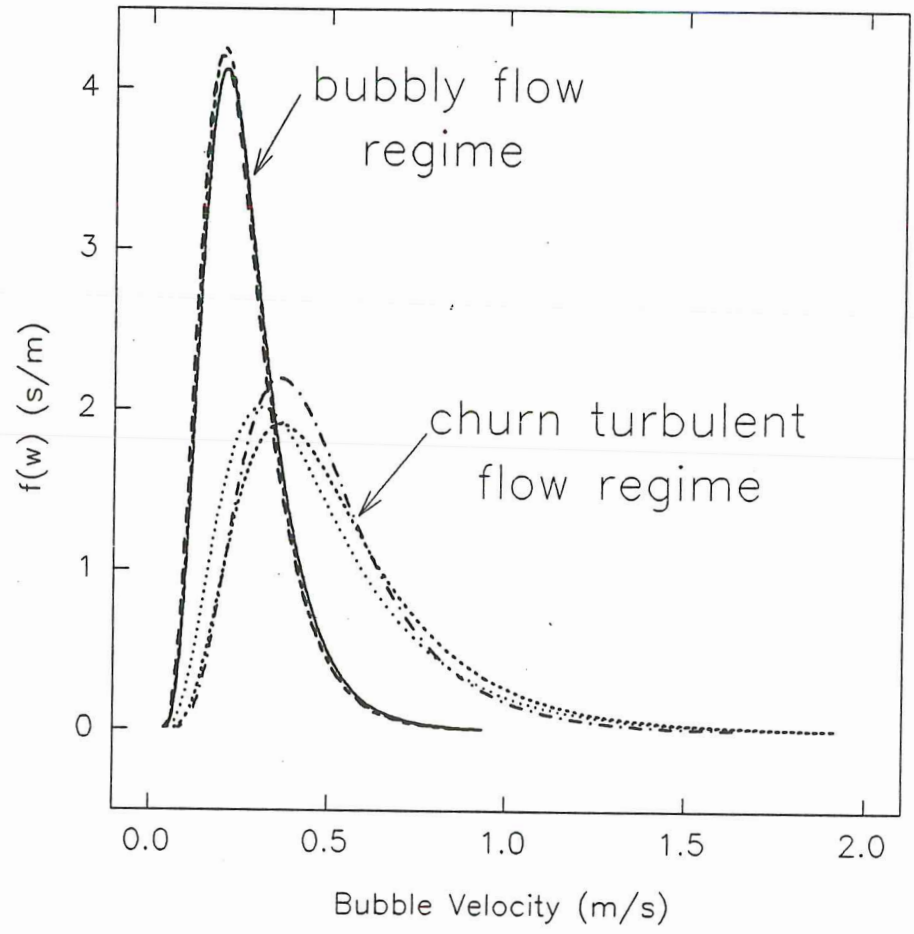

Figure 2.8: Bubble rise velocity distributions (for parameters see Table 2.6)

2.6 Conclusions

The simple tests using moments of tracer response curves (Equations 2.12 and 2.26) are capable of discriminating between convective and dispersive phenomena. These tests show that spreading observed in gas phase tracer response curves for a bubble column is principally due to a convective rather than a dispersive phenomenon in the gas phase flow. Further, V_{14}, calculated from tracer response curves which involve a control volume measurement technique, are also conclusive in eliminating the axial dispersion model to represent gas phase behaviour. In both the bubbly and churn turbulent flow regimes, the convective model fits tracer response curves well and the mean of its bubble velocity distribution corresponds to independently measured U_g/ϵ_g. Gas flow in bubble columns is convective in nature and the use of the axial dispersion model is not recommended especially in the churn turbulent regime. The proposed convective model may be used as a technique to calculate bubble rise velocity distributions from RTD data.

2.7 Acknowledgements

The authors gratefully acknowledge financial support from the Natural Sciences and Engineering Research Council of Canada and of the Fonds pour la Formation de Chercheurs et l'Aide à la Recherche (Québec). We would also like to thank Dr. G. Kennedy and J. St-Pierre for their assistance with the activation of numerous radioactive tracer samples and their advice on the application of radioactive tracers.

2.8 References

AUFDERHEIDE, E. and A. VOGELPOHL (1986), "A Convective Model to Interpret Dispersed-Phase Residence Time Measurements in Pulsed Liquid/Liquid Extractors", Chem. Eng. Sci. **41**, 1747-1757.

CHEN, R.C., J. REESE and L.-S. FAN (1994), "Flow Structure in a Three Dimensional Bubble Column and Three-Phase Fluidized Bed", AIChE J. **40**, 1093-1104.

DECKWER, W-D. and A. SCHUMPE (1993), "Improved Tools for Bubble Column Reactor Design and Scale-Up", Chem. Eng. Sci. **48**, 889-911.

FAN, L.-S. (1989), "Gas-Liquid-Solid Fluidization Engineering", Butterworth Publishers, Stoneham, MA, pp. 90-91.

FIELD, R.W. and J.F. DAVIDSON (1980), "Axial Dispersion in Bubble Columns", Trans. Inst. Chem. Eng. **58**, 228-236.

FRANZ, K., T. BÖRNER, H.J. KANTOREK and R. BUCHHOLZ (1984), "Flow Structures in Bubble Columns", Ger. Chem. Eng. **7**, 365-374.

HILLS, J.H. (1974), "Radial Non-Uniformity of Velocity and Voidage in a Bubble Column", Trans. Inst. Chem. Eng. **52**, 1-9.

JOSHI, J.B. (1982), "Gas Phase Dispersion in Bubble Columns", Chem. Eng. J. **24**, 213-216.

KAWAGOE, M., T. OTAKE and C.W. ROBINSON (1989), "Gas-Phase Mixing in Bubble Columns", J. Chem. Eng. Japan **22**, 136-142.

KUESTER, J.L. and J.H. MIZE (1973), "Optimization Techniques with Fortran", McGraw Hill, Toronto, pp. 368-385.

LEVENSPIEL, O. (1972), "Chemical Reaction Engineering", John Wiley & Sons, Toronto, pp. 275-278.

LEVENSPIEL, O. and T.J. FITZGERALD (1983), "A Warning on the Misuse of the Dispersion Model", Chem. Eng. Sci. **38**, 489-491.

MODAK, S.Y., V.A. JUVEKAR and V.C. RANE (1993), "Dynamics of the Gas Phase in Bubble Columns", Chem. Eng. Technol. **16**, 303-306.

MOLERUS, O. and M. KURTIN (1986), "Modelling of Residence Time Distributions of the Gas Phase in Bubble Columns in the Liquid Circulation Regime", Chem. Eng. Sci. **41**, 2693-2698.

PRESS, W.H., B.P. FLANNERY, S.A. TEUKOLSKY and W. VETTERLING (1989), "Numerical Recipes: The Art of Scientific Computing (FORTRAN Version)", Cambridge University Press, New York, pp. 289-293.

SHETTY, S.A., M.V. KANTAK and B.G. KELKAR (1992), "Gas Phase Backmixing in Bubble Column Reactors", AIChE J. **38**, 1013-1026.

UEYAMA, K. and T. MIYAUCHI (1979), "Properties of Recirculating Turbulent Two Phase Flow in Gas Bubble Columns", AIChE J. **25**, 258-266.

WAKAO, N. and S. KAGUEI (1982), "Heat and Mass Transfer in Packed Beds", Gordon and Breach Science Publishers, New York, pp. 1-31.

YAO, B.P., C. ZHENG, K.E. GASCHE and H. HOFMANN (1991), "Bubble Behaviour and Flow Structure of Bubble Columns" Chem. Eng. Process. **29**, 65-75.

CHAPTER III

GAS PHASE HYDRODYNAMICS IN BUBBLE COLUMNS

Reference: HYNDMAN, C.L. and C. GUY (1995), "Gas Phase Hydrodynamics in Bubble Columns", Chemical Engineering Research and Design **73**, 302-307.

Keywords: bubble columns, hydrodynamics, convective model, residence time distribution

3.1 Context[2]

In Chapter II, "Gas Phase Flow in Bubble Columns: A Convective Phenomenon", two models for gas phase flow were tested using residence time distribution (RTD) data. The axial dispersion model often reported in the literature proved to be unacceptable, particularly at higher superficial gas velocities and in the churn turbulent flow regime. A few authors have opted for modifying the axial dispersion model. On the basis of tests using moments which indicated convective rather than dispersive behaviour of the gas phase, a fully convective model was proposed. The convective model is essentially a series of plug flow models superimposed. The result is that bubble velocity distributions may be calculated from RTD data. In Chapter III, bubble velocity distributions for superficial gas velocities ranging from 0.037 to 0.095 m/s have been calculated. Bubble velocity distribution parameters are correlated with superficial gas velocity.

---

2. This section is not included in the original published paper. It merely serves as a transition between papers for the thesis.

3.2 Abstract

For bubble columns, both the influence of bubble size distribution and liquid circulation within the column result in a bubble rise velocity distribution for the gas phase. We previously determined that a convective model may be a more appropriate description of gas phase behaviour than the more commonly used axial dispersion model.

In this paper, we present bubble velocity distributions and the method for calculating them using a fully convective model. It is shown that the bubble velocity distribution is affected by the superficial gas velocity. Correlations for the mean, mode and standard deviation of the distribution are proposed as a function of superficial gas velocity for an air-water system.

3.3 Introduction

The simplest model to describe gas phase behaviour in bubble columns is a plug flow model. In gas-liquid contactors, when the hydrodynamic behaviour of the gas phase deviates from a plug flow model, an obvious choice for a hydrodynamic model has been the axial dispersion model. This model assumes an average gas velocity and an axial dispersion coefficient to account for the deviation from the average flow velocity. In the work done to date, a large scatter in the dispersion coefficients reported (Deckwer and Schumpe, 1993) shows that the model is perhaps over simplified.

Convective type modifications have been made to the axial dispersion model by assuming two average bubble rise velocities and an axial dispersion coefficient for each velocity. In their two-bubble group model, Kawagoe et al. (1989) assume there are two average bubble velocities, one attributed to the core or upflow region of the bubble column where higher rise velocities tend to occur, and an annulus or downflow region where lower bubble rise velocities occur. Bubbles from one group are assumed not to interact with those from the other group. More recently Modak et al. (1993) have presented a modified two-bubble class model which assumes large and small bubble phases with a cross-mixing coefficient to account for interaction between the phases. (Their model is verified using the data from Kawagoe et al. (1989).) The

large bubble phase is also assumed to have a negligible axial dispersion coefficient in comparison to the small bubble phase.

Whether the axial dispersion model or these modified models are used, a Fickian dispersion coefficient is being used to explain a large part of the "mixing" phenomena seen in residence time distribution curves for the gas phase. A fundamental assumption in the axial dispersion models is that the dispersion coefficient is constant over the length of the column. Levenspiel and Fitzgerald (1983) argued that the axial dispersion model could be misused to represent a convective flow. In a previous publication (Hyndman and Guy, 1994a), we showed that while the axial dispersion model was capable of fitting RTD (residence time distribution) curves, it could not accurately represent the mean convective velocity. The fully convective model was capable of fitting both the RTD curves and the independently measured mean convective velocity U_g/ϵ_g. It was concluded that gas flow in bubble columns is convective in nature and that the axial dispersion model does not accurately describe the gas phase behaviour. Here we use the convective model to describe gas phase behaviour in a bubble column from the bubbly to churn turbulent flow regimes.

3.4 Experimental Method[3]

An acrylic bubble column having an inside diameter of 0.2 m and a height of 1.9 m was used for the residence time distribution experiments (refer to Figure 3.1). The distributor is a perforated plate with 69, 1 mm diameter orifices arranged in a square pattern. Experiments are conducted in semi-batch mode with a water level of 1.4 m. An air-argon-water system is used for all experiments. Two rotameters are used to control gas flow: one is used to control filtered process air from a central supply system, while the other simultaneously allows gas from a pressurized gas cylinder to be fed to the bubble column. A mercury filled manometer is used to measure the pressure at the rotameters. Two vented gage pressure transmitters (Lucas Schaevitz P3061 100"WG and 20"WG) connected near the bottom and top of the column allow measurement of the average gas hold-up over the column. A syringe is used to introduce the gas phase tracer (approximately 7 mL at atmospheric pressure) into the feed gas via a septum on the gas line. The injection requires less than 0.5 s.

Residence time distributions are measured using radioactive argon gas as tracer which is detected at four different axial positions outside the column. (Detectors are 0.083 m in diameter and the heights of their centres above the distributor are as follows:

---

3. The reader should note that aside from some information on the detectors and tracer injection given in section 3.4 a more detailed description of the experimental procedure for RTD is given in section 2.3.

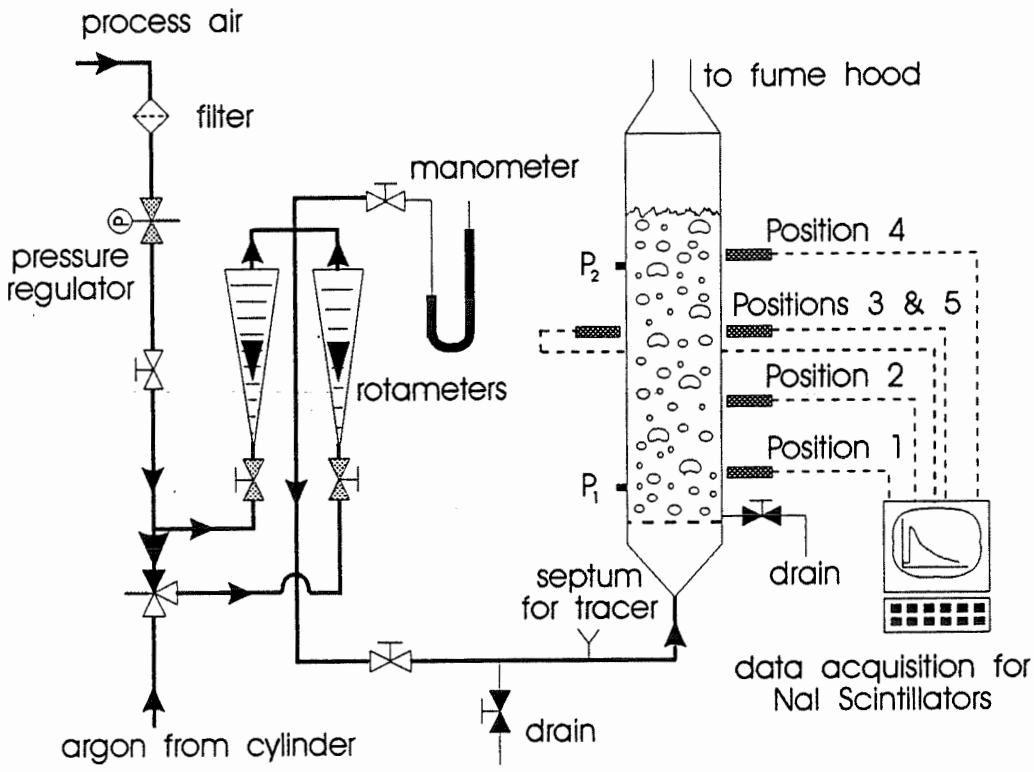

Figure 3.1: Experimental set-up.

positions 1 = 0.211 m, 2 = 0.608 m, 3 = 1.006 m, 4 = 1.408 m and 5 = 1.008 m; detector 5 is located opposite 3.) Argon gas is irradiated in a Slowpoke nuclear reactor immediately prior to each experiment. NaI scintillation detectors (EG&G ORTEC) measure gamma radiation released by the radioactive argon gas as it decays ($t_{1/2}$ = 1.8 h). All five detectors are surrounded by lead brick shielding having the same geometry. Gamma rays detected in each 0.05 s interval by each of the five detectors are counted by the data acquisition system and recorded. Only gamma rays which enter a detector directly and from within the control volume before it are counted. All other gamma rays are eliminated because of their lower energies. Data acquisition continues for a period of 180 s. Because argon dissolves in water, it is fed simultaneously with air in a fixed ratio. Passage of the radioactive tracer into water which is already saturated in argon occurs only as a result of the dynamic equilibrium. This effect is negligible since baseline signals, which include radioactivity in the liquid phase, are the same before and after an experiment. A fixed ratio of air/argon (3.3:1.0) is used so as to eliminate gas density as a variable in experiments. Superficial gas velocities from 0.037 to 0.095 m/s are examined.

Baselines of detector signals (due to background radiation) are removed, signals are filtered to remove high frequency noise and then resampled at 0.1 s to reduce the amount of data. Signals are normalized with respect to the area under their curves. For a complete description of the data treatment refer to Hyndman and Guy (1994a).

3.5 Convective Hydrodynamic Model

The present investigation involves the use of the convective model to determine the bubble rise velocity distributions. Development and testing of the model has been presented elsewhere (Hyndman and Guy, 1994). The distribution of bubble velocity is the combination of the distributions for liquid and relative bubble velocity.

The calculation procedure for the model is as follows. A form for the velocity distribution must be assumed. A log-normal distribution has been assumed in accordance with data presented by Fan (1989) for bubble velocities in the dispersed and coalesced flow regimes of three phase flow. The volume distribution function of bubbles having a velocity w has the following form.

$$f(w) = \exp[-(\ln w-\alpha)^2/(2\beta^2)]/[\beta w(2\pi)^{\frac{1}{2}}] \qquad (3.1)$$

The mode of this distribution is e^{α} and β is an indication of its skewness. Parameters α and β are chosen and the distribution is discretized between the cutoff points w_{min} and w_{max}. Cutoff points for bubble velocity distributions were determined by allowing a tolerance of 10^{-4} on the fraction of bubbles at the upper and lower limits. Spreading of tracer response curves is caused by the distribution in rise velocities so that bubbles containing tracer having higher rise velocities pass the second, third and fourth detectors sooner than those with slower velocities. The effect of the control volume

on the tracer response curve is accounted for by defining time $t_{pass,i}$ as the time required for bubbles rising at velocity w_i to move through a detector window. The bubble velocity distribution is thus corrected by weighting it with $t_{pass,i}$.

$$g(w_i) = f(w_i)t_{pass,i} / \int_{w_{min}}^{w_{max}} f(w)t_{pass}\,dw \tag{3.2}$$

Since the geometry of the lead bricks which create the detector windows is the same for all five detectors ($t_{pass,i} = h_{win}/w_i$), h_{win} cancels out of Equation 3.2. Area under the weighted velocity distribution corresponding to the slowest rise velocities is matched with the tracer which passes in front of the detectors last. The inverted cumulative velocity distribution ($1-g^c$) is matched to the first cumulative tracer response curve in order to link velocities w_i with arrival times at the first detector (t_{i1}).

$$1 - g^c(w_i) = n_1^c(t_{i1}) \tag{3.3}$$

If the parameters chosen for the log-normal distribution curve are correct then the other tracer response curves will be predicted accurately. The cumulative tracer response curves for detectors 2 and above are calculated as follows.

$$\begin{aligned} n_k^c(t_{ik}) &= n_1^c(t_{i1}) \\ \textit{where} \quad t_{ik} &= t_{i1} + L_{1k}/w_i \end{aligned} \tag{3.4}$$

The log-normal velocity distribution parameters (α and β) are optimized using a

downhill simplex method (Press et al. 1989) with an objective function consisting an absolute error between the calculated and experimental response curves.[4]

$$\epsilon = \sum_i (t_{ik}^{calc} - t_{ik}^{expt})^2 \tag{3.5}$$

To evaluate the average bubble velocity distribution in the column, only ϵ at detector 4 is used as a criterion for precision of fit. As it takes longer for bubbles to travel between detectors 1 and 4, the accuracy of calculations is thus greater. Predicted tracer response curves are the derivative of cumulative response curves. Calculated tracer response curves were also produced for detectors 2, 3 and 5 to confirm the validity of the model throughout the column.

4. See Appendix I for details on the objective function.

3.6 Results and Discussion

Gas hold-up as function of superficial velocity is presented in Figure 3.2 for RTD experiments. Also presented on Figure 3.2 are hold-up measurements done with the same air/argon ratio as used in RTD experiments (a volumetric ratio of 3.3) and with air only as the feed gas.[5] These results show that the replacement of a fraction of the gas flow with argon (necessary for the tracer experiments) does not affect gas hold-up in the column.

Examples of predicted and experimental tracer response curves are presented in Figures 3.3 and 3.4 for the bubbly and churn turbulent flow regimes respectively. The signal from detector 1, Equations 3.1 to 3.5, and optimized values for α and β are used to reconstruct the tracer response at detector 4. Despite not being fitted, responses at detectors 2, 3 and 5, are well predicted (data not shown). The response curves predicted by the convective model are not smooth (especially at the peaks) because they result from derivatives of the predicted cumulative response curves. Bubble velocity distributions for three experiments in the bubbly flow regime and six experiments in churn turbulent flow are presented in Figure 3.5. As would be expected, the distributions are narrower and have a smaller mode (e^{α}) at lower superficial gas velocity.

---

5. The three air only gas hold-up experiments at the lowest superficial gas velocities were later found to be unrepeatable refer to Chapters II and IV for accurate meaurements at low superficial velocity.

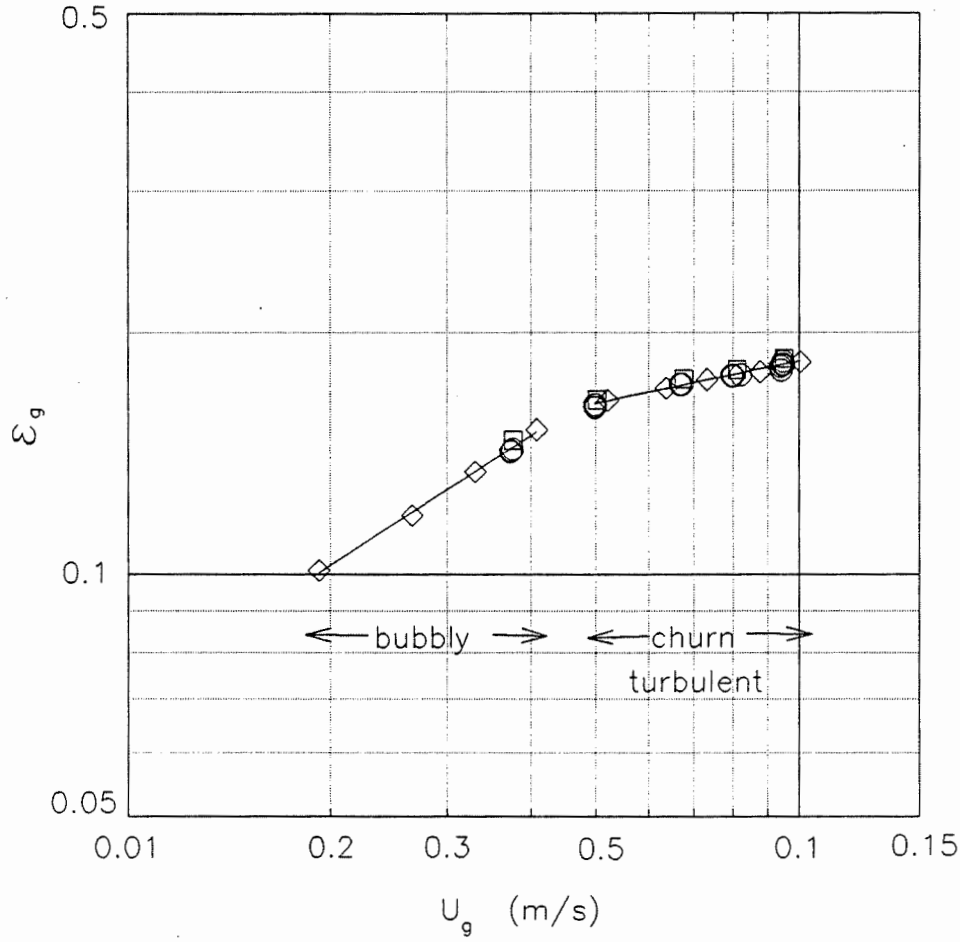

Figure 3.2: Gas hold-up versus superficial velocity (m/s) (RTD experiments O, hold-up experiments with a fixed air/argon ratio□ and air only ◇).

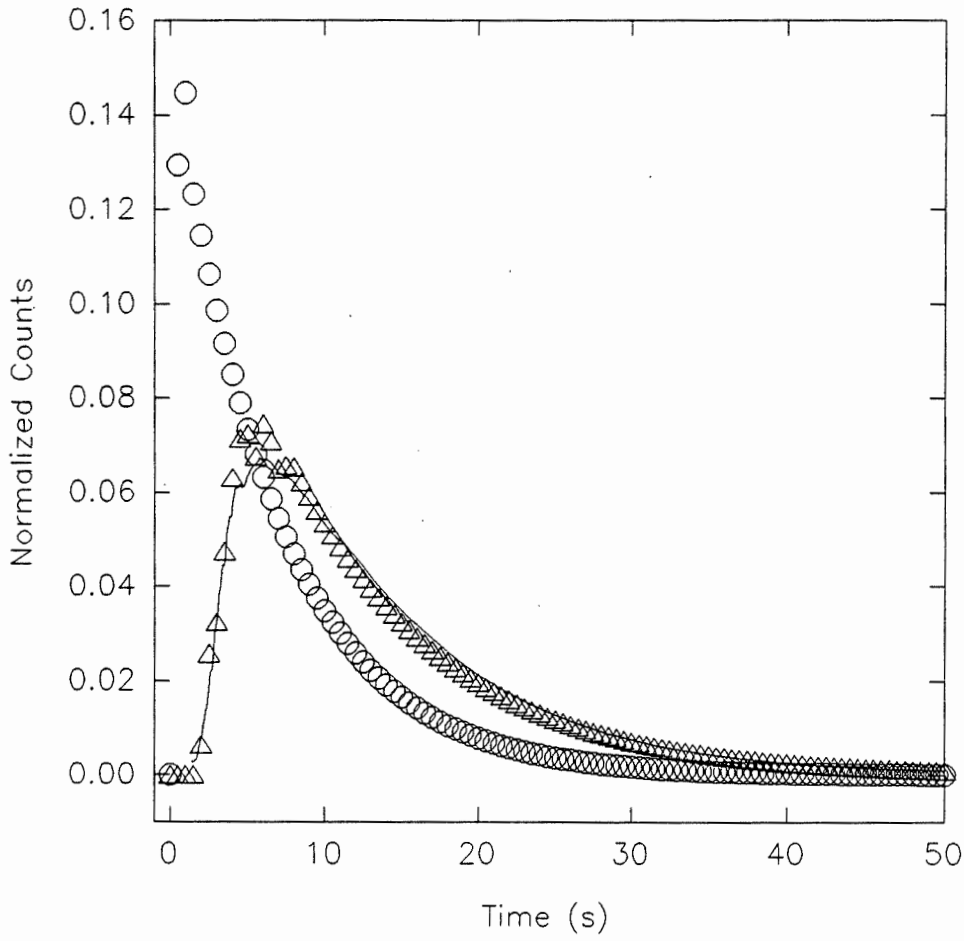

Figure 3.3: Convective model tracer response curve predictions versus experiment for U_g = 0.038 m/s; Response at detector 1 (data O, 1/5 of data points are shown for clarity); Response at detector 4 (data ▵; prediction ——).

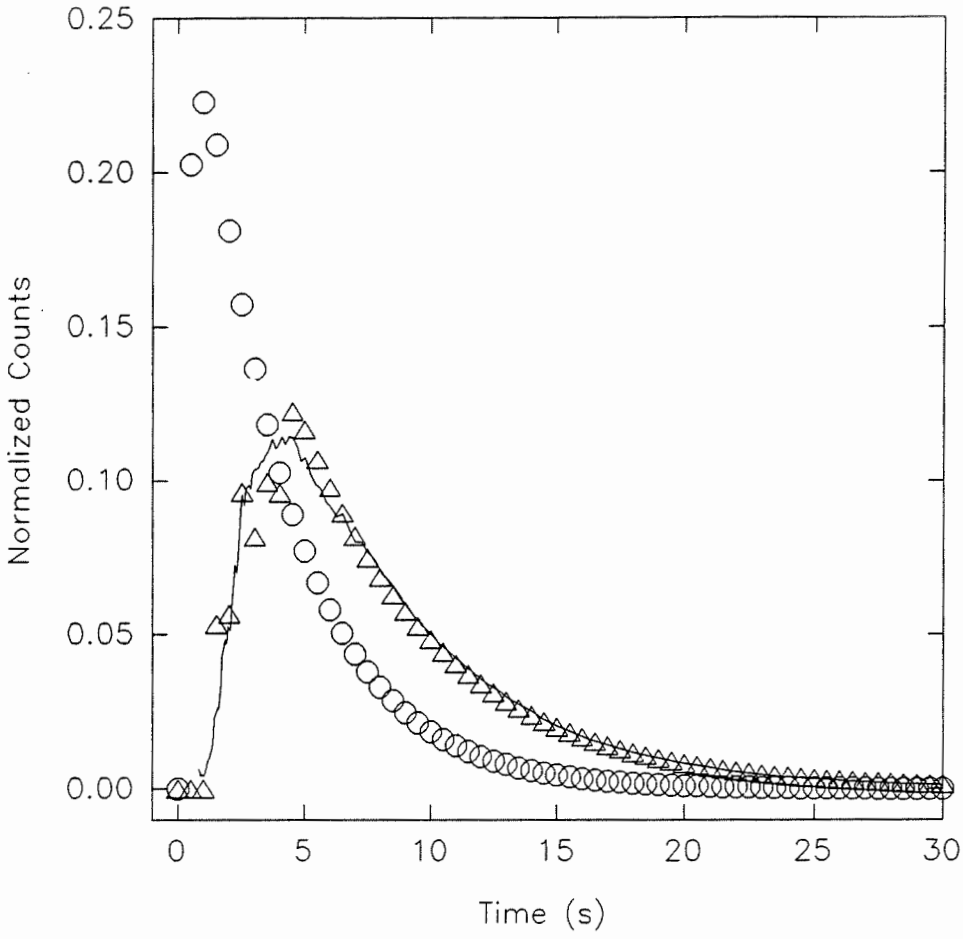

Figure 3.4: Convective model tracer response curve predictions versus experiment for U_g = 0.080 m/s; Response at detector 1 (data O, 1/5 of data points are shown for clarity); Response at detector 4 (data Δ ; prediction ——).

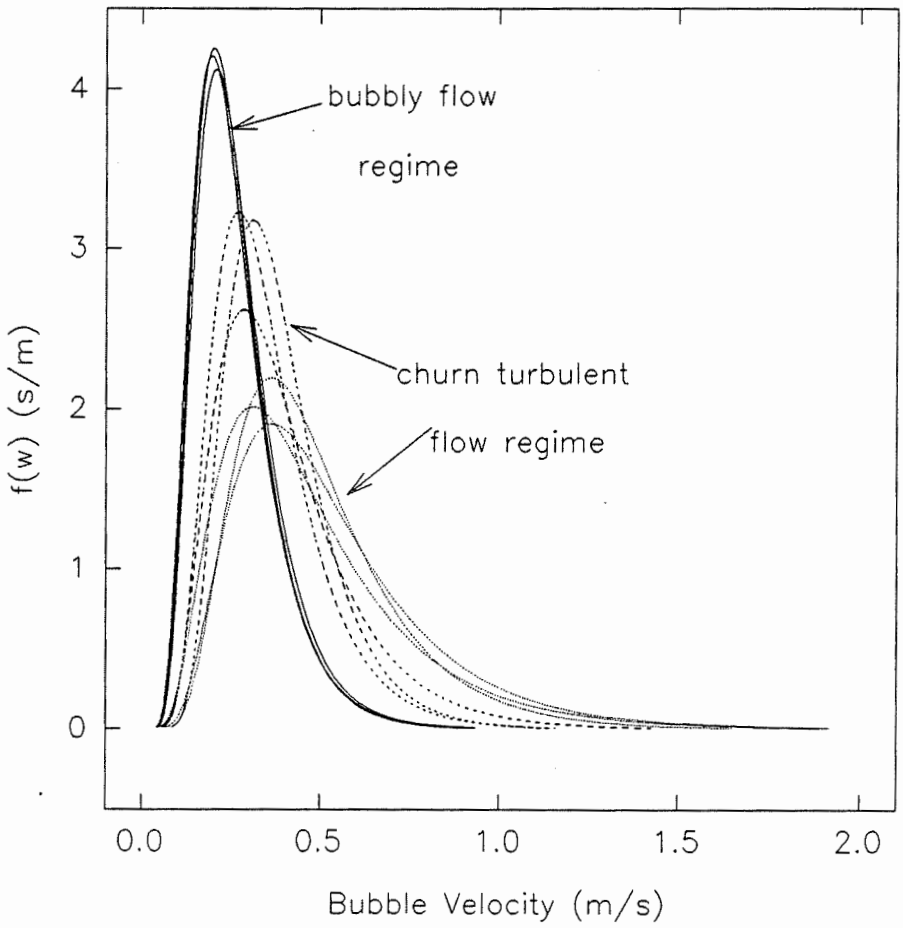

Figure 3.5: Bubble rise velocity distributions for experiments in the bubbly (U_g = 0.037 m/s ——) and churn turbulent (U_g = 0.067 m/s ---- and U_g = 0.094 m/s ·····) flow regime.

Figure 3.6 compares the first moment of the bubble velocity distributions (some of which are presented in Figure 3.5) to mean gas velocities.

$$\overline{w} = \int_{w_{min}}^{w_{max}} w f(w) dw \tag{3.6}$$

The bubble velocity distributions are calculated using only the tracer response curves. Thus, U_g/ϵ_g is a completely independent measure of the gas velocity, as U_g is obtained from flow rate data and ϵ_g from pressure tap data. Good agreement between the mean velocity as determined from RTD data ($\overline{w}$) and U_g/ϵ_g indicates that the convective model adequately represents gas hydrodynamics in the column. The standard deviation of the bubble rise velocity distribution as calculated from the second moment characterizes the broadness of the distribution.

$$\sigma_w = \sqrt{\int_{w_{min}}^{w_{max}} (w-\overline{w})^2 f(w) dw} \tag{3.7}$$

For a log-normal distribution, the mean and standard deviation are defined as follows.

$$\overline{w} \equiv \exp(\alpha + \beta^2/2) \tag{3.8}$$

$$\sigma_w \equiv \exp(\alpha + \beta^2/2)\sqrt{\exp(\beta^2) - 1} \tag{3.9}$$

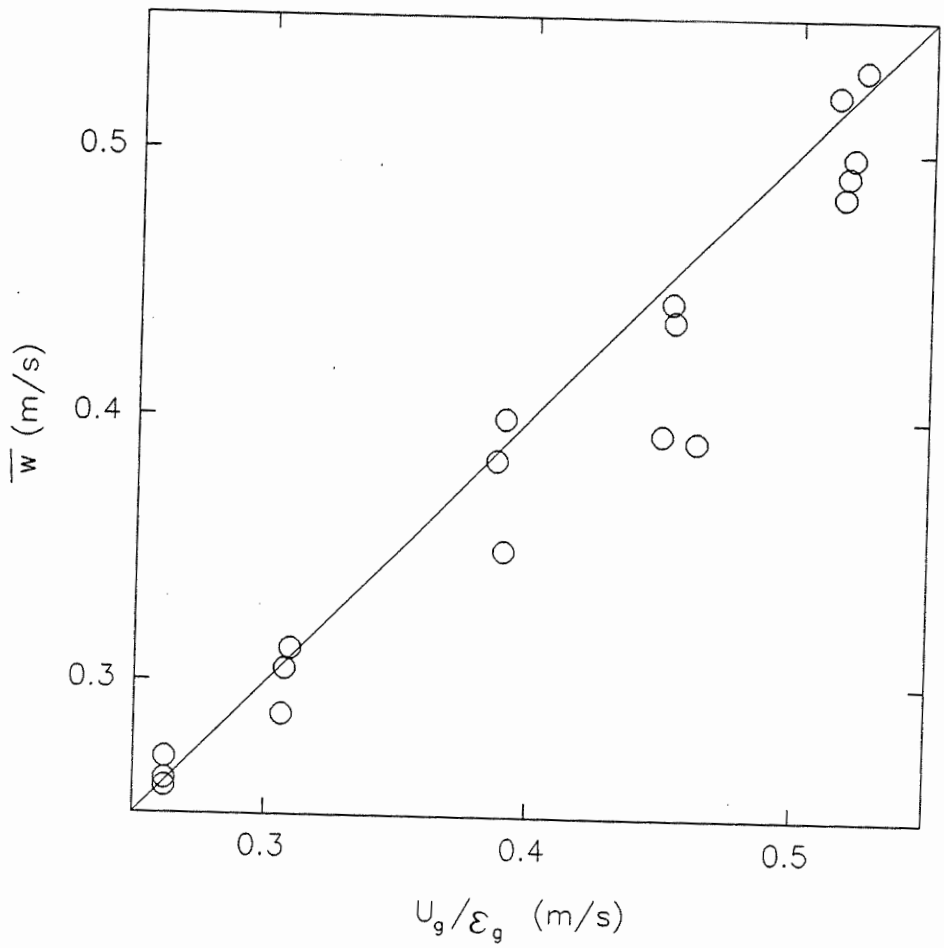

Figure 3.6: First moments of bubble rise velocity distributions versus mean gas velocity.

Table 3.1 summarizes the first moment of the bubble velocity distribution curves (Equation 3.6), their standard deviations (Equation 3.7) and the optimized values of

Table 3.1

Summary of Experimental Results

Regime	U_g (m/s)	U_g/ϵ_g (m/s)	$\bar{w}$ (m/s)	σ_w (m/s)	α ($e^{\alpha} \equiv$ m/s)	ß
churn	0.0942	0.52	0.53	0.27	-0.75	0.51
turbulent	0.0948	0.51	0.52	0.31	-0.81	0.59
	0.0948	0.52	0.50	0.24	-0.80	0.47
	0.0944	0.52	0.48	0.27	-0.87	0.55
	0.0939	0.52	0.49	0.23	-0.81	0.45
	0.0800	0.45	0.44	0.22	-0.92	0.48
	0.0800	0.45	0.44	0.19	-0.92	0.43
	0.0821	0.46	0.39	0.19	-1.0	0.47
	0.0796	0.45	0.39	0.20	-1.0	0.49
	0.0672	0.39	0.40	0.20	-1.0	0.48
	0.0672	0.39	0.35	0.15	-1.1	0.42
	0.0667	0.39	0.38	0.15	-1.0	0.38
	0.0499	0.31	0.30	0.12	-1.3	0.38
	0.0499	0.31	0.31	0.13	-1.2	0.40
	0.0497	0.31	0.29	0.11	-1.3	0.38
bubbly	0.0374	0.26	0.27	0.12	-1.4	0.43
	0.0376	0.26	0.26	0.12	-1.4	0.44
	0.0373	0.26	0.26	0.12	-1.4	0.43

α and β. There is a slight difference between $\bar{w}$ and σ_w as calculated using Equations 3.6 and 3.7 versus values which would be calculated using their definitions (Equations 3.8 and 3.9). This difference is a result of the cutoff points w_{min} and w_{max}.

The mean of the bubble velocity distribution (Equation 3.6) may be expressed as a function of the superficial velocity (see Figure 3.7).

$$\bar{w} = 2.5\, U_g^{0.69} \tag{3.10}$$

The mode of the distribution may also be expressed in terms of the superficial velocity (see Figure 3.8).

$$e^{\alpha} = 2.0\, U_g^{0.65} \tag{3.11}$$

The standard deviation of the bubble rise velocity (Equation 3.7) is correlated with superficial velocity as follows (see Figure 3.9).

$$\sigma_w = 2.1\, U_g^{0.91} \tag{3.12}$$

The experiments conducted in the bubbly flow regime are close to the transition point (refer to Figure 3.2) and thus experiments at yet lower superficial gas velocities would be required to truly validate Equations 3.10, 3.11 and 3.12 for the bubbly flow regime. As seen in Figure 3.5, the mean, mode (e^{α}) and standard deviation of the bubble velocity distribution are all increasing functions of the superficial gas velocity.

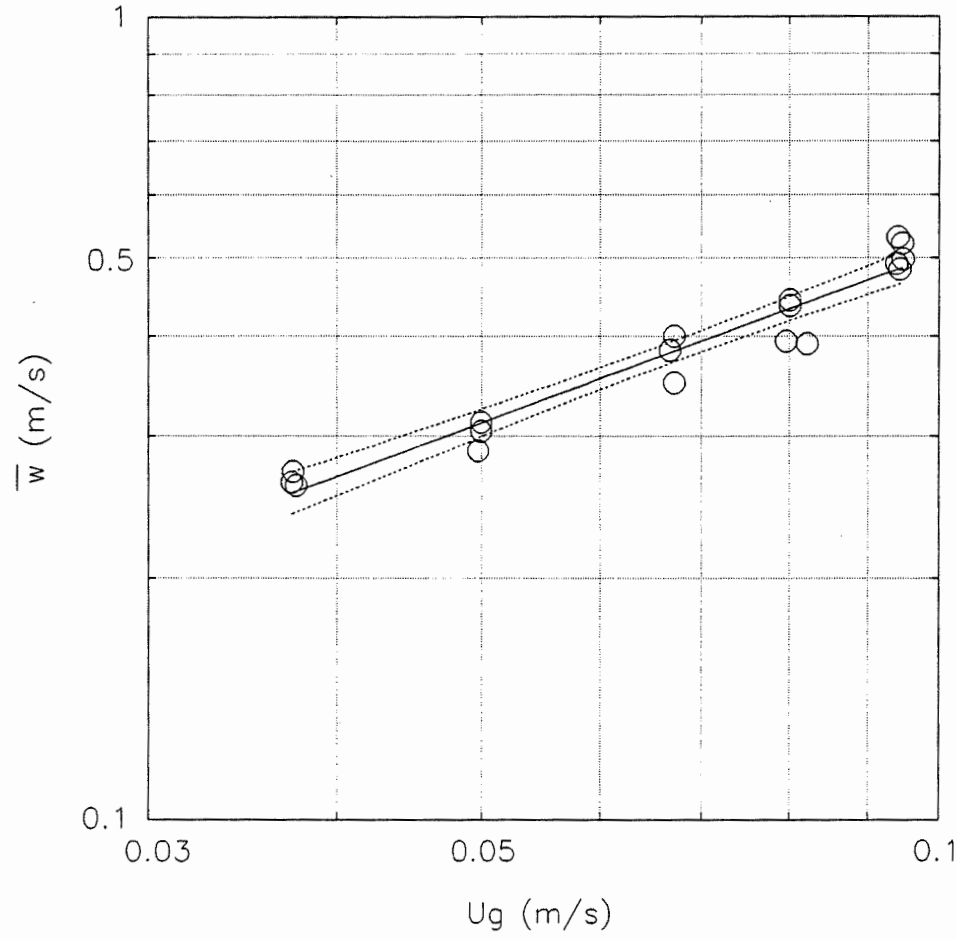

Figure 3.7: Mean bubble velocity ($\overline{w}$) versus superficial gas velocity (data O; Equation 3.10 —— ; 95 percent confidence interval ------).

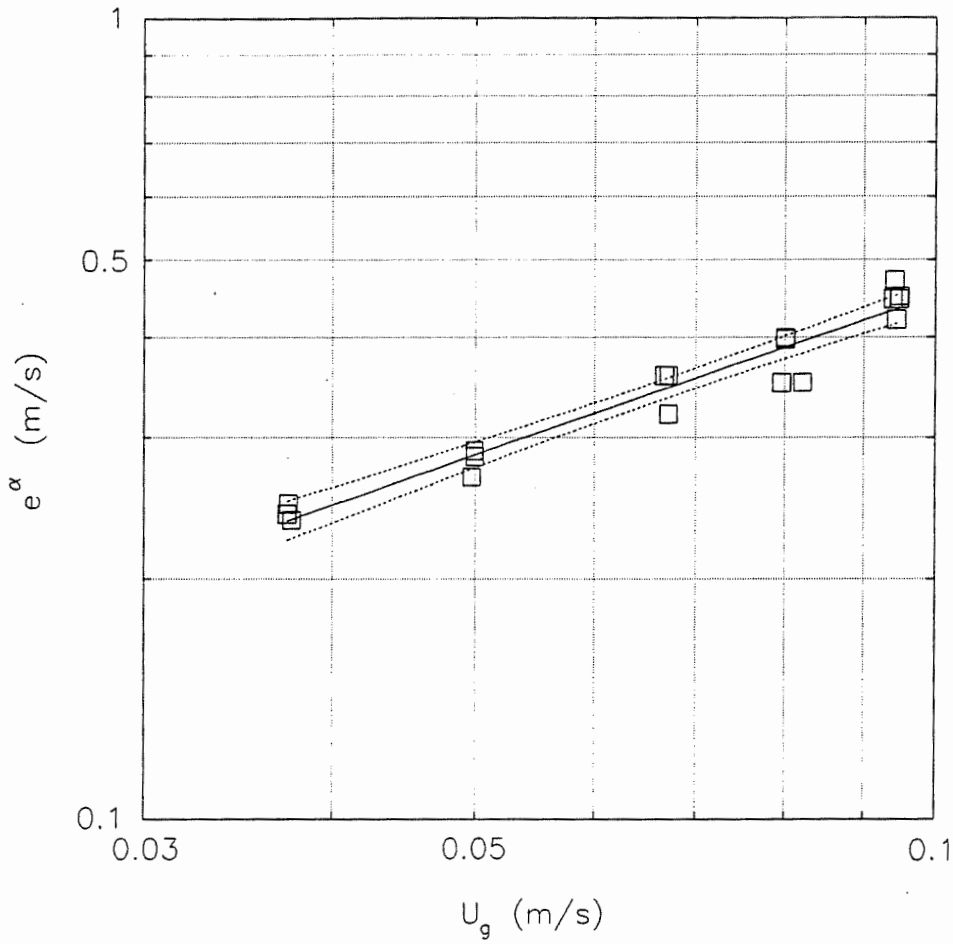

Figure 3.8: Mode of the bubble velocity distribution (e^{α}) versus superficial gas velocity (data□ ; Equation 3.11 —— ; 95 percent confidence interval ------).

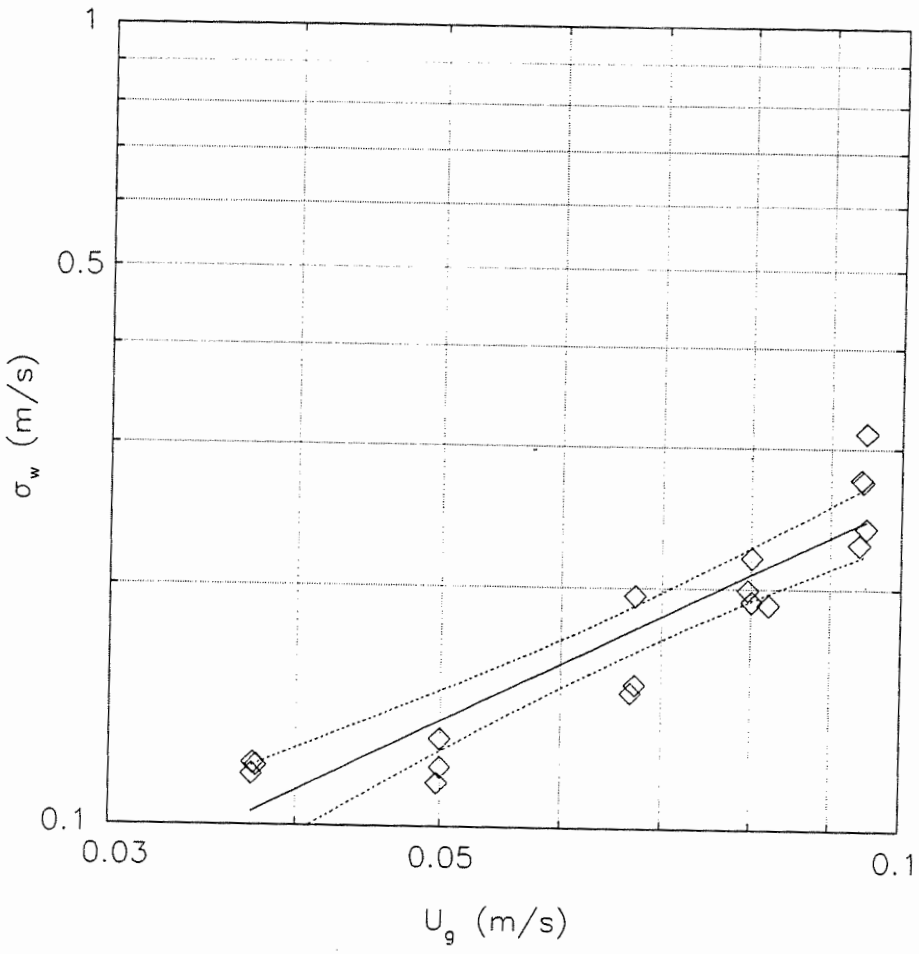

Figure 3.9: Standard deviation of the bubble velocity distribution (σ_w)versus superficial gas velocity (data ◇; Equation 3.12 —— ; 95 percent confidence interval ------).

A bubble velocity distribution calculated by the convective model is an average over the column and is a result of a relative bubble velocity distribution superimposed upon a liquid circulation pattern. Bubbles are hindered and accelerated by liquid movement in the column; hindered bubbles are easily observed near the transparent column walls. In the bubbly flow regime, small σ_w is indicative of both a narrow relative bubbly velocity distribution (homogeneous bubble sizes) and a gentle liquid circulation. In the churn turbulent regime, larger σ_w is indicative of a wider relative bubble velocity distribution (large bubbles are observed) and a more vigorous circulation of the liquid phase.

3.7 Conclusions

Correlations for the bubble velocity distribution are proposed for the convective model of gas phase hydrodynamics in a bubble column. The above correlations for the mean, mode and standard deviation of the log-normal bubble rise velocity distribution (Equations 3.10, 3.11 and 3.12 respectively) were calculated using RTD data from an air-water system in a bubble column 0.2 m in diameter. The correlations indicate that the mean, mode and standard deviation increase with increasing superficial gas velocity as would be expected.

3.8 References

DECKWER, W-D. and A. SCHUMPE (1993), "Improved Tools for Bubble Column Reactor Design and Scale-Up", Chem. Eng. Sci. **48**, 889-911.

FAN, L.-S. (1989), "Gas-Liquid-Solid Fluidization Engineering", Butterworth Publishers, Stoneham, MA, pp. 90-91.

FIELD, R.W. and J.F. DAVIDSON (1980), "Axial Dispersion in Bubble Columns", Trans. Inst. Chem. Eng. **58**, 228-236.

HYNDMAN, C.L. and C. GUY (1995a), "Gas Phase Flow in Bubble Columns: A Convective Phenomenon", Can. J. Chem. Eng. **73**, 426-434. (Chapter II)

KAWAGOE, M., T. OTAKE and C.W. ROBINSON (1989), "Gas-Phase Mixing in Bubble Columns", J. Chem. Eng. Japan **22**, 136-142.

LEVENSPIEL, O. and T.J. FITZGERALD (1983), "A Warning on the Misuse of the Dispersion Model", Chem. Eng. Sci. **38**, 489-491.

MODAK, S.Y., V.A. JUVEKAR and V.C. RANE (1993), "Dynamics of the Gas Phase in Bubble Columns", Chem. Eng. Technol. **16**, 303-306.

PRESS, W.H., B.P. FLANNERY, S.A. TEUKOLSKY and W. VETTERLING (1989), "Numerical Recipes: The Art of Scientific Computing (FORTRAN Version)", Cambridge University Press, New York, pp. 289-293.

CHAPTER IV

UNDERSTANDING GAS PHASE HYDRODYNAMICS IN BUBBLE COLUMNS: A CONVECTIVE MODEL BASED ON KINETIC THEORY

Reference: HYNDMAN, C.L., F. LARACHI and C. GUY (1995), "Understanding Gas Phase Hydrodynamics in Bubble Columns: A Convective Model Based on Kinetic Theory", submitted to Chemical Engineering Science (August, 1995)

Keywords: bubble columns, hydrodynamics, dynamic gas disengagement, convective model, kinetic theory, pressure fluctuations

4.1 Context[6]

In the previous two chapters a convective model was proposed. The model fits tracer response curves as well as average gas velocity. Using the convective model and RTD data, absolute bubble velocity distributions have been calculated for superficial gas velocities from 0.037 to 0.095 m/s. Log-normal bubble velocity distribution parameters have been correlated to superficial gas velocity.

Gas hold-up and flow regime, two factors which greatly influence gas phase hydrodynamics, are examined in this chapter. In the homogeneous flow regime, the gas hold-up consists of relatively uniformly-sized bubbles. When operating in the heterogeneous flow regime (as the name suggests) a range of bubble sizes is observed. Therefore, gas hold-up structure differs in the two regimes.

A variety of methods may be used to distinguish between the bubbly and churn turbulent flow regimes. Wall pressure fluctuations have been used quite extensively in gas-solid fluidized beds, but only a few reports have used this technique in bubble columns. Pressure fluctuations and overall gas hold-up are examined for distinguishing flow regime boundaries.

---

6. This section is not included in the original manuscript. It merely serves as a transition between papers for the thesis.

Dynamic gas disengagement (DGD) is a technique which has been used to determine large and small bubble hold-ups. Theoretical disengagement curves calculated using the convective model proposed in Chapters II and III are compared to DGD data.

A kinetic model which unifies the treatment of the bubbly and churn turbulent flow regimes is proposed. The model is capable of demarcating the transition between the flow regimes, as well as determining overall gas hold-up in the bubbly flow regime and the fraction of the gas hold-up in the form of large bubbles in the churn turbulent flow regime.

4.2 Abstract

Bubble column hydrodynamics exhibit a bubbly flow regime at low superficial gas velocity and a churn turbulent regime at higher superficial gas velocity, except in small diameter columns where slugging is observed. A convective model developed previously (Hyndman and Guy, 1995a) is compared to dynamic gas disengagement (DGD) data. Theoretical disengagement curves calculated from the convective model bubble velocity distribution (at steady-state) compare well to DGD curves at the transition point. Our analysis of DGD curves using the convective model indicates that in the churn turbulent regime, gas hold-up consists of a superposition of large bubbles on a transition point bubble velocity distribution. A kinetic model for gas phase hydrodynamics capable of describing both the bubbly and churn turbulent flow regimes is proposed. Absolute bubble velocity distributions are calculated based on an ideal bubble velocity distribution and rules of bubble-bubble interaction. In the bubbly flow regime, overall gas hold-up is calculated, while in the churn turbulent flow regime the fraction of gas hold-up in the form of large bubbles is determined by the model. The model is in good agreement with experiment in both flow regimes.

4.3 Introduction

The hydrodynamic behaviour of multiphase reactors is strongly dependent on the flow regime. Bubble columns are commonly known to operate in the bubbly flow regime at low superficial velocity and in the churn turbulent or slugging flow regime at high superficial gas velocity. Slugging is observed only in laboratory columns of small diameter, while the churn turbulent regime is observed in larger diameter and industrial-sized columns. The bubbly flow regime is characterized by small bubbles with relatively gentle mixing in the column. By contrast, the churn turbulent flow regime is characterized by vigorous mixing and a range of bubble sizes. Larger bubbles rise quickly through the dispersion in complex patterns entraining smaller bubbles and liquid in their wake. Bubbles also tend to rise in clusters through the column. Flow regimes have been further subdivided into dispersed bubble flow regime at very low superficial velocities (superficial velocities less than 0.021 m/s for a semi-batch bubble column, D_c = 0.102 m) a vortical spiral flow regime (for superficial gas velocities from 0.021 m/s to 0.049 m/s) followed by turbulent flow (Chen et al., 1994). Vortical-spiral flow has a unique flow pattern, but nevertheless represents a gradual transition from bubbly to churn turbulent flow.

In modelling this complex behaviour, simplifications must be made. Studies on liquid phase behaviour have generally concluded that the liquid velocity has a maximum upward

velocity at the centre of the column. A minimum (or maximum downward) velocity occurs near the column wall (see for example Ueyama and Miyauchi, 1979; Franz et al., 1984). Absolute bubble velocities (i.e. relative to the column wall) are a combination of the relative bubble velocity which is related to bubble size and the continuous or liquid phase velocity.

For describing gas phase behaviour, the axial dispersion model has been popular and correlations exist in the literature to calculate the axial dispersion coefficient based on operating conditions and geometric parameters (Deckwer, 1993; Fan, 1989). Given the heterogeneity observed in the churn turbulent regime because of the existence of a range of bubble sizes and the vigorous mixing of the liquid phase, the assumption of a single average gas velocity and dispersion coefficient is quite far from the observed reality. Researchers have proposed bimodal axial dispersion models and two-bubble-class models for the churn turbulent regime (Kawagoe et al., 1989; Shah et al., 1985; Shetty et al., 1992). These models assume bimodal average gas velocities to represent the small and large bubble phases. Kawagoe et al. (1989) assumed a unique average velocity and a unique dispersion coefficient for each bubble group. By contrast Shah et al. (1985) and Shetty et al. (1992) have assumed that the large bubble phase travels in plug flow. Molerus and Kurtin (1986b) have proposed a core-annulus model for the churn turbulent regime which assumes that large bubbles rise only in the core region. In a previous contribution (Hyndman and Guy, 1995a), we examined the axial dispersion model using

residence time distribution (RTD) data and showed its inapplicability for a bubble column operating in the churn turbulent regime. Instead of the bimodal axial dispersion models mentioned above, a fully convective model was developed which enables the determination of an absolute bubble velocity distribution. An interesting hydrodynamic model for bubble column reactors has been proposed by Iordache and Jinescu (1986) to explain gas phase behaviour using a kinetic theory approach. Their model is also a convective model based upon an absolute bubble rise velocity distribution. The elegance of the model is that a single equation describes gas phase flow in both the bubbly and churn turbulent flow regimes. Bubble-bubble interactions described by the model infer a transition point and the existence of a large bubble phase in the heterogeneous flow regime.

Krishna et al. (1993) have used analogous behaviours between gas-liquid bubble columns and gas-solid fluidized beds to describe gas hold-up in bubble columns in terms of small and large bubble phases. Their description is based on the transition velocity from bubbly to churn turbulent flow. In order to understand hydrodynamics of bubble columns, knowledge about the transition from bubbly to churn turbulent flow is key. While visual observation may be possible in transparent laboratory columns, researchers are focusing on other methods which may also be used in an industrial context. The dependence of gas hold-up on superficial velocity is expressed as $\epsilon_o \sim U_o^B$ (Deckwer, 1992). Since the exponent n is dependent on the flow regime, the transition point can be described as the

intersection of the equations in the bubbly and churn turbulent flow regime. Wallis (1969) outlined a procedure to determine flow regime changes using drift flux as a function of gas hold-up. A change in slope indicated a flow regime change. Krishna et al. (1991) have used a plot of average bubble swarm velocity versus superficial gas velocity. Since the swarm velocity is essentially invariant in the bubbly flow regime and increases with superficial gas velocity in the churn turbulent flow regime, the transition point may be determined as the point where average swarm velocity starts to increase. They have used the intersection of two fitted straight lines to demarcate the transition superficial velocity (U_{tran}). Thimmapuram et al. (1992) have examined statistical functions including the variance, autocorrelation function and power spectral density function of temperature-history records of a heat transfer probe to distinguish flow regimes in a bubble column. In gas-solid reactors, much emphasis has been placed on the change in the character of pressure fluctuations in the transition from a bubbling to a turbulent fluidized bed (Bi and Grace, 1995; Brereton and Grace, 1992; Chehbouni et al., 1994). Pressure fluctuations have also been used to examine flow regime transition in gas-liquid-solid fluidized beds (Fan et al., 1986; Nishiyama et al., 1989; Yashima et al., 1992). Drahoš and Čermák (1989) have reviewed various methods, including pressure fluctuations, for distinguishing flow regimes in gas-liquid flow. More recently statistical characteristics (Drahoš et al., 1991) and fractals (Drahoš et al., 1992) have been used to analyze pressure fluctuation data to characterize flow regimes in bubble columns.

All two-bubble-group models for the churn turbulent flow regime require a knowledge of the small and large bubble fractions of the gas hold-up. Generally these have been obtained by a procedure known as dynamic gas disengagement (DGD) which involves following dispersion height in the column after the gas feed has been shut off (Sriram and Mann, 1977). Most reports involve experimental procedures requiring a transparent column or manometers and time consuming analysis of video tape to follow the decline in dispersion height with time. Lee et al. (1985) developed a digital sensor with a wooden buoy that floats on the top of the gas-liquid mixture. This method has the advantage of directly recording dispersion height versus time data, but would be difficult to implement at high pressure and temperature. Daly et al. (1992) have proposed the use of a pressure transducer connected just below the clear liquid height to follow a DGD experiment. Their method is easily implemented with standard equipment, automates data acquisition, does not require a transparent column and may be used at high pressure and temperature.

In the present paper the transition from bubbly to churn turbulent flow in a bubble column is examined using steady-state hold-up data and pressure fluctuation data. DGD experiments have also been performed in both flow regimes. DGD is used to calculate small and large bubble hold-ups in the churn turbulent flow regime. Simple equations proposed by Krishna et al. (1994) are used to calculate bimodal bubble velocities. The gas behaviour in churn turbulent flow is examined in terms of a superposition of large,

fast bubbles upon small bubbles. Finally, a hydrodynamic model based on kinetic theory is proposed to describe both the bubbly and churn turbulent flow regimes.

4.4 Experimental method

An acrylic bubble column with an inside diameter of 0.2 m and a height of 1.9 m has been used for dynamic gas disengagement experiments (Figure 4.1). The distributor is a perforated plate with 69, 1-mm diameter orifices arranged in a square pattern. Orifice spacing is 20.5 mm centre to centre. Two rotameters are used to control gas flow: one is used to control filtered process air from a central supply system; the other simultaneously allows gas from a pressurized gas cylinder to be fed to the bubble column. A mercury filled manometer is used to measure the pressure at the rotameters. Two vented gauge pressure transducers (Lucas Schaevitz, Pennsauken, NJ, P3061 100"WG (P_d) and 20"WG (P)) are used to measure pressure in the column. P_d is the pressure in the chamber under the perforated plate distributor. The pressure transducer which is used to follow the progress of gas disengagement is connected to the column (at h_{PT}) a few centimetres below the non-aerated liquid height (h_{nae}). A solenoid valve (8210G34 Ascolectric Ltd., Brantford, ONT) located just before the distributor chamber (Figure 4.1) is used to rapidly close the gas feed for disengagement experiments. A Labview (Version 3.1, National Instruments, Austin, TX) virtual instrument controls the data acquisition and the closing of the solenoid valve.

Experiments are conducted in semi-batch mode with a water level of 1.4 m (h_{PT}= 1.37 m). (Some experiments at superficial velocities exceeding 0.11 m/s were performed

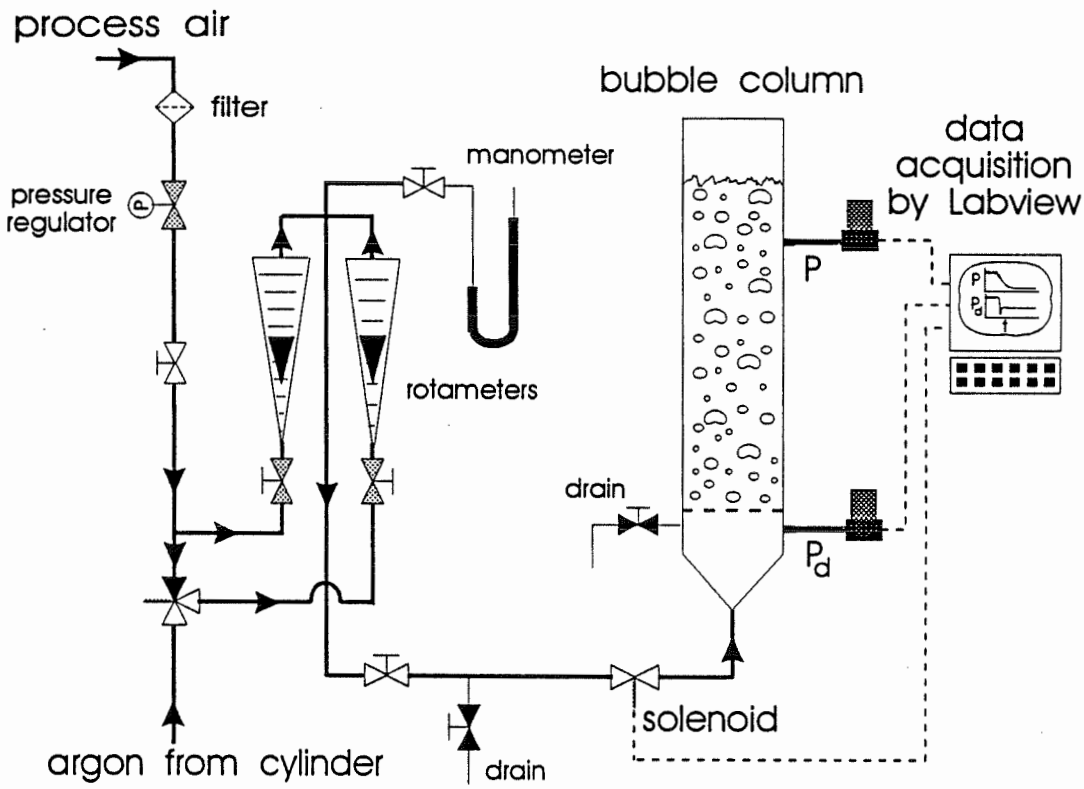

Figure 4.1: Experimental set-up.

with a water level of 1.3 m (h_{PT}= 1.26 m). During subsequent experiments, at high U_O a 1.4 m water level was maintained. Because the height to diameter ratio was sufficiently high, H_{nae} did not affect the results.) An air-argon-water system (with a fixed ratio of 3.3:1.0 air to argon) is used to replicate conditions in residence time distribution (RTD) experiments (refer to Hyndman and Guy, 1995a for details of RTD experiments). An air-water system is used for all other experiments. Once operating conditions are set, an equilibration period of 5 minutes is allowed before commencing an experiment. Measurements for the superficial velocity (mercury manometer, rotameters) are taken just before starting an experiment. Data acquisition is carried out at a scan rate of 100 Hz for all dynamic gas disengagement (DGD) experiments. For each experiment P_d and P are recorded continuously for a period including 10 s before closing the solenoid valve and 40 s afterwards (for some experiments 40 s of data was recorded before closing the valve).

Immediately following the disengagement experiment, the non-aerated pressure (P_{nae}) and water temperature are measured. Overall instantaneous gas hold-up in the column below the connection point for the pressure transducer may be calculated: the volume of gas below h_{PT} is the same as the equivalent difference in height of clear liquid above h_{PT}.

$$\epsilon = \frac{h - h_{nae}}{h_{PT}} = \frac{P - P_{nae}}{\rho g h_{PT}} \tag{4.1}$$

As Equation 4.1 indicates, the calculated gas hold-up is sensitive to P_{nae} ($=\rho g h_{nae}$). Measurement of P_{nae} immediately following each gas disengagement ensures that calculations are accurate since there is negligible change in h_{nae} as a result of evaporation during disengagement. Superficial velocities ranging from 0.019 to 0.154 m/s are examined.

4.5 Transition from Bubbly to Churn Turbulent Flow

The transition from bubbly to churn turbulent flow in a bubble column with increasing superficial gas velocity is in reality a gradual process. However, when modelling the complex hydrodynamics of bubble columns the simplification of the gradual process by defining a transition point is useful for modelling the hydrodynamic behaviour.

Transition velocities between bubbly and churn turbulent flow regimes (U_{tran}) have been determined by Krishna et al. (1991) using a plot of interstitial gas velocity U_o/ϵ_o versus superficial gas velocity. Using their method for our air-water experiments, we find U_{tran}=0.0375 m/s and ϵ_{tran}=0.137 (Figure 4.2). U_o/ϵ_o deviates from a straight line at higher superficial gas velocity. However, Krishna et al. (1991) did not plot any points beyond U_{tran}+0.06 m/s. Deviation from a straight line shown in Figure 4.2 occurs just beyond that point. Their method is useful since it clearly defines a transition point between the two flow regimes. The transition point determined in Figure 4.2 will be used in all subsequent analyses presented here.

Pressure fluctuations have been used in gas-solid, gas-liquid and gas-liquid-solid reactors to distinguish between flow regimes (Bi and Grace, 1995; Brereton and Grace, 1992; Chehbouni et al., 1994; Drahos et al., 1991 and 1992; Fan et al. 1986; Nishiyama et al., 1989; Yashima et al., 1992). Brereton and Grace (1992) recommend using the

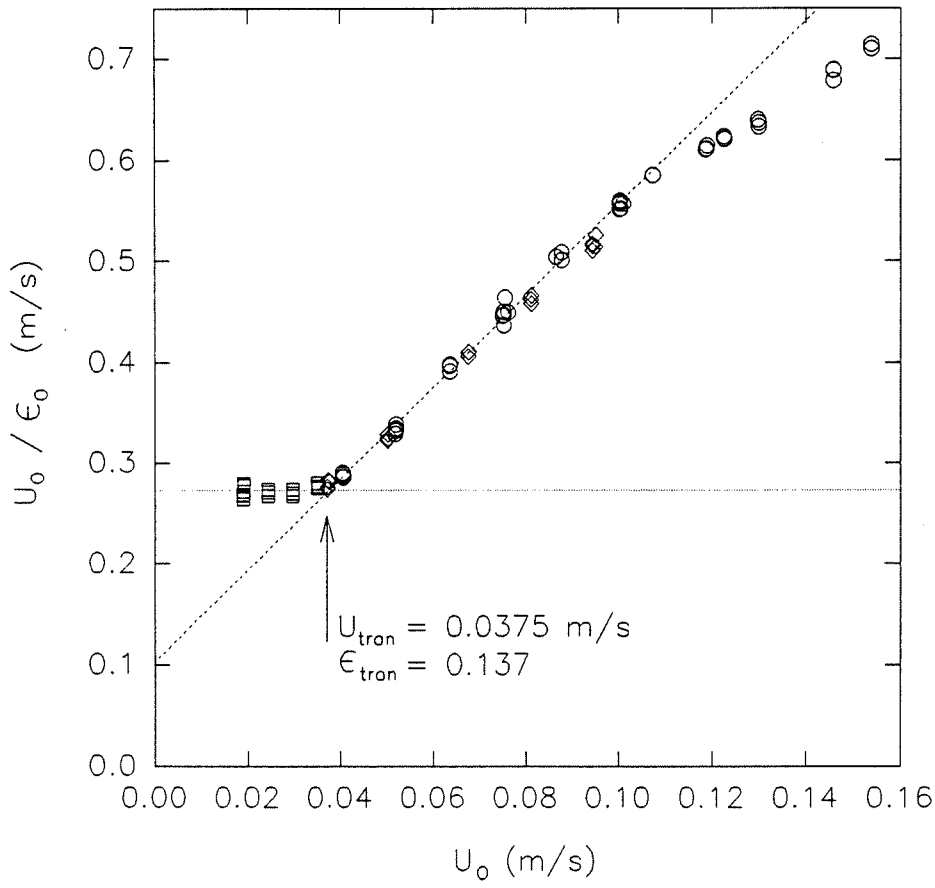

Figure 4.2: Interstitial gas velocity (U_o/ϵ_o) versus superficial gas velocity (bubbly flow regime □ ; churn turbulent flow regime ○; air/argon mixture ◇; average velocity in bubbly flow ·····; regression in churn turbulent flow up to U_o = 0.107 m/s ------).

normalized standard deviation of the pressure fluctuations recorded by a differential pressure transducer. For gas-solid fluidized beds they recommend placing the lower pressure tap less than two column diameters above the distributor plate. Chehbouni et al. (1995) however recommend the use of absolute pressure transducers for analysis of pressure fluctuations. The present analysis has been done using vented gauge (i.e. absolute) pressure transducers. Because there is no agreement yet as to the preferred data analysis method both standard deviation ($\sigma_{\epsilon o}$) and normalized standard deviation ($\sigma_{\epsilon o}/\epsilon_O$) of the gas hold-up are shown in Figure 4.3 as a function of superficial gas velocity. Fluctuations in ϵ during steady-state operation are directly proportional to pressure fluctuations (Equation 4.1). Standard deviation is relatively invariant in the bubbly flow regime and increases linearly with superficial velocity in the churn turbulent flow regime. Note that this is in contradiction with results presented by Drahos et al. (1991). They were unable to distinguish flow regimes using standard deviation of pressure fluctuations. In our system, the transition point determined by the standard deviation or normalized standard deviation is slightly lower but generally confirms the transition point from Figure 4.2.

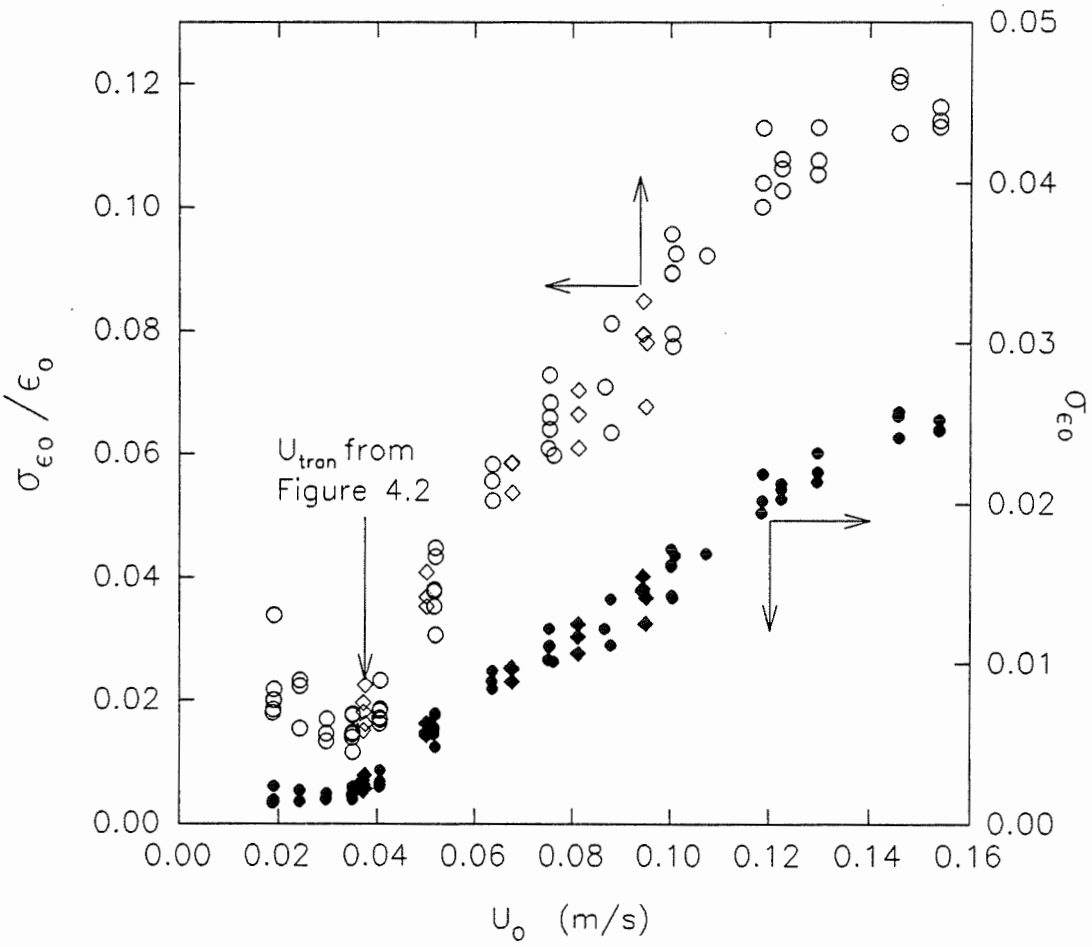

Figure 4.3: Normalized standard deviation and standard deviation of fluctuations in instantaneously measured gas hold-up (ϵ) as a function of superficial gas velocity (air ○ ●; air/argon mixture ◇ ◆; open symbols are normalized standard deviation filled symbols are standard deviation).

4.6 Dynamic Gas Disengagement

The experimental technique of dynamic gas disengagement experiments developed by Sriram and Mann (1977) has typically involved following the decline in dispersion height with time (Vermeer and Krishna, 1981; Schumpe and Grund, 1986; Patel et al., 1989). Daly et al. (1992) have instead used a pressure tap located just below the non-aerated liquid height to follow the evolution of the gas disengaging from the column after the gas supply has been suddenly switched off. A typical disengagement profile for the churn turbulent regime using their technique is shown in Figure 4.4. The solenoid valve on the gas supply was closed at time t=0. Equation 4.1 is used to transform the pressure data to overall hold-up in the section of the column below the pressure tap. As shown in Figure 4.4, hold-up data have the same form as pressure data. In the churn turbulent regime, two distinct phases to the disengagement are observed. During Phase I the large bubbles are evacuated from the column and large oscillations are observed in the pressure profile. Mixing in the upper part of the column resembles that seen at steady-state then gradually undergoes what could be described as a flow regime change to bubbly flow. Phase II of the disengagement is characterized by a linear descent in pressure and hold-up below h_{PT}. Small, slower-moving bubbles (some of which disengage simultaneously with the larger, faster-moving bubbles in Phase I) continue to move up the column in a more orderly fashion during Phase II. No large bubbles are present during Phase II, as can be attested by the disappearance of large oscillations.

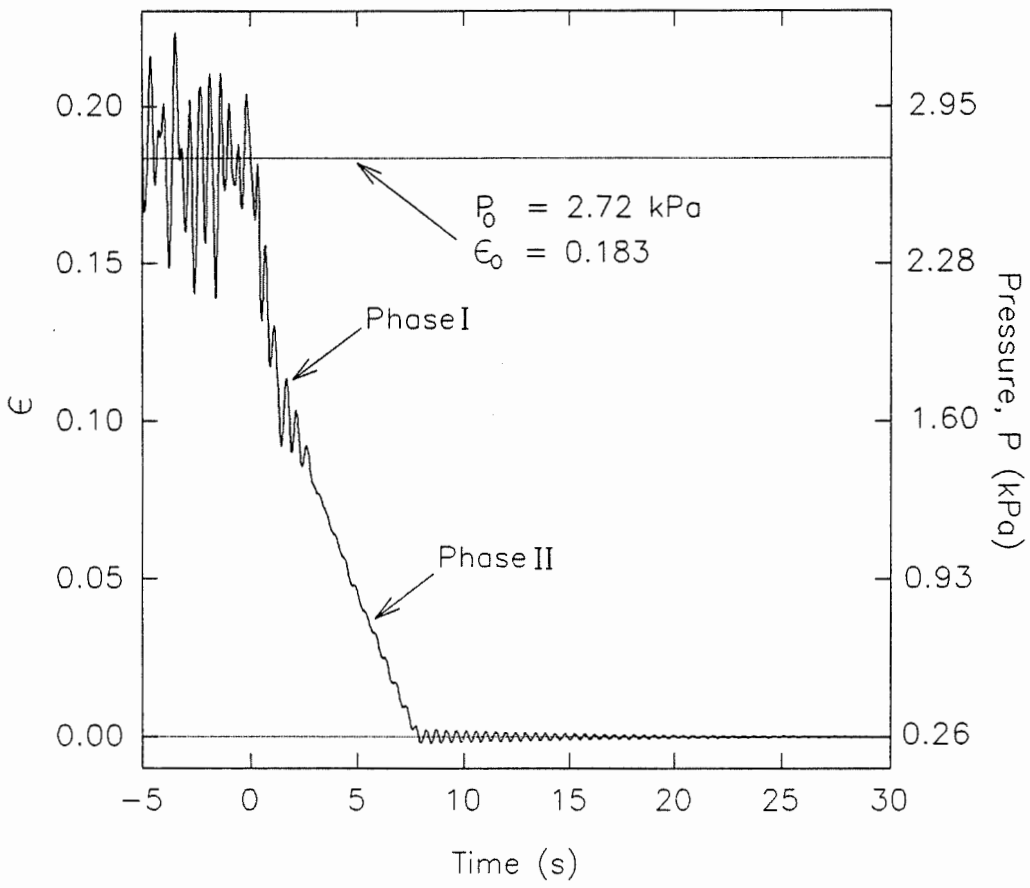

Figure 4.4: Instantaneous gas hold-up and pressure versus time for a typical disengagement experiment in the churn turbulent regime (U_o = 0.107 m/s).

Smaller oscillations which gradually decrease in amplitude after Phase II of the disengagement are due to waves in the water level and not to more bubbles leaving the column. Oscillations in the height of the water observed visually at the pressure tap connection, matched well with oscillation height calculated from the pressure data ($h=P/\rho g$).

The evolution of pressure in the distributor chamber during the same DGD experiment, as shown in Figure 4.4, is presented in Figure 4.5. Visual observation indicated gas feed leaving the distributor plate is interrupted immediately when the air supply is shut off. The sudden drop of P_d below the equilibrium ($\rho g H_{nae}$) pressure shown in Figure 4.5 confirms visual observations. Small groups of 5 to 10 bubbles occasionally left the distributor causing P_d to dip slightly (for example at approximately 5 and 20 seconds in Figure 4.5). Not enough gas volume was added by these bubbles to adversely affect the disengagement experiment. The release of small groups of bubbles may be due to imperfect sealing of the solenoid valve since they were more frequent for experiments at higher superficial gas velocity (and higher shut-off pressure).

DGD profiles with gas hold-up normalized to steady-state hold-up (ϵ_o) for air-water experiments at three superficial gas velocities are shown together in Figure 4.6. The experiment at a superficial velocity of 0.035 m/s is just below the transition velocity and

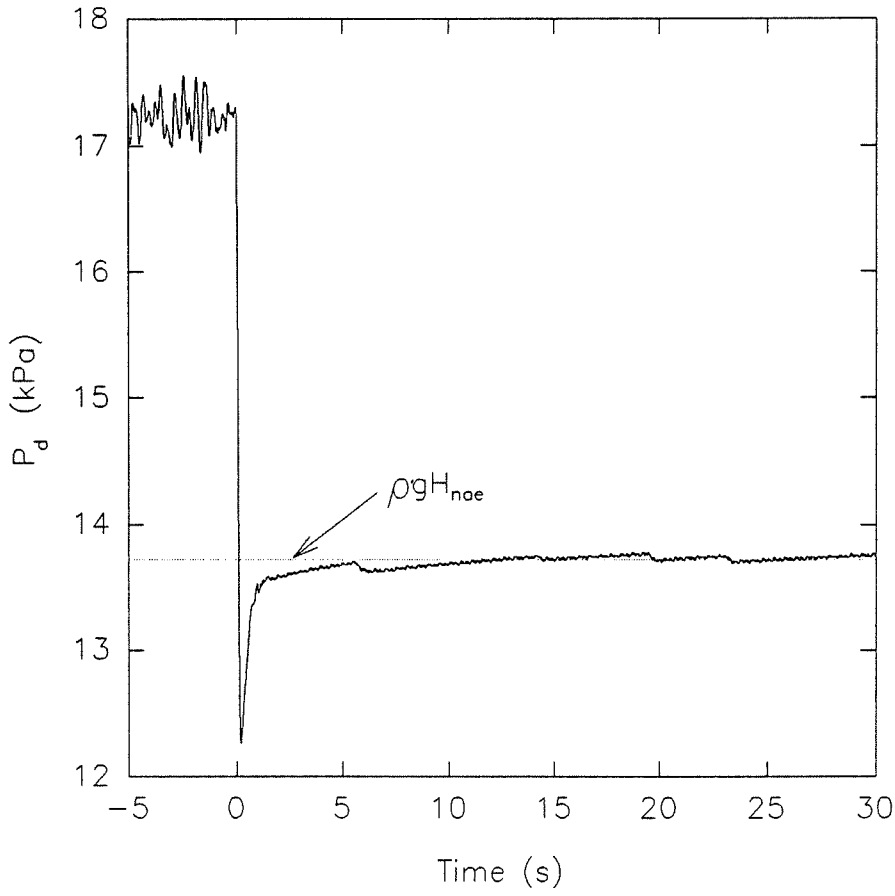

Figure 4.5: Pressure in the distributor chamber (P_d) versus time.

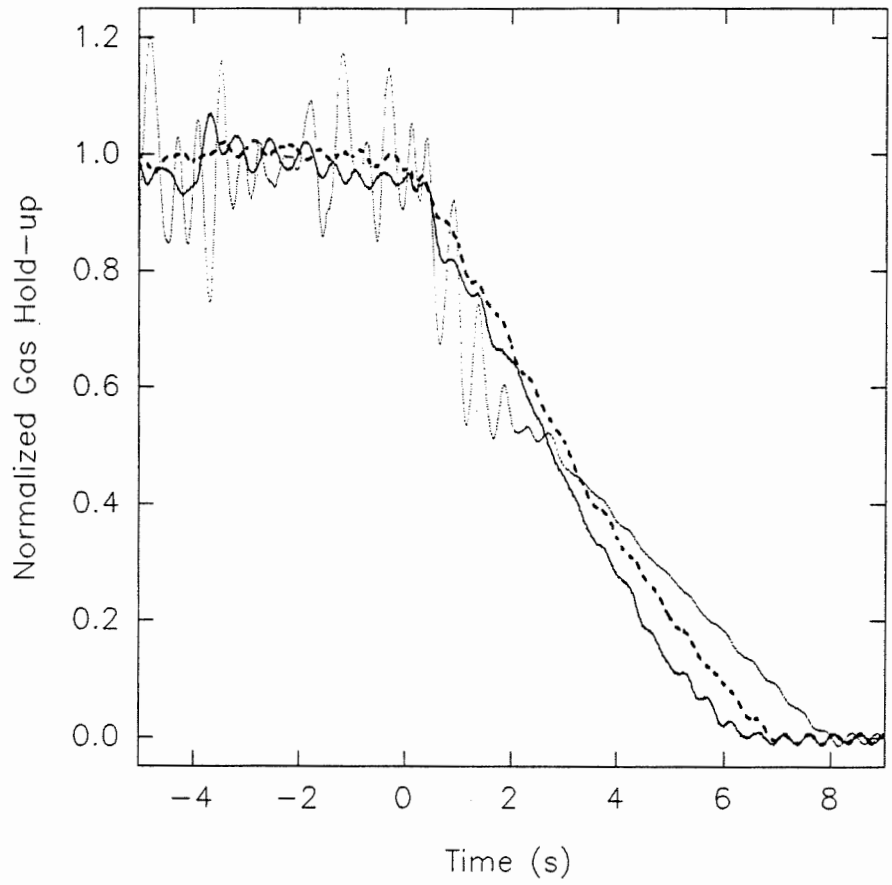

Figure 4.6: Dynamic gas disengagement profiles, normalized gas hold-up (ϵ/ϵ_o) versus time (bubbly flow regime U_o = 0.019 m/s —— ; bubbly flow regime close to the transition velocity U_o = 0.035 m/s ----; churn turbulent flow regime U_o = 0.101 m/s ·····).

has a similar concave upward form to the experiment at a superficial velocity of 0.019 m/s. The disengagement for the churn turbulent flow regime (0.101 m/s) clearly displays Phases I and II. Figure 4.6 also illustrates that normalized pressure fluctuations are larger in the churn turbulent regime; numerical results ($\sigma_{\epsilon o}/\epsilon_O$) were presented in Figure 4.3. Slopes on normalized plots differ from ϵ versus time plots by ϵ_O.

Fitting a straight line to the small bubble (or Phase II) portion of a DGD profile and a straight line to the entire DGD profile in the bubbly flow regime reveals a marked change in slope at the transition point (Figure 4.7). Linear regression (on an ϵ versus t plot) in the bubbly flow regime has been forced through the known intercept, ϵ_O. A simple linear regression is used to fit the Phase II portion of churn turbulent DGD profiles. The slope in Phase II of the disengagement is invariant, whereas in the bubbly flow regime the steepness of the profile increases with superficial gas velocity. The invariance of the Phase II slopes indicates that the small bubble hold-up and the behaviour of small bubbles in the churn turbulent regime do not change significantly with superficial gas velocity.

Assuming that the gas does not expand substantially over the height of the column, a volume balance may be performed for each phase of the disengagement in churn turbulent flow. Dividing each term in the volume balance by the cross-sectional area of the column the following expression is obtained for Phase I.

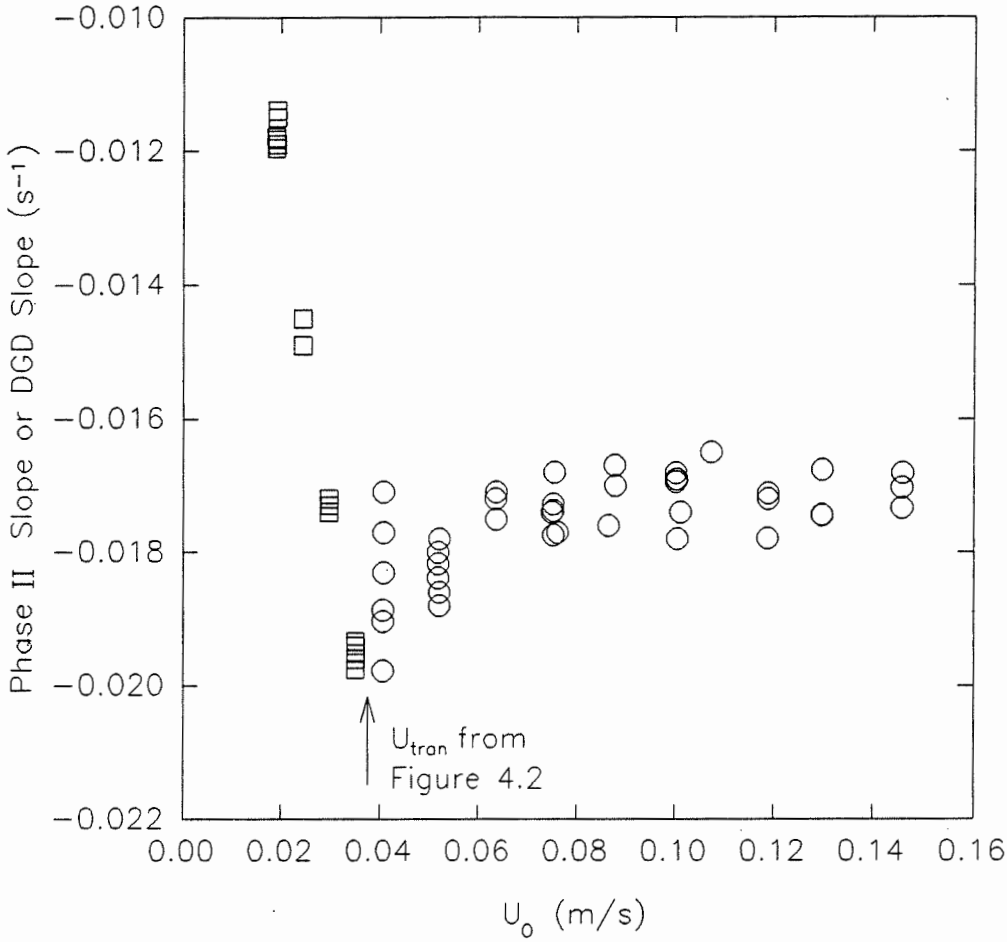

Figure 4.7: Slope of DGD profile (Phase II only for churn turbulent flow) versus superficial gas velocity (regression forced through ϵ_0□ ; Phase II regression ○).

$$h_I = h_o - U_o t \tag{4.2}$$

In developing the above equation we have followed a procedure similar to that of Daly et al. (1992) but have incorporated the knowledge that the superficial gas velocity of bubbles leaving during Phase I is the same as during steady-state operation (Schumpe and Grund, 1986; Vermeer and Krishna, 1981). In terms of pressure this equation becomes

$$P_I = P_o - \frac{U_o \rho g}{1000} t \tag{4.3}$$

If instead the equation is expressed in terms of instantaneous hold-up as defined by Equation 4.1

$$\epsilon_I = \epsilon_O - \frac{U_o}{h_{PT}} t \tag{4.4}$$

Assuming that the small bubbles leave the column at a constant rate throughout the disengagement process (Phases I and II), a similar expression may be developed for Phase II.

$$\epsilon_{II} = \epsilon_{Os} - \frac{U_{Os}}{h_{PT}} t \tag{4.5}$$

Equation 4.5 indicates that the small bubble hold-up (ϵ_{Os}) may be directly read from a plot of ϵ versus t as the intercept of the Phase II regression line. Large bubble hold-up is therefore simply calculated as follows.

$$\epsilon_{OL} = \epsilon_O - \epsilon_{Os} \tag{4.6}$$

Small and large bubble hold-ups are calculated here based on the reactor volume below the pressure tap. Total hold-up and small bubble hold-up determined by the Phase II intercept are shown in Figure 4.8. The value of ϵ_{Os} remains approximately constant and close to the value of ϵ_{tran} determined in Figure 4.2.

Using the following simplified equations (Krishna et al., 1994), small and large bubble velocities may be calculated.

$$u_{bs} = \frac{U_{tran}}{\epsilon_{tran}} \tag{4.7}$$

$$u_{bL} = \frac{U_g - U_{tran}}{\epsilon_O - \epsilon_{tran}} \tag{4.8}$$

The resulting values for u_{bs} and u_{bL} are shown in Figure 4.9 along with air-water data from Schumpe and Grund (1986)(cf. their Figure 7; D_c = 0.3 m) and from Grund et al. (1992)(cf. their Figure 3; D_c = 0.15 m). As a consequence of Equation 4.7 u_{bs} is a constant; despite this simplified approach, u_{bs} concurs with values determined by Schumpe and Grund (1986) and Grund et al. (1992) using their more complicated iterative procedure. Absolute bubble rise velocities of large bubbles calculated using Equation 4.8 compare well with data from Schumpe and Grund (1986) in the 0.3 m

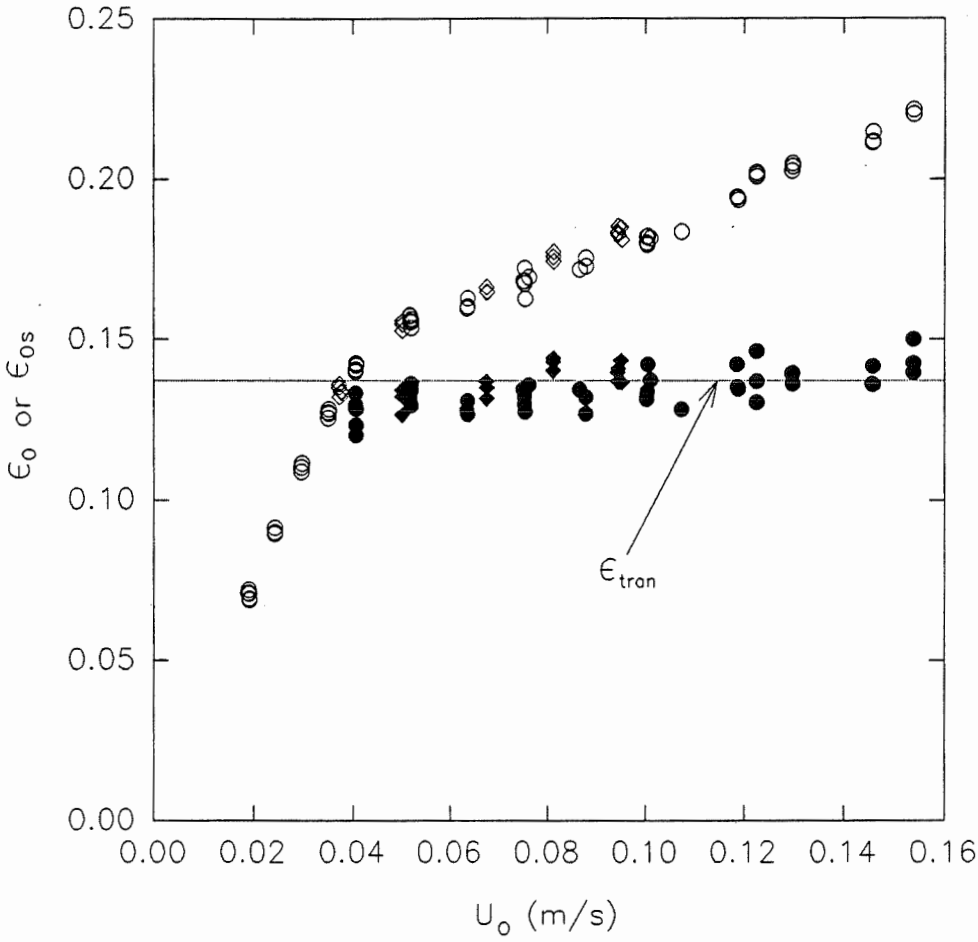

Figure 4.8: Total gas hold-up (open symbols) and small bubble hold-up from the Phase II intercept (filled symbols) (air ○ ●; air/argon mixture ◇ ◆).

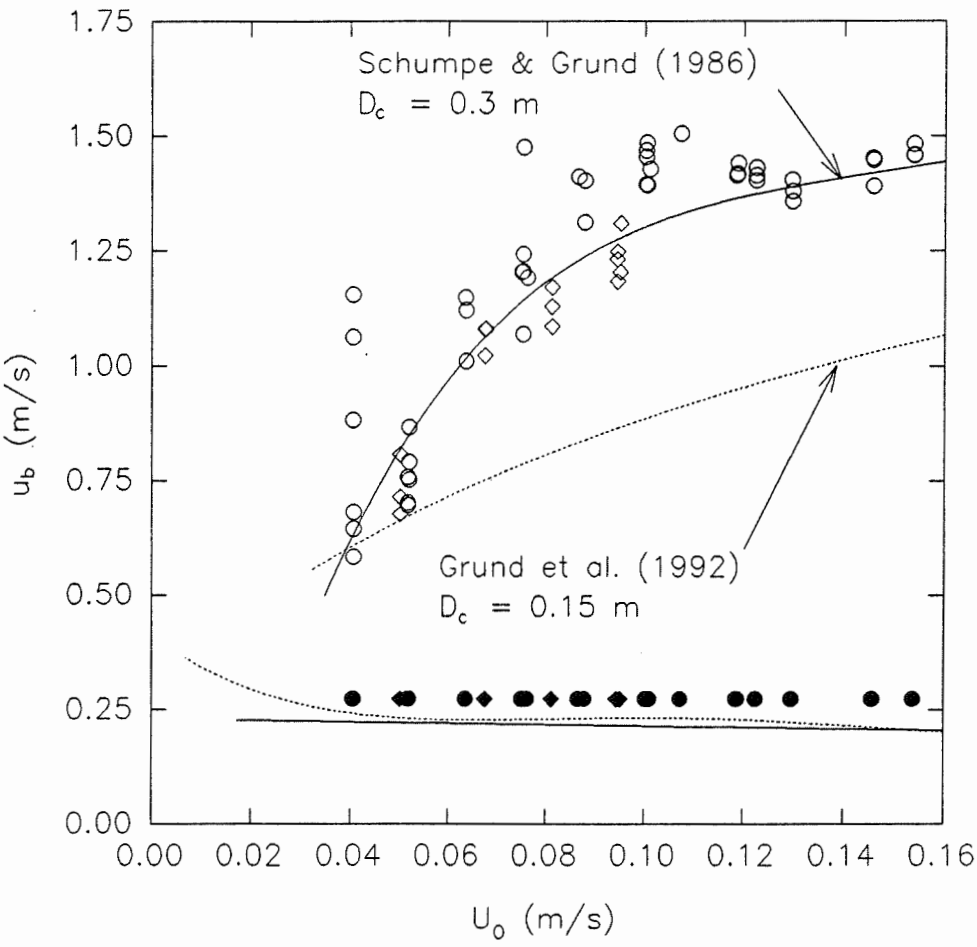

Figure 4.9: Large bubble velocity and small bubble velocity as calculated using Equations 4.7 and 4.8 (same symbols as Figure 4.8) (air-water data from Grund et al., 1992; Schumpe and Grund, 1986).

diameter column. Perhaps the dependence of u_{bL} on column diameter is more important with columns smaller that 0.2 m in diameter. The deviation from a straight line seen in Figure 4.2 may be explained by u_{bL} levelling off at higher superficial velocity (see Figure 4.9 and Equation 4.8).

It can then be concluded that the total gas hold-up in a bubble column in the churn turbulent regime is composed of two components: large, fast bubbles and small, slow bubbles. The contribution of small bubbles in the churn turbulent regime appears to be constant and equal to the transition hold-up. Large bubble velocities may be essentially scale independent for bubble columns 0.2 m in diameter and larger.

4.6.1 Convective Flow of Bubbles and Dynamic Gas Disengagement

Bubble velocity distributions calculated using the convective model proposed by Hyndman and Guy (1995a and 1995b) are a combination of the velocity distributions for liquid and relative bubble velocities. The volume distribution function of bubbles having a velocity w was assumed to be log-normal.

$$f(w) = \frac{1}{\beta w\sqrt{2\pi}}\exp[-\frac{(\ln w-\alpha)^2}{2\beta^2}] \qquad (4.9)$$

The mode of this distribution is e^{α} and β is an indication of its skewness. The distribution was discretized and normalized to have an area of one between cutoff points w_{min} and

w_{max}.

Bubbles having a single rise velocity have linear disengagement curves with the slope depending on the bubble rise velocity, assuming the liquid velocity does not markedly decrease during disengagement. Therefore, for each velocity on the distribution curve, the theoretical disengagement curve would be a straight line.

Since the distribution is discretized it may be treated as a histogram. The fraction of the normalized gas hold-up remaining in the column below h_{PT} at time t which rises at velocity w_m (midpoint of a histogram interval from w_i to w_{i+1}) is calculated as follows.

$$x_m(t) = f(w_m)(w_{i+1} - w_i) = f(w_m)\Delta w_m \qquad for\ t \leq t_o$$

$$x_m(t) = f(w_m)\Delta w_m\left(1 - \frac{w_m}{h_{PT}}t\right) \qquad for\ t_o < t < t_{PT,m} \qquad (4.10)$$

$$x_m(t) = 0 \qquad for\ t \geq t_{PT,m} = \frac{h_{PT}}{w_m}$$

$t_{PT,m}$ is the time at which there will be no more gas travelling at w_m below h_{PT}. Negative values for $x_m(t)$ are not permissable; zero is assigned to $x_m(t)$ for times greater than $t_{PT,m}$. Theoretical disengagement curves for the entire bubble velocity distribution are calculated by summing x_m at each time t until the normalized gas hold-up is zero.

$$x(t) = \sum x_m(t) \qquad (4.11)$$

No gas will remain in the column below h_{PT} at $t_{PT,max} = h_{PT}/w_{m,min}$. These calculations assume that the disengagement of slower velocity bubbles is not hindered by the faster velocity bubbles or by the waterfall effect, and that the liquid velocity remains the same during the dynamic disengagement as during the steady-state RTD measurements. The disengagement profile is scaled to ϵ by multiplying by ϵ_o.

Velocity distributions have been calculated using the correlations presented in a previous publication (Hyndman and Guy, 1995b) with the same 10^{-4} tolerance on f(w) for w_{min} and w_{max} proposed in Hyndman and Guy (1995a). These correlations were developed from data at superficial velocities from 0.037 to 0.095 m/s. The correlations could not be extrapolated to superficial velocities lower than the transition velocity (0.037 m/s) because the flow regime changes.

In Figure 4.10, the disengagement profile calculated using Equations 4.9 to 4.11 is compared to an air-argon-water experiment performed at the transition point (U_o = 0.0376 m/s). Also shown on Figure 4.10 is a linear regression through ϵ_o: slopes of the linear regression were presented in Figure 4.7. The disengagement calculated using the convective model describes the experimental disengagement well. The good fit indicates that the upper part of the column where disengagement is occurring behaves as if it were operating at steady-state. Since the absolute bubble velocity couples the relative bubble velocity with local liquid velocity, dynamic gas disengagement does not greatly affect the

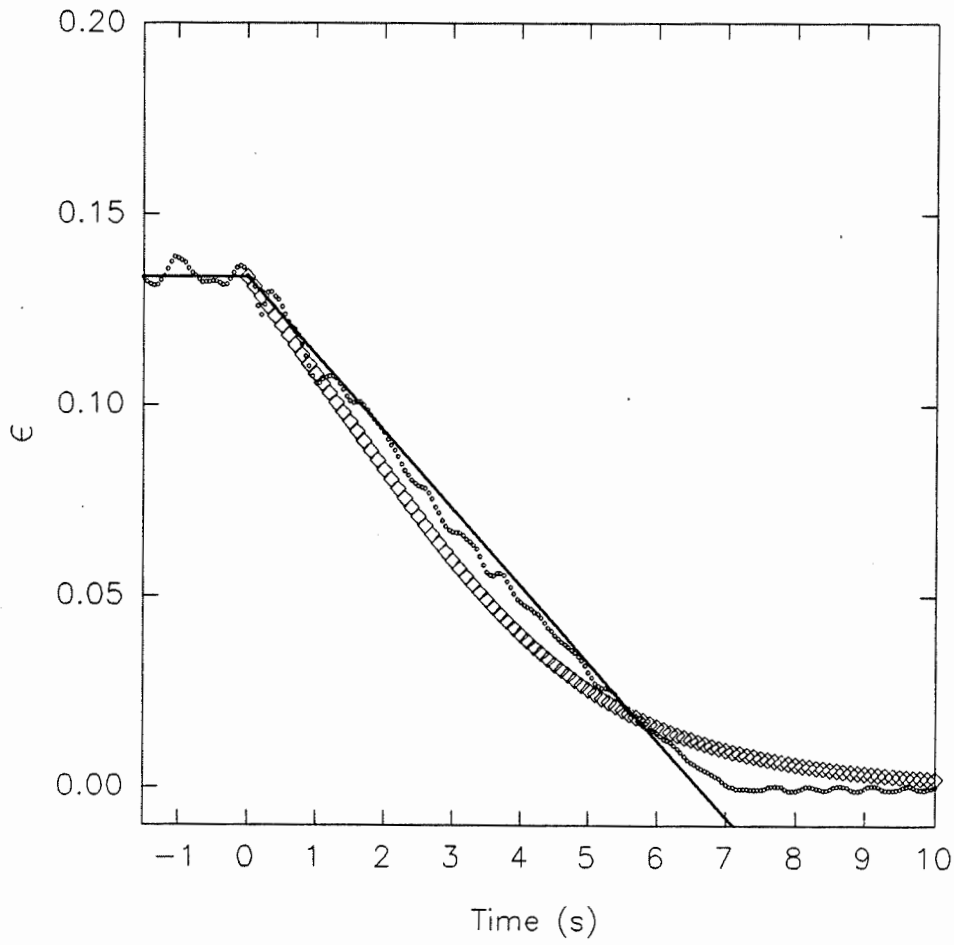

Figure 4.10: Transition point DGD experiment (U_o = 0.0376 m/s, ϵ_o = 0.1335) compared to convective model theoretical disengagement (α = -1.4 and β = 0.43) (DGD data ○, 1/5 of points shown for clarity; convective model ◇; regression through ϵ_o ——).

liquid velocity profile imposed upon bubbles in the upper portion of the column which still contains a gas-liquid mixture.

Above the transition point, the model calculations at the steady-state superficial velocity, U_O, predict a much faster disengagement than experimental values (see Figure 4.11). The convective model follows the Phase I disengagement described by Equation 4.4 much longer than does the experimental data. The convective model disengagement is based upon steady-state operation and similarly Equations 4.2 to 4.4 assume that during Phase I of a churn turbulent disengagement experiment, gas leaves the column at the same rate as during steady-state. In the churn turbulent regime, the overall gas hold-up during steady-state is composed of a superposition of a large bubble fraction on a small bubble fraction (ϵ_{Os}). In Figure 4.8, ϵ_{Os} is shown to be approximately constant and equal to the steady-state gas hold-up at the transition point. In Figure 4.11, Phase II of the DGD experiment is compared to a theoretical disengagement calculated at the transition point (U_{tran} = 0.0375 m/s, α = -1.4, β = 0.43).

The starting point for the transition model disengagement profile in Figure 4.11 is where the Phase I line (Equation 4.4 or equivalently the model calculation at U_O) descends to the transition hold-up (ϵ_{tran}). The gas hold-up presented in the disengagement profiles is the hold-up referenced to the reactor volume below h_{PT}. Since bubbles disengage from the bottom up, there is a portion of the column height during disengagement occupied

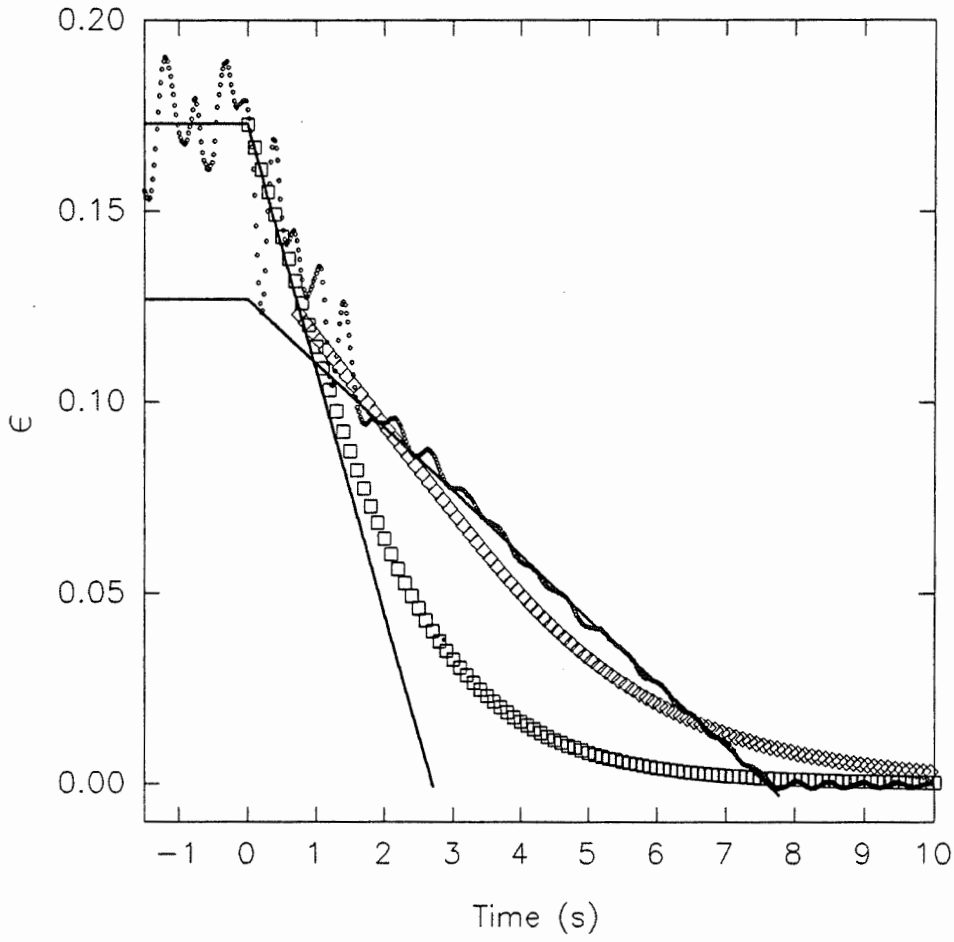

Figure 4.11: Churn turbulent DGD experiment (U_o = 0.0878 m/s, ϵ_o = 0.173) compared to convective model theoretical disengagement (α = -0.89 and β = 0.50) and theoretical disengagement at the transition point (U_o = 0.0375 m/s, α = -1.4 and β = 0.43) (DGD data ○, 1/2 of points shown for clarity; model□ ; transition model ◇; Equations 4.4 and 4.5 are shown as fine lines).

only by liquid ($h_{PT,l}$). Convective model disengagement calculations are based upon starting at steady-state operation when there is gas throughout the column. To compare the Phase II portion of a churn turbulent disengagement to a theoretical disengagement at the transition velocity, the transition hold-up (ϵ_{tran}) is matched to ϵ corrected for $h_{PT,l}$. The same type of correction for the clear liquid height has been used by Schumpe and Grund (1986) to correct or convert ϵ so that it is referenced to the height within the column still containing a gas-liquid mixture. Since the Phase II slope is constant, a reasonable assumption may be made that the back of the small bubble front moves up the column at a constant velocity.

$$\frac{h_{PT,l}}{h_{PT}} = \frac{t_{corr}}{t_{nae}} \tag{4.12}$$

t_{nae} is the time when all bubbles have risen past the pressure tap and $h_{PT,l}$ is the bottom portion of the column occupied by clear liquid at t_{corr}.

$$\epsilon_{corr} = \frac{h - h_{nae}}{h_{PT} - h_{PT,l}} \tag{4.13}$$

Substituting Equations 4.1 and 4.12 into Equation 4.13, gas hold-up may be expressed as

$$\epsilon = \epsilon_{corr}\left(\frac{t_{nae} - t_{corr}}{t_{nae}}\right) \tag{4.14}$$

The time at which the corrected gas hold-up reaches ϵ_{tran} must be found ($\epsilon_{corr} = \epsilon_{tran}$). A

combination of the Equation 4.4 at t = t_{corr} with Equation 4.14 is used for this purpose.

$$t_{corr} = \frac{(\epsilon_O - \epsilon_{corr}) t_{nae}}{[\frac{U_O t_{nae}}{h_{PT}} - \epsilon_{corr}]} \tag{4.15}$$

The transition velocity convective model disengagement is then plotted on the ϵ versus time curve (Figure 4.11) starting at the point (t_{corr}, ϵ) which is calculated using Equations 4.15 and 4.14 respectively with $\epsilon_{corr} = \epsilon_{tran}$.

At the transition point and in the bubbly flow regime DGD profiles have an upwardly concave form which is well described by the theoretical convective model disengagement curve (Figure 4.10). Contrary to the bubbly flow regime where the liquid velocity profile is not greatly affected over the course of a transient DGD experiment, disengagement of large bubbles during Phase I of a churn turbulent DGD experiment probably cause a rapid deceleration of liquid circulation. Less mixing is observed in Phase II of a disengagement than in a bubbly flow regime experiment. Considering the convective model disengagement assumes no deceleration in liquid velocity, the model fits Phase II very well (Figure 4.11). The good fit indicates that the small bubble fraction of the hold-up in the churn turbulent regime has the same behaviour as at the transition point.

From the above analysis we may conclude that the convective model disengagement profile seems to accurately describe the upwardly concave shape of the disengagement

profiles seen in the bubbly flow regime. However, we only have data which can confirm that good match at the transition velocity. Our analysis of transient disengagement curves in the churn turbulent flow regime, shows that they are well represented by a convective model at the steady-state velocity, U_o, during Phase I and a convective model at the transition velocity, U_{tran}, during Phase II. Churn turbulent gas phase hydrodynamics may thus be described as the superposition of large bubbles upon the transition point bubble velocity distribution.

4.7 Convective Model Based on Kinetic Theory

In this section a simplified conceptual model to describe the gas hold-up structure based on kinetic theory is presented. The model describes gas phase flow in bubble columns in both the bubbly and churn turbulent flow regimes and is based upon a stochastic model for bubble interaction first suggested by Iordache and Muntean (1981), extended to churn turbulent flow by Iordache and Jinescu (1986), and applied to a gas-solid reactor by Iordache et al. (1995). The major advance proposed here is to treat bubble-bubble interactions as volume interactions, thereby replacing "linear" concentration in their model by gas hold-up.

The evolution of the absolute bubble velocity distribution f(v,z,t) with increasing gas hold-up is explained by a combination of bubble-bubble and bubble-liquid interaction. The model is based upon an ideal bubble velocity distribution, $f^o(v,z,t)$, which would exist for a given set of operating conditions in the absence of bubble-bubble interactions. The actual bubble velocity distribution f(v,z,t) which exists at a specific operating condition is determined by $f^o(v,z,t)$ and the rules of bubble-bubble interactions. Two assumptions have been made about bubble-bubble interactions in the kinetic model. First, when two bubbles having the same velocity interact, there is no change in bubble velocity. This rule may seem untenable. For example if two bubbles coalesce to form a larger bubble it would probably rise faster. Theoretically, however, bubbles moving up

the column with the same velocity will not meet to interact. Second, when two bubbles having different velocities interact, the slower bubble is accelerated to the same velocity as the faster one. The beauty of the interaction rule is that it is not important whether or not the bubbles coalesce; bubbles may simply move collectively in a cluster or instead they may coalesce. A complete derivation of the model may be found in Hyndman (1995).[7] The following equation is capable of describing both the bubbly and churn turbulent flow regimes in a bubble column.

$$\frac{\partial f}{\partial t} + v\frac{\partial f}{\partial z} = -a^o(f-f^o) + a\epsilon_o(v-\bar{v})f \qquad (4.16)$$

Equation 4.16 is based upon the following hypotheses:

i) velocity distribution variations are due to bubble-liquid interactions (first RHS term) and to bubble-bubble interactions (second RHS term),

ii) the bubble-liquid interaction term describes the relaxation of the bubble velocity distribution f(v,z,t) towards the ideal velocity distribution f^o(v,z,t),

iii) interaction between two bubbles results in the slower bubble being accelerated to the same velocity as the faster one.

iv) both f(v,z,t) and f^o(v,z,t) are normalized to the steady-state gas hold-up ϵ_o.

For the stationary, space independent case Equation 4.16 simplifies as follows.

---

7. See Appendix IV.

$$f^o(v) - f(v)[1 + \frac{a}{a^o}(\bar{v} - v)\epsilon_o] = 0 \qquad (4.17)$$

In solving Equation 4.17 for the bubble velocity distribution f(v) a singularity appears when the factor $[1 + (a/a^o)(\bar{v} - v)\epsilon_o]$ diminishes to zero. The singularity appears at higher gas hold-ups starting at the transition to the churn turbulent flow regime. f(v) rewritten as a function of $f^o(v)$ therefore has the following form.

$$f(v) = \frac{f^o(v)}{1 + \frac{a}{a^o}(\bar{v} - v)\epsilon_o} + b\epsilon_o\delta(1 + \frac{a}{a^o}(\bar{v} - v)\epsilon_o) \qquad (4.18)$$

In Equation 4.18, $b\epsilon_o$ represents the fraction of the gas hold-up which rises at a singular large-bubble velocity, u_{bL}, designated by a delta-Dirac function.

4.7.1 Bubbly Flow Regime

For the bubbly flow regime only the non-singular portion of Equation 4.18 is required (i.e. b=0). If it is rewritten in the terms of $f^o(v)$, multiplied by v, and integrated for all v, the following relation results.

$$\bar{v} - \frac{a}{a^o}\epsilon_o\sigma^2 = \bar{v}^o \qquad (4.19)$$

$\bar{v}^o$ denotes the mean gas velocity in ideal flow and σ^2 is the variance of f(v). Equation

4.19 may be rewritten in a familiar form.

$$\bar{v} = \frac{\bar{v}^o}{1 - A\epsilon_o} \qquad (4.20)$$

$$where \quad A = \frac{a}{a^o}\frac{\sigma^2}{\bar{v}}$$

Equation 4.20 may be verified for the two limiting conditions ($\epsilon=0$ and $\epsilon=1$). At very low gas hold-ups the flow is ideal and $\bar{v} = \bar{v}^o$. If gas hold-up were to increase to one (flooding or transport flow regime), $\bar{v}$ should increase indefinitely. To fulfil this second condition A is chosen equal to one. With A = 1 Equation 4.20 ressembles the drift flux model (Wallis, 1969). The ratio of the constants a and a° for the bubbly flow regime can thus be determined.

$$\frac{a}{a^o} = \frac{\bar{v}}{\sigma^2} \qquad (4.21)$$

From the denominator of the non-singular portion of Equation 4.18 and Equation 4.21 an accommodation function is defined.

$$\Omega = 1 + \frac{\bar{v}}{\sigma^2}(\bar{v} - v_{max})\epsilon_o \qquad (4.22)$$

v_{max} is the last bubble class in f(v) and f°(v). Ω tends toward zero as ϵ_o (and U_o) increase to a critical value indicating the transition condition. Combining Equations 4.18 and 4.21 enables area under the velocity distribution f(v) for the bubbly flow regime to be

expressed as follows.

$$\epsilon_o = \int_0^{v_{max}} \frac{f^o(v)}{1 + \frac{\bar{v}}{\sigma^2}(\bar{v} - v)\epsilon_o} dv \tag{4.23}$$

The first and second central moments of the normalized velocity distributions are shown below for the bubbly flow regime.

$$\bar{v} = \int_0^{v_{max}} \frac{v(f^o(v)/\epsilon_o)}{1 + \frac{\bar{v}}{\sigma^2}(\bar{v} - v)\epsilon_o} dv \tag{4.24}$$

$$\sigma^2 = \int_0^{v_{max}} \frac{(v - \bar{v})^2 \ (f^o(v)/\epsilon_o)}{1 + \frac{\bar{v}}{\sigma^2}(\bar{v} - v)\epsilon_o} dv \tag{4.25}$$

Equations 4.24 and 4.25 are independent and may be solved simultaneously for $\bar{v}$ and σ^2 at a given ϵ_o if $f^o(v)/\epsilon_o$ is known.

4.7.2 Churn Turbulent Flow Regime

In comparing the convective model at the transition point to Phase II of the disengagement, we concluded that the transition velocity distribution accurately represented the small bubble hold-up. Similarly Iordache and Jinescu (1986) have

represented churn turbulent flow conceptually by combining a pseudo-homogeneous portion of the gas hold-up with a singularity in the form of a delta-Dirac function for large bubbles or bubbles moving in clusters. Representing the large bubbles by a single velocity u_{bL} is a reasonable assumption as seen in Figure 4.11. Other researchers have made the same assumption in their two-bubble-group models by representing the large bubbles by plug flow (Shah et al., 1985; Shetty et al., 1992).

For the heterogeneous or churn turbulent flow regime Equation 4.18 applies and the constant a/a° is determined using the singularity condition.

$$1 + \frac{a}{a^o}(\bar{v} - u_{bL})\epsilon_0 = 0$$
$$or \quad \frac{a}{a^o} = \frac{1}{(u_{bL} - \bar{v})\epsilon_O} \tag{4.26}$$

Substituting a/a° from Equation 4.26 into Equation 4.18 gives the following result.

$$f(v) = \frac{(u_{bL} - \bar{v})f^o(v)}{(u_{bL} - v)} + b\epsilon_O\delta(u_{bL} - v) \tag{4.27}$$

The value of b in Equation 4.26 differs from the model presented by Iordache and Jinescu (1986). In their model b=1 for churn turbulent flow. Here $b\epsilon_0$ is defined as the large bubble hold-up or ϵ_{OL} from DGD experiments. Normalizing the area to one, the fraction of bubbles moving at u_{bL} may be determined.

$$b = 1 - (u_{bL} - \bar{v}) \int_0^{v_{max}} \frac{(f^o(v)/\epsilon_O)}{u_{bL} - v} dv \qquad (4.28)$$

The first and second central moments are not independent equations as was the case for homogeneous flow. Therefore, only b as a function of $\bar{v}$ may be determined by the kinetic model in churn turbulent flow. More information is required to determine the large ($b\epsilon_O$) and small ($(1-b)\epsilon_O$) bubble hold-ups. From our DGD experiments and as proposed by Krishna et al. (1991), we know that $\epsilon_{Os} = (1-b)\epsilon_O \approx \epsilon_{tran}$. Relating this to the proposed kinetic model, the overall gas hold-up may be calculated.

$$\epsilon_O = \frac{\epsilon_{tran}}{1 - b} \qquad (4.29)$$

In the churn turbulent regime, the large bubble fraction of the total gas hold-up (b) may be determined for a given $\bar{v}$ if $f^o(v)/\epsilon_O$ and $u_{bL}(\bar{v})$ are known. Total, large and small gas hold-ups may be calculated as a function of U_O using the kinetic model if in addition ϵ_{tran} is known.

4.7.3 Kinetic Model Implementation

As mentioned previously, the model requires an ideal bubble velocity distribution ($f^o(v)/\epsilon_O$). With a bubble velocity distribution in the bubbly flow regime, $f^o(v)/\epsilon_O$ may be calculated from Equation 4.17. Convective model correlations proposed by Hyndman and

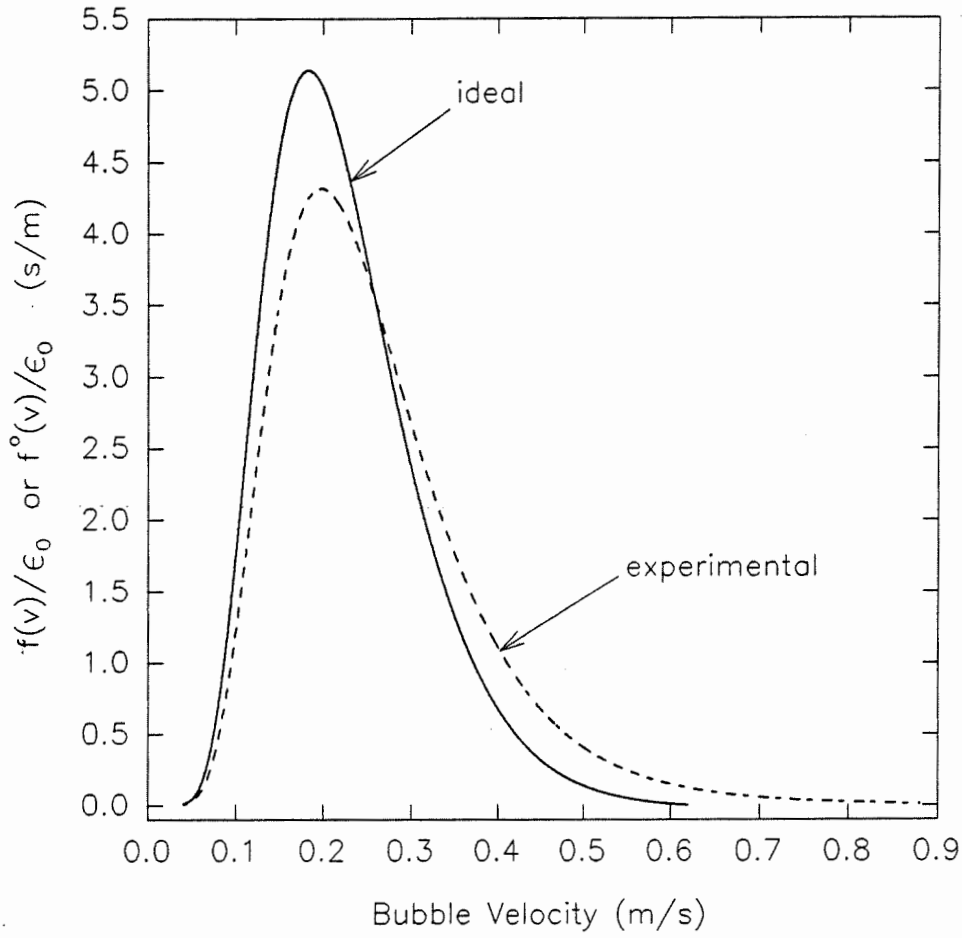

Figure 4.12: Convective model bubble velocity distribution at the transition point (----) and ideal bubble velocity distribution for the kinetic model (f°/ϵ_0 ——).

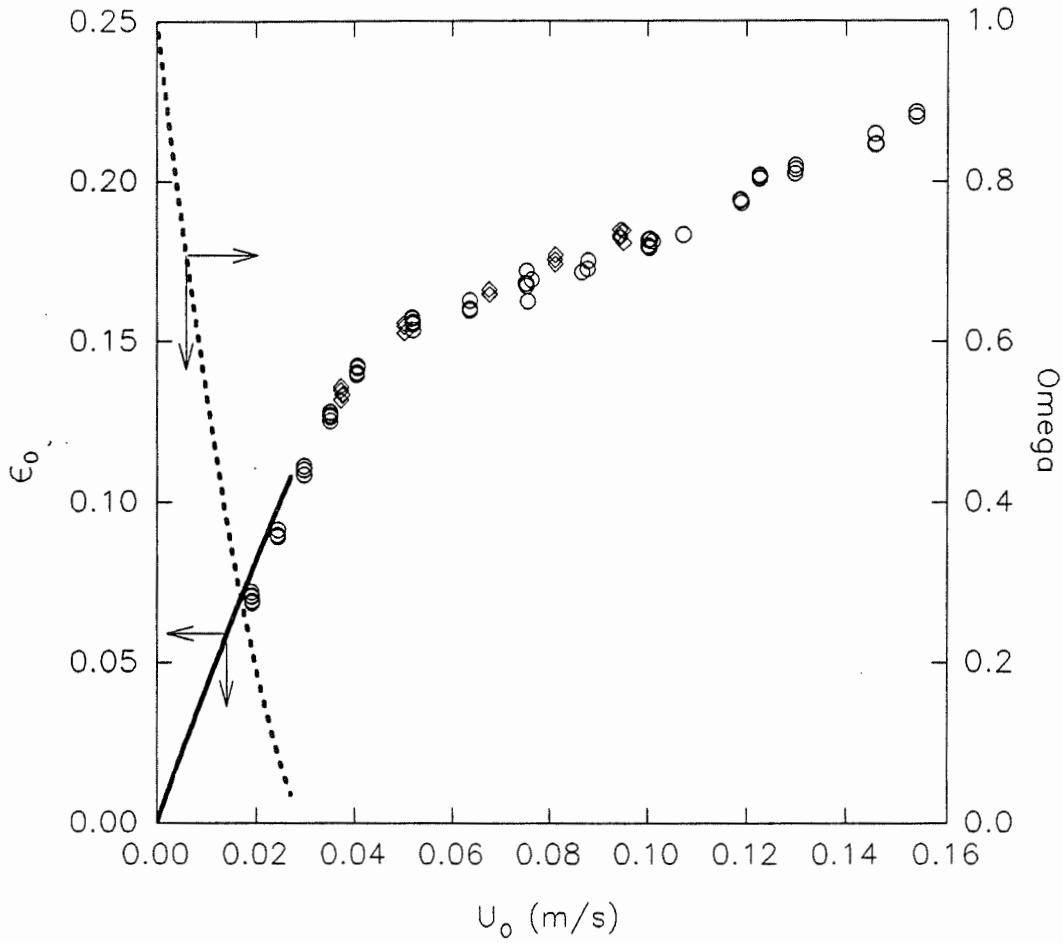

Figure 4.13: Comparison of the kinetic model to gas hold-up for the bubbly flow regime (same symbols as Figure 4.8; kinetic model ϵ_o —— ; Ω ----).

Guy (1995b) fill this purpose as they are valid for the transition point. Further, the DGD data at the transition point have shown an upwardly concave form, characteristic of the bubbly flow regime. The experimental convective model bubble velocity distribution is normalized to one and is equivalent to $f(v)/\epsilon_o$ in the bubbly flow regime. Further analysis is based upon $f^o(v)/\epsilon_o$ calculated using Equations 4.9 and 4.17 with α and β determined at $U_o = 0.0375$ m/s by Equations 3.10 and 3.11 from Hyndman and Guy (1995b). $f^o(v)/\epsilon_o$ and $f(v)/\epsilon_o$ are presented in Figure 4.12. The ideal distribution shown in Figure 4.12 has a shorter tail than the experimentally determined distribution because Equations 4.9 and 4.17 produce negative values of $f^o(v)/\epsilon_o$ at higher velocities. Negative values of $f^o(v)/\epsilon_o$ have no physical meaning and the distribution was truncated accordingly (v_{max} was the last positive value). The calculated gas hold-up for the bubbly flow regime (Equations 4.23 and 4.24) are in good agreement with experimental data as shown in Figure 4.13. It should be noted that the kinetic model presented here has no fitting parameters and calculations are based only on knowledge of an experimental bubble velocity distribution. The accommodation function is also presented in Figure 4.13. A critical value for Ω is reached at $\epsilon_o \approx 0.108$ which is below the transition hold-up as determined in Figure 4.2 ($\epsilon_{tran} = 0.137$).

DGD experiments and calculations with gas hold-up data have shown that the large bubble velocity, u_{bL}, varies with superficial velocity. Using a fourth order polynomial

expression (not shown)[8] a function for $u_{bL}(\bar{v})$ has been fitted for the purposes of model calculations. The polynomial was fit to u_{bL} as calculated by Equation 4.8 since the results were equivalent to those from DGD data and have less variation.

The ideal distribution along with three calculated f(v) in the churn turbulent regime are shown in Figure 4.14. The proportion of the area under the pseudo-homogeneous portion of the curve is reduced as $\bar{v}$ and fraction b of gas hold-up in the form of large bubbles (represented by the Dirac) increases. In Figure 4.15, the fraction of large bubbles calculated from DGD experiments is compared to the kinetic model calculations. The model and data are in good agreement.

Finally in Figure 4.16, experimental data is compared to overall gas hold-up calculated using Equation 4.29. Small bubble hold-up is simply ϵ_{tran} as we have shown previously in Figure 4.8. Good agreement is achieved as would be expected from Figure 4.15. Again, note that there is no fitting parameter. However, gas hold-up at the transition point and velocity of large bubbles must be known in addition to an experimental bubble velocity distribution in the bubbly flow regime (for calculation of $f^o(v)/\epsilon_o$). Also shown in Figure 4.16 is the kinetic model description of gas hold-up in the bubbly flow regime. There is a gap between where Ω and b indicate the transition point for bubbly to churn turbulent flow. One explanation may be that the two extremities of a gradual transition

8. See Appendix III.

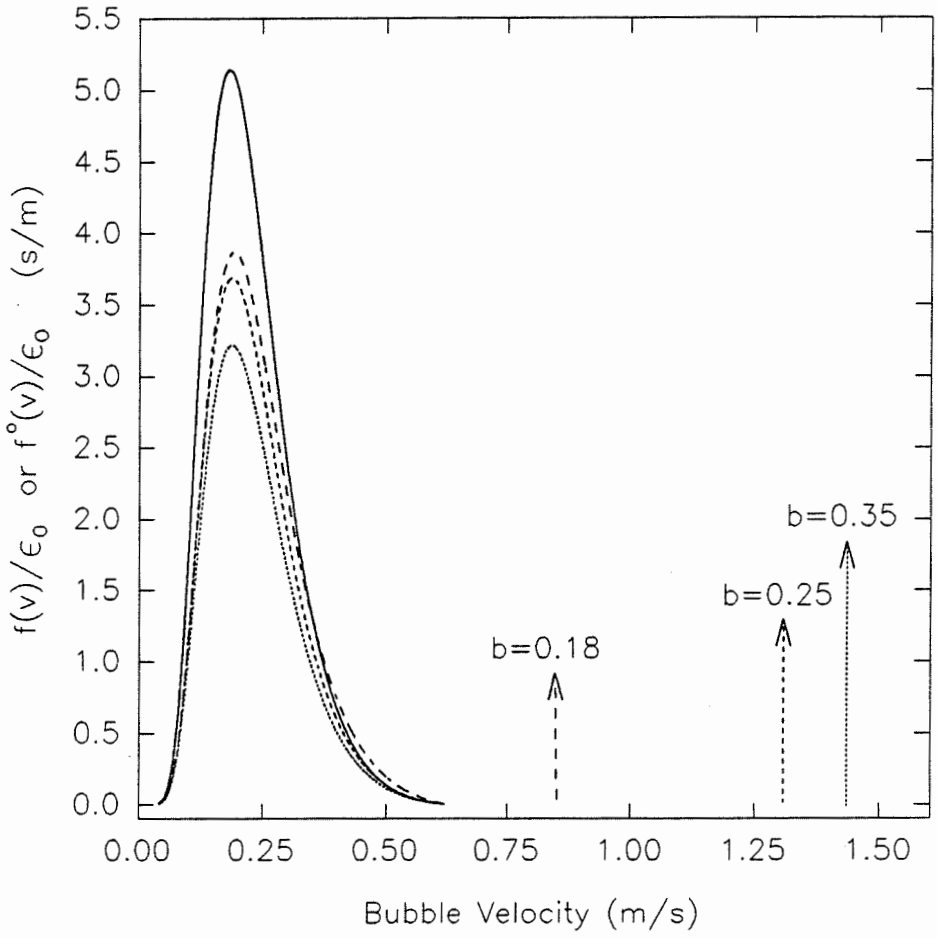

Figure 4.14: Kinetic model ideal (——) and churn turbulent velocity distributions ($\bar{v}$ = 35 ———, $\bar{v}$ = 50 ----, $\bar{v}$ = 65 m/s ------).

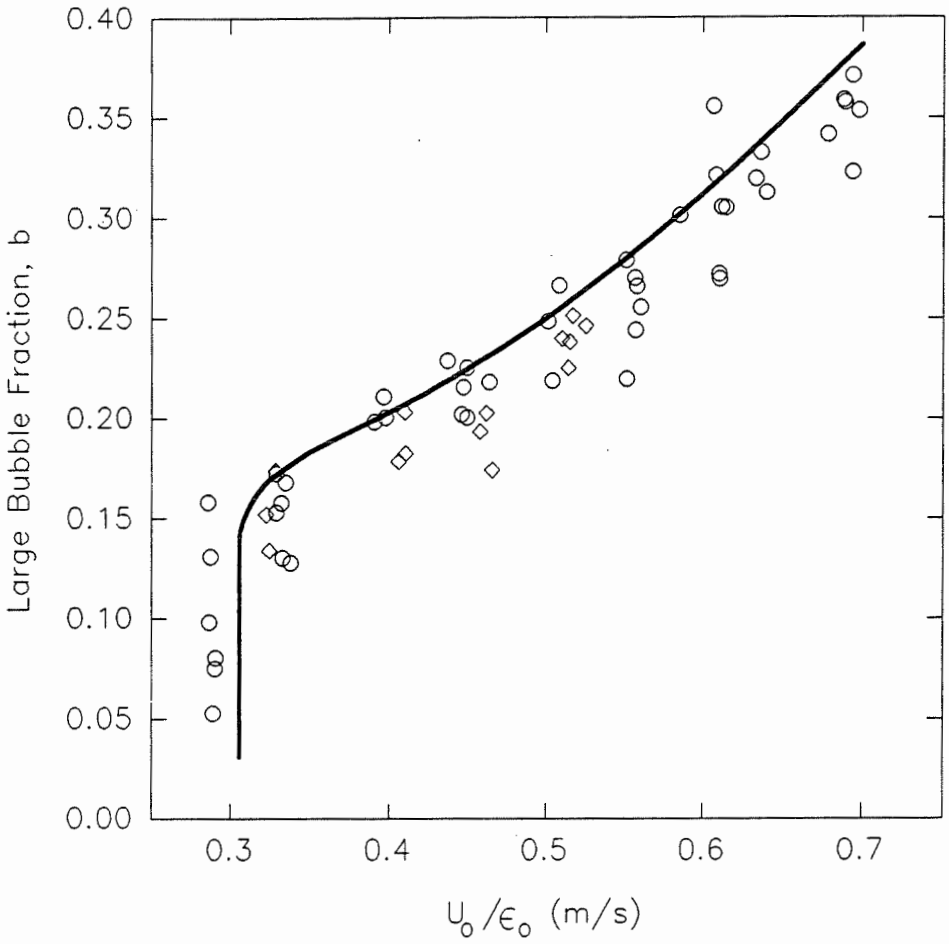

Figure 4.15: Comparison of calculated to experimental large bubble fraction in the churn turbulent flow regime (air only DGD data O; air/argon mixture DGD data ◇ ; kinetic model ——).

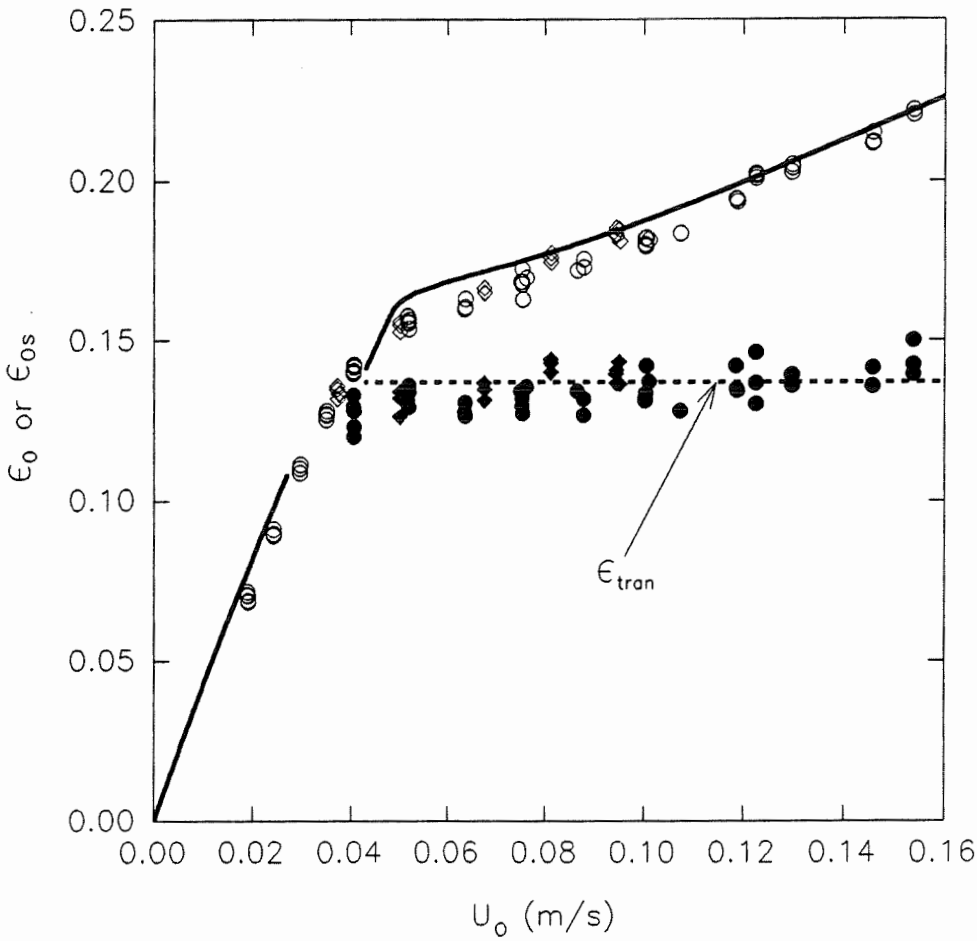

Figure 4.16: Comparison of the kinetic model to gas hold-up for the bubbly and churn turbulent flow regimes (same symbols as Figure 4.8; kinetic model ϵ_0 —— ; ϵ_{tran} ----).

are indicated. Omega indicates that $U_{tran} \approx 0.027$ m/s and b indicates that $U_{tran} = \bar{v}_{tran}$ $\epsilon_{tran} \approx 0.043$ m/s. These values are similar to values found by Chen et al. (1994) (D_c = 0.102 m) as boundaries for the vortical-spiral flow regime.

4.8 Conclusions

In a 0.2 m bubble column, the transition point for an air-water system from bubbly to churn turbulent flow is found to occur at 0.038 m/s using gas hold-up data. Pressure fluctuation data (whether normalized or not) concur with the transition point determined using gas hold-up data. Small bubble hold-up is found to be a constant equal to the transition hold-up over the range of churn turbulent superficial velocities examined in this study (0.037 to 0.15 m/s). Large bubble velocities, calculated only using gas hold-up data and information on the transition superficial velocity, agree well with literature data determined using the dynamic gas disengagement technique. The scale dependence of large bubble velocity reported by Grund et al. (1992) may apply to columns smaller than 0.2 m in diameter. Theoretical disengagement curves calculated from the convective model proposed in a previous publication (Hyndman and Guy, 1995a) compared well with DGD data in the bubbly flow regime. However, the fit could only be verified at the transition point since RTD data were not available at lower superficial velocities. In the churn turbulent flow regime, the convective model disengagement curves fit Phase I of the disengagement well. Phase II is well represented by a transition point convective model disengagement curve. This analysis indicates that the steady-state behaviour of the gas phase is composed of a superposition of large bubbles upon a transition bubble velocity distribution. Finally, a theoretical model based on kinetic theory which is capable of describing gas phase behaviour in the bubbly and churn turbulent flow regimes

was examined. The kinetic model describes the evolution of the bubble velocity distribution with increasing gas hold-up. Model calculations which determine the fraction of gas hold-up in the form of large bubbles agree well with DGD data.

4.9 Acknowledgements

The authors gratefully acknowledge financial support from the Natural Sciences and Engineering Research Council of Canada and of the Fonds pour la Formation de Chercheurs et l'Aide à la Recherche (Québec). The authors would also like to thank Richard Caron for his assistance in conducting the disengagement experiments.

4.10 References

BI, H.T. and J.R. GRACE (1995), "Effect of Measurement Method on the Velocities Used to Demarcate the Onset of Turbulent Fluidization", Chem. Eng. J. **57**, 261-271.

BRERETON, C.M.H and J.R. GRACE (1992), "The Transition to Turbulent Fluidization", Chem. Eng. Res. Des. **70**, 246-251.

CHEHBOUNI, A., J. CHAOUKI, C. GUY and D. KLVANA (1994), "Characterization of the Flow Transition between Bubbling and Turbulent Fluidization", Ind. Eng. Chem. Res. **33**, 1889-1896.

CHEN, R.C., J. REESE and L.-S. FAN (1994), "Flow Structure in a Three Dimensional Bubble Column and Three-Phase Fluidized Bed", AIChE J. **40**, 1093-1104.

DALY, J.G., S.A. PATEL and D.B. BUKUR (1992), "Measurement of Gas Holdups and Sauter Mean Diameters in Bubble Column Reactors by Dynamic Gas Disengagement Method", Chem. Eng. Sci. **47**, 3647-3654.

DECKWER, W.-D. (1992), "Bubble Column Reactors", John Wiley and Sons, West Sussex, England, p. 171.

DECKWER, W.-D. and A. SCHUMPE (1993), "Improved Tools for Bubble Column Reactor Design and Scale-Up", Chem. Eng. Sci. **48**, 889-911.

DRAHOŠ, J., F. BRADKA and M. PUNČOCHÁŘ (1992), "Fractal Behaviour of Pressure Fluctuations in a Bubble Column", Chem. Eng. Sci. **47**, 4069-4075.

DRAHOŠ, J., J. ČERMÁK (1989), "Diagnostics of Gas-Liquid Flow Patterns in Chemical Engineering Systems", Chem. Eng. Process. **26**, 147-164.

DRAHOŠ, J., J. ZAHRADNÍK, M. PUNČOCHÁŘ, M. FIALOVÁ and F. BRADKA (1991), "Effect of Operating Conditions on the Characteristics of Pressure Fluctuations in a Bubble Column", Chem. Eng. Process. **29**, 107-115.

FAN, L.-S. (1989), "Gas-Liquid-Solid Fluidization Engineering", Butterworth Publishers, Stoneham, MA, pp. 270-272.

FAN, L.-S., S. SATIJA and K. WISECARVER (1986), "Pressure Fluctuation Measurements and Flow Regime Transitions in Gas-Liquid-Solid Fluidized Beds", AIChE J. **32**, 338-340.

FRANZ, K., T. BÖRNER, H.J. KANTOREK and R. BUCHHOLZ (1984), "Flow

Structures in Bubble Columns", Ger. Chem. Eng. **7**, 365-374.

GRUND, G., A. SCHUMPE and W.-D. DECKWER (1992), "Gas-Liquid Mass Transfer in a Bubble Column with Organic Liquids", Chem. Eng. Sci. **47**, 3509-3516.

HYNDMAN, C.L. (1995), "Gas Phase Hydrodynamics of Bubble Columns", Thèse de doctorat (in english), École Polytechnique de Montréal, Canada.

HYNDMAN, C.L. and C. GUY (1995a), "Gas Phase Flow in Bubble Columns: A Convective Phenomenon", Can. J. Chem. Eng. **73**, 426-434. (Chapter II)

HYNDMAN, C.L. and C. GUY (1995b), "Gas Phase Hydrodynamics in Bubble Columns", Chem. Eng. Res. Des. **73**, 302-307. (Chapter III)

IORDACHE, O., Y. BLOISE, J. CHAOUKI and R. LEGROS (1995), "Clusters in Circulating Fluidized Beds: Kinetic Theory Approach", Chem. Eng. Comm. **131**, 53-71.

IORDACHE, O. and G. JINESCU (1986), "The Stability of Flow in Bubble Columns", Chem. Eng. Sci. **41**, 2585-2588.

IORDACHE, O.M. and O.L. MUNTEAN (1981), "Stochastic Approach to the

Hydrodynamics of Gas-Liquid Dispersions", Ind. Eng. Chem. Fundam. **20**, 204-207.

KAWAGOE, M., T. OTAKE and C.W. ROBINSON (1989), "Gas-Phase Mixing in Bubble Columns", J. Chem. Eng. Japan **22**, 136-142.

KRISHNA, R., J.W.A. DE SWART, D.E. HENNEPHOF, J. ELLENBERGER and H.C.J. HOEFSLOOT (1994), "Influence of Increased Gas Density on Hydrodynamics of Bubble-Column Reactors", AIChE J. **40**, 112-119.

KRISHNA, R., J. ELLENBERGER and D.E. HENNEPHOF (1993), "Analogous Description of the Hydrodynamics of Gas-Solid Fluidized Beds and Bubble Columns", Chem. Eng. J. **53**, 89-101.

KRISHNA, R., P.M. WILKINSON and L.L. VAN DIERENDONCK (1991), "A Model for Gas Hold-up in Bubble Columns Incorporating the Influence of Gas Density on Flow Regime Transitions", Chem. Eng. Sci. **46**, 2491-2496.

LEE, Y.H., Y.J. KIM, B.G. KELKAR and C.B. WEINBERGER (1985), "A Simple Digital Sensor for Dynamic Gas Holdup Measurements in Bubble Columns", Ind. Eng. Chem. Fundam. **24**, 105-107.

MOLERUS, O. and M. KURTIN (1986b), "Hydrodynamics of Bubble Columns in the Liquid Circulation Regime", Chem. Eng. Sci. **41**, 2685-2692.

NISHIYAMA, M., T. KAWANO, N. OTOTAKE and N. YUTANI (1989), "Fluctuations in Static Pressure and the Mode of Flow in a Three-Phase Fluidized Bed", Int. Chem. Eng. **29**, 287-294.

PATEL, S.A., J.G. DALY and D.B. BUKUR (1989), "Holdup and Interfacial Area Measurements Using Dynamic Gas Disengagement", AIChE J. **35**, 931-942.

SCHUMPE, A. and G. GRUND (1986), "The Gas Disengagement Technique for Studying Gas Holdup Structure in Bubble Columns", Can. J. Chem. Eng. **64**, 891-896.

SHAH, Y.T., S. JOSEPH, D.N. SMITH and J.A. RUETHER (1985), "Two-Bubble Class Model for Churn Turbulent Bubble-Column Reactor", Ind. Eng. Chem. Process Des. Dev. **24**, 1096-1104.

SHETTY, S.A., M.V. KANTAK and B.G. KELKAR (1992), "Gas Phase Backmixing in Bubble Column Reactors", AIChE J. **38**, 1013-1026.

SRIRAM , K. and R. MANN (1977), "Dynamic Gas Disengagement: A New Technique

for Assessing the Behaviour of Bubble Columns", Chem. Eng. Sci. **32**, 571-580.

THIMMAPURAM, P.R., N.S. RAO and S.C. SAXENA (1992), "Characterization of Hydrodynamic Regimes in a Bubble Column", Chem. Eng. Sci. **47**, 3355-3362.

UEYAMA, K. and T. MIYAUCHI (1979), "Properties of Recirculating Turbulent Two Phase Flow in Gas Bubble Columns", AIChE J. **25**, 258-266.

VERMEER, D.J. and R. KRISHNA (1981), "Hydrodynamics and Mass Transfer in Bubble Columns Operating in the Churn-Turbulent Regime", Ind. Eng. Chem. Process Des. Dev. **20**, 475-482.

WALLIS, G.B. (1969), "One-Dimensional Two-Phase Flow", McGraw-Hill, Inc., Toronto, ON.

YASHIMA, M., R. NASSAR, L.T. FAN and Y. KANG (1992), "Stochastic Modelling of Pressure Fluctuations in a Three-Phase Fluidized Bed", AIChE J. **38**, 629-634.

CHAPTER V

CONCLUDING DISCUSSION

In Chapters II and III gas phase residence time distribution (RTD) experiments and analysis have been presented. The traditional axial dispersion model with a single average bubble velocity and an axial dispersion coefficient has been examined using the radioactive gas phase tracer data. On the basis of a combination of the tests using statistical moments of tracer response curves and the underestimation by the model of the interstitial gas velocity the traditional axial dispersion model has been invalidated for description of gas phase behaviour in the churn turbulent flow regime. A purely convective model for discrete phase flow of the gas phase has been presented. This model is based upon a log-normal volume distribution of bubble velocities. The dominant mechanism in gas phase flow has been shown to be convection using the RTD data. Two elements were involved in the analysis of RTD data which confirm this conclusion: the convective model test developed for tracer response curve moments and the good fit of mean gas velocity (as calculated from the convective model bubble velocity distributions) with experimental interstitial gas velocity. Convective behaviour is the dominant mechanism involved in gas phase flow and the purely convective model presented in this thesis represents an important step in modelling of gas phase flow. There are however number of alternatives in pursuing further work with convective-type models for gas phase flow in bubble columns. There may be some dispersion superimposed upon a

mainly convective behaviour. Also the convective model presented here has not considered negative bubble velocities. One can observe some smaller bubbles close to the wall moving downward. Negative bubble velocities occur as a result of liquid circulation patterns within the column: small bubbles are swept along by the liquid flow. Radial profiles of local axial liquid velocity will be an important next step convective modelling of gas phase flow. At higher superficial gas velocities than those examined here, and for columns of larger diameter, downward flow of bubbles is expected to be a more important part of the overall gas phase flow.

Dynamic gas disengagement (DGD) experiments and the kinetic model to describe gas hold-up structure presented in Chapter IV have shown that a bimodal velocity distribution in the churn turbulent flow regime could alternatively have been used as the bubble velocity distribution in the convective model. Confirmation of the appropriate form for the bubble velocity distribution is required. The log-normal volume bubble velocity distribution may be the most appropriate form for the bubbly flow regime. However, a bimodal distribution could be examined for the churn turbulent flow regime.

CONCLUSIONS

The first objective of this study was to model gas phase flow in bubble columns. Toward this end, residence time distribution experiments with radioactive argon gas as a tracer were used to analyze gas phase hydrodynamics. The axial dispersion model, commonly used for gas phase flow in the literature, was shown to be inapplicable in the churn turbulent flow regime. While the model was capable of fitting tracer response curves, the average gas velocity was under-predicted especially at higher gas velocity. A new approach to gas phase hydrodynamics is proposed by the use of a fully convective model for gas phase flow. Simple tests based on residence time distribution (RTD) curve moments were developed to distinguish dispersive from convective flow of the gas phase. Tests showed that the gas phase flow is convective rather than dispersive in nature. The convective model fits RTD tracer response curves well and matched independently measured average swarm velocity. The model can be used to calculate bubble velocity distributions from RTD data. Bubble velocity distribution parameters calculated from RTD data were correlated with superficial gas velocities from 0.037 to 0.095 m/s.

The second objective was to model gas hold-up structure in bubble columns. Since the hold-up structure differs in the bubbly and churn turbulent flow regimes, the transition between flow regimes was analyzed. The transition point determined using pressure fluctuation data concurs with calculations from overall gas hold-up data. Dynamic gas

disengagement was used to experimentally determine gas hold-up structure. Theoretical convective model disengagement curves match dynamic gas disengagement data at the transition point between bubbly and churn turbulent flow. In the churn turbulent flow regime, the disengagement process consists of two distinct phases. During Phase I large bubbles leave the column; during Phase II small bubbles (some of which disengage during Phase I) continue to disengage. Theoretical disengagement curves match Phase I of the disengagement process. Phase II data compare well with a transition point theoretical disengagement curve. Gas hold-up in the churn turbulent flow regime is the superposition of large bubbles on a transition bubble velocity distribution. Large bubble velocities increase with superficial gas velocity; this function may be scale independent for columns 0.2 m in diameter and larger. A kinetic model to describe gas hold-up structure over the bubbly and churn turbulent flow regimes was developed. It indicates the boundaries for a gradual transition from bubbly to churn turbulent flow. In the bubbly flow regime, overall gas hold-up may be calculated using the model. The fraction of gas hold-up in the form of large bubbles may be calculated in the churn turbulent flow regime. Overall hold-up data and large bubble hold-up (from DGD experiments) compare well with kinetic model calculations.

RECOMMENDATIONS

• Residence time distribution experiments at lower superficial gas velocity to test the validity of the convective model in the bubbly flow regime would be valuable. According to the kinetic theory developed in Chapter IV, the bubble velocity distribution should not change significantly with superficial gas velocity. This would also allow for comparison of theoretical disengagement curves in the bubbly flow regime to DGD data.

• Local bubble velocity data (for example using a fibre optic probe) would provide number frequency distributions. Coupled with the volume distributions at the same operating conditions, information on bubble size could be determined. Since the fibre optic probes are also capable of measuring chord lengths, the convective model could be further validated.

• Measurements of radial profiles of local axial liquid velocity will be valuable in combination with absolute bubble velocity distributions from the convective modelling of gas phase flow. Further, negative bubble velocities which should be considered in future modelling efforts result from the liquid circulation pattern (especially the downward liquid velocities known to exist near the column wall). RTD data and local liquid velocity data from the same column would constitute a valuable contribution to the literature on bubble columns.

- Bubble columns as unit operations involve mass transfer. The integration of mass transfer with convective-type models, and discrete phase flow models in general, will be an important step in the further development of gas phase flow models for bubble columns.

GENERAL BIBLIOGRAPHY

AUFDERHEIDE, E. and A. VOGELPOHL (1986), "A Convective Model to Interpret Dispersed-Phase Residence Time Measurements in Pulsed Liquid/Liquid Extractors", Chem. Eng. Sci. **41**, 1747-1757.

BI, H.T. and J.R. GRACE (1995), "Effect of Measurement Method on the Velocities Used to Demarcate the Onset of Turbulent Fluidization", Chem. Eng. J. **57**, 261-271.

BRERETON, C.M.H and J.R. GRACE (1992), "The Transition to Turbulent Fluidization", Chem. Eng. Res. Des. **70**, 246-251.

CHABOT, J. and H.I. DE LASA (1993), "Gas Holdups and Bubble Characteristics in a Bubble Column Operated at High Temperature", Ind. Eng. Chem. Res. **32**, 2595-2601.

CHEHBOUNI, A., J. CHAOUKI, C. GUY and D. KLVANA (1994), "Characterization of the Flow Transition between Bubbling and Turbulent Fluidization", Ind. Eng. Chem. Res. **33**, 1889-1896.

CHEN, R.C., J. REESE and L.-S. FAN (1994), "Flow Structure in a Three Dimensional Bubble Column and Three-Phase Fluidized Bed", AIChE J. **40**, 1093-1104.

DALY, J.G., S.A. PATEL and D.B. BUKUR (1992), "Measurement of Gas Holdups and Sauter Mean Diameters in Bubble Column Reactors by Dynamic Gas Disengagement Method", Chem. Eng. Sci. **47**, 3647-3654.

DECKWER, W.-D. (1992), "Bubble Column Reactors", John Wiley and Sons, West Sussex, England, p. 171.

DECKWER, W-D. and A. SCHUMPE (1993), "Improved Tools for Bubble Column Reactor Design and Scale-Up", Chem. Eng. Sci. **48**, 889-911.

DEVANATHAN, N., D. MODLEMIAN and M.P. DUDUKOVIĆ (1990), "Flow Mapping in Bubble Columns Using CARPT", Chem. Eng. Sci. **45**, 2285-2291.

DRAHOŠ, J., F. BRADKA and M. PUNČOCHÁŘ (1992), "Fractal Behaviour of Pressure Fluctuations in a Bubble Column", Chem. Eng. Sci. **47**, 4069-4075.

DRAHOŠ, J., ČERMÁK (1989), "Diagnostics of Gas-Liquid Flow Patterns in Chemical Engineering Systems", Chem. Eng. Process. **26**, 147-164.

DRAHOŠ, J., J. ZAHRADNÍK, M. PUNČOCHÁŘ, M. FIALOVÁ and F. BRADKA (1991), "Effect of Operating Conditions on the Characteristics of Pressure Fluctuations in a Bubble Column", Chem. Eng. Process. **29**, 107-115.

FAN, L.-S. (1989), "Gas-Liquid-Solid Fluidization Engineering", Butterworth Publishers, Stoneham, MA.

FAN, L.-S., S. SATIJA and K. WISECARVER (1986), "Pressure Fluctuation Measurements and Flow Regime Transitions in Gas-Liquid-Solid Fluidized Beds", AIChE J. **32**, 338-340.

FIELD, R.W. and J.F. DAVIDSON (1980), "Axial Dispersion in Bubble Columns", Trans. Inst. Chem. Eng. **58**, 228-236.

FRANZ, K., T. BÖRNER, H.J. KANTOREK and R. BUCHHOLZ (1984), "Flow Structures in Bubble Columns", Ger. Chem. Eng. **7**, 365-374.

GRUND, G., A. SCHUMPE and W.-D. DECKWER (1992), "Gas-Liquid Mass Transfer in a Bubble Column with Organic Liquids", Chem. Eng. Sci. **47**, 3509-3516.

HILLS, J.H. (1974), "Radial Non-Uniformity of Velocity and Voidage in a Bubble Column", Trans. Inst. Chem. Eng. **52**, 1-9.

HYNDMAN, C.L. and C. GUY (1995a), "Gas Phase Flow in Bubble Columns: A Convective Phenomenon", Can. J. Chem. Eng. **73**, 426-434. (Chapter II)

HYNDMAN, C.L. and C.GUY (1995b), "Gas Phase Hydrodynamics in Bubble Columns", Chem. Eng. Res. Des. **73**, 302-307. (Chapter III)

IORDACHE, O., Y. BLOISE, J. CHAOUKI and R. LEGROS (1995), "Clusters in Circulating Fluidized Beds: Kinetic Theory Approach", Chem. Eng. Comm. **131**, 53-71.

IORDACHE, O. and G. JINESCU (1986), "The Stability of Flow in Bubble Columns", Chem. Eng. Sci. **41**, 2585-2588.

IORDACHE, O.M. and O.L. MUNTEAN (1981), "Stochastic Approach to the Hydrodynamics of Gas-Liquid Dispersions", Ind. Eng. Chem. Fundam. **20**, 204-207.

JOSHI, J.B. (1982), "Gas Phase Dispersion in Bubble Columns", Chem. Eng. J. **24**, 213-216.

KAWAGOE, M., T. OTAKE and C.W. ROBINSON (1989), "Gas-Phase Mixing in Bubble Columns", J. Chem. Eng. Japan **22**, 136-142.

KRISHNA, R., J.W.A. DE SWART, D.E. HENNEPHOF, J. ELLENBERGER and H.C.J. HOEFSLOOT (1994), "Influence of Increased Gas Density on Hydrodynamics of Bubble-Column Reactors", AIChE J. **40**, 112-119.

KRISHNA, R., J. ELLENBERGER and D.E. HENNEPHOF (1993), "Analogous Description of the Hydrodynamics of Gas-Solid Fluidized Beds and Bubble Columns", Chem. Eng. J. **53**, 89-101.

KRISHNA, R., P.M. WILKINSON and L.L. VAN DIERENDONCK (1991), "A Model for Gas Hold-up in Bubble Columns Incorporating the Influence of Gas Density on Flow Regime Transitions", Chem. Eng. Sci. **46**, 2491-2496.

KUESTER, J.L. and J.H. MIZE (1973), "Optimization Techniques with Fortran", McGraw Hill, Toronto, pp. 368-385.

LEVENSPIEL, O. (1972), "Chemical Reaction Engineering", John Wiley & Sons, Toronto, pp. 275-278.

LEE, Y.H., Y.J. KIM, B.G. KELKAR and C.B. WEINBERGER (1985), "A Simple Digital Sensor for Dynamic Gas Holdup Measurements in Bubble Columns", Ind. Eng. Chem. Fundam. **24**, 105-107.

LEVENSPIEL, O. and T.J. FITZGERALD (1983), "A Warning on the Misuse of the Dispersion Model", Chem. Eng. Sci. **38**, 489-491.

MODAK, S.Y., V.A. JUVEKAR and V.C. RANE (1993), "Dynamics of the Gas Phase in Bubble Columns", Chem. Eng. Technol. **16**, 303-306.

MODAK, S.Y., V.A. JUVEKAR and V.C. RANE (1994), "Comparison of the Single-Bubble-Class and Modified Two-Bubble-Class Models of Bubble Column Reactors", Chem. Eng. Technol. **17**, 313-322.

MOLERUS, O. and M. KURTIN (1986a), "Modelling of Residence Time Distributions of the Gas Phase in Bubble Columns in the Liquid Circulation Regime", Chem. Eng. Sci. **41**, 2693-2698.

MOLERUS, O. and M. KURTIN (1986b), "Hydrodynamics of Bubble Columns in the Liquid Circulation Regime", Chem. Eng. Sci. **41**, 2685-2692.

NISHIYAMA, M., T. KAWANO, N. OTOTAKE and N. YUTANI (1989), "Fluctuations in Static Pressure and the Mode of Flow in a Three-Phase Fluidized Bed", Int. Chem. Eng. **29**, 287-294.

PATEL, S.A., J.G. DALY and D.B. BUKUR (1989), "Holdup and Interfacial Area Measurements Using Dynamic Gas Disengagement", AIChE J. **35**, 931-942.

PRESS, W.H., B.P. FLANNERY, S.A. TEUKOLSKY and W. VETTERLING (1989), "Numerical Recipes: The Art of Scientific Computing (FORTRAN Version)", Cambridge University Press, New York, pp. 289-293.

SCHUMPE, A. and G.GRUND (1986), "The Gas Disengagement Technique for Studying Gas Holdup Structure in Bubble Columns" **64**, 891-896.

SHAH, Y.T., S. JOSEPH, D.N. SMITH and J.A. RUETHER (1985), "Two-Bubble Class Model for Churn Turbulent Bubble-Column Reactor", Ind. Eng. Chem. Process Des. Dev. **24**, 1096-1104.

SHETTY, S.A., M.V. KANTAK and B.G. KELKAR (1992), "Gas Phase Backmixing in Bubble Column Reactors", AIChE J. **38**, 1013-1026.

SRIRAM , K. and R. MANN (1977), "Dynamic Gas Disengagement: A New Technique for Assessing the Behaviour of Bubble Columns", Chem. Eng. Sci. **32**, 571-580.

THIMMAPURAM, P.R., N.S. RAO and S.C. SAXENA (1992), "Characterization of Hydrodynamic Regimes in a Bubble Column", Chem. Eng. Sci. **47**, 3355-3362.

UEYAMA, K. and T. MIYAUCHI (1979), "Properties of Recirculating Turbulent Two Phase Flow in Gas Bubble Columns", AIChE J. **25**, 258-266.

VERMEER, D.J. and R. KRISHNA (1981), "Hydrodynamics and Mass Transfer in Bubble Columns Operating in the Churn-Turbulent Regime", Ind. Eng. Chem. Process Des. Dev. **20**, 475-482.

WAKAO, N. and S. KAGUEI (1982), "Heat and Mass Transfer in Packed Beds", Gordon and Breach Science Publishers, New York, pp. 1-31.

WALLIS, G.B. (1969), "One-Dimensional Two-Phase Flow", McGraw-Hill, Inc., Toronto, ON.

YAO, B.P., C. ZHENG, K.E. GASCHE and H. HOFMANN (1991), "Bubble Behaviour and Flow Structure of Bubble Columns", Chem. Eng. Process. **29**, 65-75.

YASHIMA, M., R. NASSAR, L.T. FAN and Y. KANG (1992), "Stochastic Modelling of Pressure Fluctuations in a Three-Phase Fluidized Bed", AIChE J. **38**, 629-634.

APPENDICES

APPENDIX I

GAS PHASE RESIDENCE TIME DISTRIBUTION

A1.1 Radioactive Argon Preparation

Irradiated argon was used as the gas phase tracer. Prepurified argon (Air Liquide Canada, Inc.) was put into small plastic containers suitable for the Slowpoke reactor. The container was placed under water and argon gas displaced the water in the container. Argon was irradiated (to Ar^{41}; $t_{0.5}=1.8$ h) for 45 minutes and then transported in a small lead container to our laboratory where the bubble column was already prepared for an experiment to begin. Up to 3 injections (3 containers) could be done in a period of 20 to 30 minutes so that the radiation did not vary greatly. Again under water, a syringe was used to remove Ar^{41} from the container. Note that many factors come into play which determine the initial "concentration" injected including how much argon was initially put into the container (approximately 7 ml), how large of a bubble remained in the container after emptying it into a syringe, how long ago the argon left the Slowpoke reactor, etc.

A1.2 Detector Placement

NaI scintillation detectors are surrounded by lead brick shielding in Figure A1.1. Lead bricks are 51 x 102 x 203 mm or 51 x 102 x 102 mm. The front of the lead brick shielding was placed flush with the column wall and detector faces were placed 57 mm from the column wall (or 0.37 m as measured from the back of the photomultiplier). Wood supports were placed under each detector to centre the detector in the lead brick arrangement. The front of the detector extended out over the support 76 mm so as to fully expose the NaI crystal to radiation.

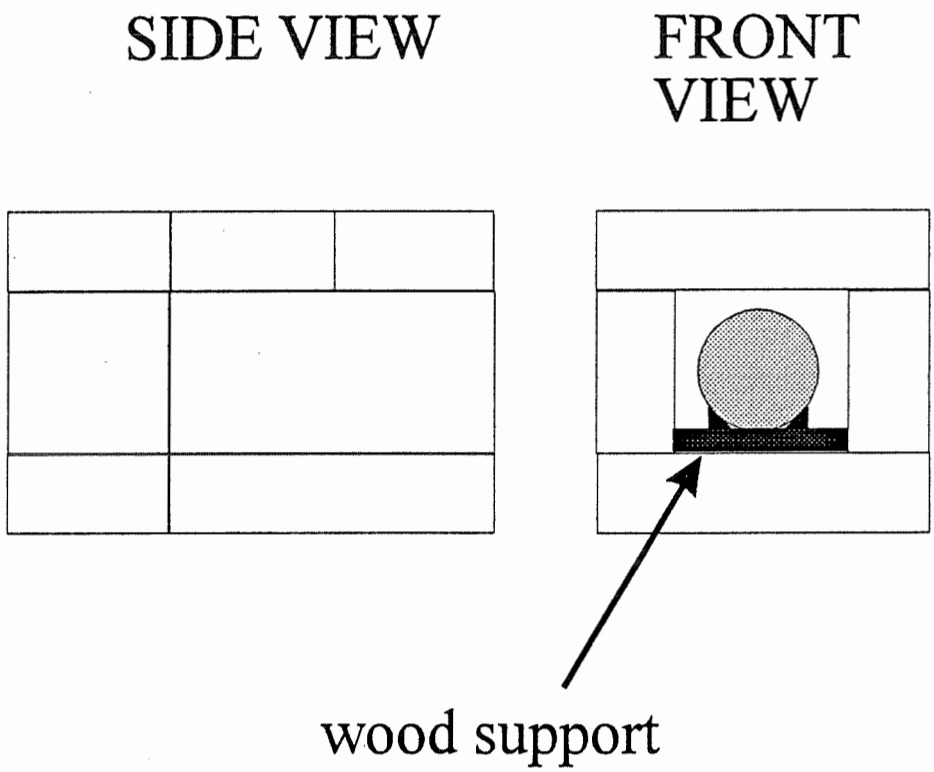

Figure A1.1: Lead brick shielding.

A1.3 Amplifier Gain Adjustment

Figure A1.2 shows the decay spectrum for Ar^{41}. The experimental spectrum was obtained with a multichannel analyzer. Also shown on the figure are the energy cutoff points around the argon energy peak. These cutoff points are used as the lower and upper limits on the amplifier (EG&G ORTEC Ace Mate and Bias Supply Model 925-Scint). In order that the upper (UL) and lower limits (LL) appear as shown in Figure A1.2 the gain on the amplifiers must be adjusted. Gain are adjusted as follows (this procedure is used with the detectors already in place). An argon source is placed near the detector in a easily repeatable location. (If placed just inside the bricks at the back of the detector, a source container of argon irradiated for about 2.5 minutes gives acceptable reading.) A comparison of a restricted reading (RR) (LL = 5.87 V, UL = 7.40 V) to a standard full scale reading (FSR)(LL = 0.2 V, UL = 9.00 V) was made. The ratio RR/FSR was found to be approximately 0.25 ± 0.01. That is one quarter of the counts were due to the argon peak. (This ratio will vary with source placement.)

To readjust or verify a gain after detectors have been moved, the gain was set at a low value then slowly increased until a maximum occurred in the RR. FSR is measured at the same gain and RR_{max}/FSR calculated. It should be equal to about 0.25 if the gain has been set correctly.

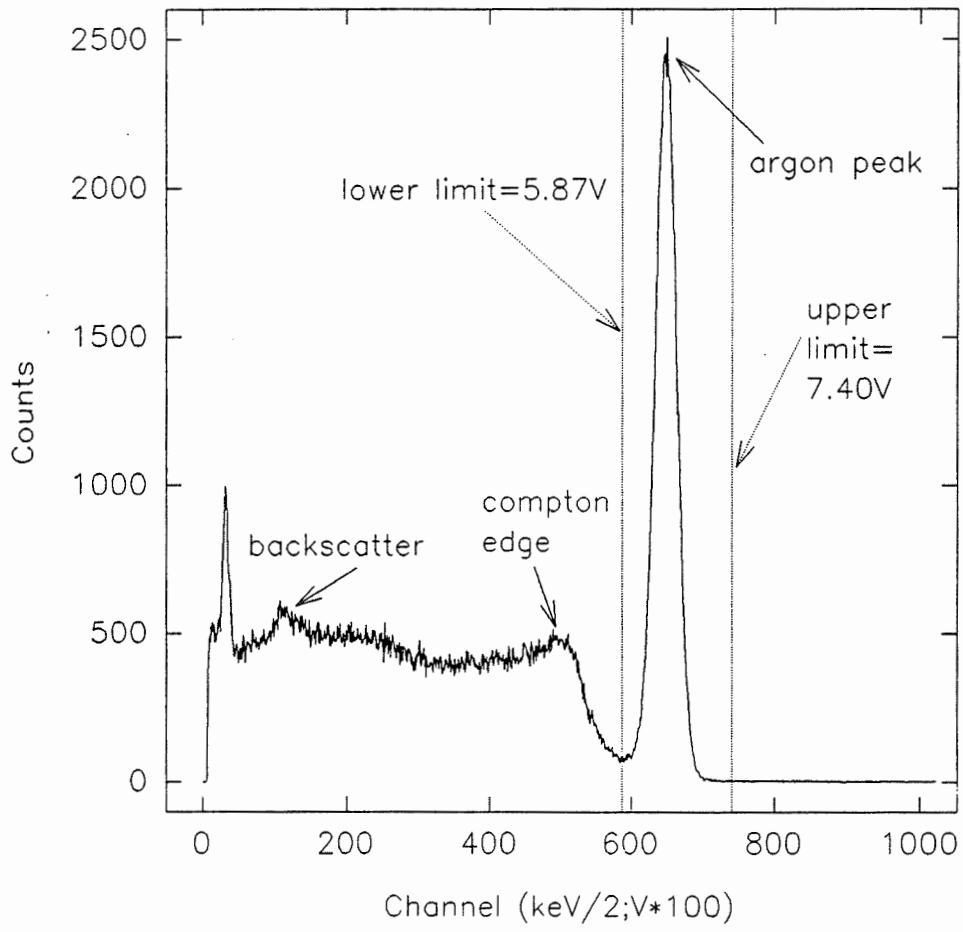

Figure A1.2: Decay Spectrum for Ar^{41}.

Once gains are set detectors should be left in place until experiments are finished. This procedure must be followed each time detectors have to be moved (eg. to another reactor).

A1.4 Gas Feed Mixture

To ensure that there is no driving force for mass transfer of radioactive argon tracer to the liquid phase, a mixture of air and argon is fed to the bubble column on a continuous basis during RTD experiments (volume ratio of air:argon is 3.3:1.0). To allow saturation of the liquid, the gas mixture and gas superficial velocity are set 10 minutes before a first injection at a particular operating condition.

Despite the absence of a driving force for mass transfer of argon molecules to the liquid phase, a dynamic equilibrium implies a continual absorption and desorption of argon molecules (exchange of those molecules in the gas phase with those in the liquid). However there are three factors that come into play when considering the possibility of losing marked molecules into the liquid phase: the ratio of argon molecules in the gas as compared to liquid, the proportion of marked molecules fed, and the kinetics of transfer versus the rate of convection through the column. First there is at least (minimum occurs at lowest U_g) 4.5 molecules of gaseous versus every 1 molecule of dissolved argon. Second, the proportion of marked molecules fed is less than 10 percent of the total argon fed to the column (maximum occurs at lowest U_g). Finally, the kinetics of transfer versus the rise velocity in the absence of a driving force may be described by a theory of mass transfer to an interface such as Higbie's penetration theory or Danckwert's surface renewal theory. From Higbie's penetration theory, the Stanton number, which is the ratio

of mass transport to convective transport ($St = 2(D/d_b u_B)^{0.5}$), best compares the kinetics involved in the possible transfer of marked argon molecules to the liquid phase in the absence of a driving force for mass transfer. For the superficial gas velocities tested, the Stanton number is less than 0.1. The combination of these factors leads us to conclude that the transfer of marked argon molecules by the dissolution/desorption mechanism under equilibrium conditions is negligible.

A further confirmation that mass transport of radioactive argon molecules to the liquid phase did not occur to any significant degree was obtained experimentally. The baseline levels of ratioactive counts were the same before and just following a RTD experiment.

A1.5 Lead Shielding Configuration

For an RTD measurement to be valid the detector must see all the bubbles at the level of the detector. For scintillation detectors there is a decreasing relationship between signal intensity and distance from the detector. In short, the detector sees all the bubbles in the detector control volume but it does not see them all to the same degree. Liquid attenuates gamma radiation emitted by the radioactive argon. Thus, a bubble containing radioactive argon will emit gamma rays and the measured signal intensity depends on its distance from the detector and the media which gamma rays must pass through to reach the detector. The media includes the liquid, gas (little attenuation), column wall (approximately the same for all gamma rays) and lead shielding. The measured signal will over-emphasize bubbles which are close and under-emphasize bubbles on the far side of the column. As mentioned in section A1.2 the detector faces were placed 57 mm from the column wall. The position of the detector with respect to the column wall affects whether the counts are evenly averaged over the detector control volume (i.e. bubbles in the centre versus those close to the column wall). Placement of the detectors was chosen so that average counts on a radial shell (N_{rs} i.e. integrate over the volume) are equivalent to those measured in a cylinder at the centre of the column (N_c). The configuration was verified by comparing the counts of a plugged tygon tube filled with radioactive tracer hung at the centre of the column to the average counts obtained from the same tube at eight angles (0° to 315°) and a given radius. The tube was placed in the

column filled with tap water and centred vertically with respect to the detector window. The tube was slightly longer than the window seen by the detector. Results for the detector at Position 2 are tabulated below.

Table A1.1

Integrated counts on a radial shell.

Radius (m)	N_{rs}/N_c eight angle measurement	N_{rs}/N_c 24 angle measurement
0.025	1.03	--
0.051	1.09	--
0.083	1.18	1.12

Since the eight angle measurement is a poor approximation to the integral for the outer radial shell, the measurement was also performed at 24 angles around the circle. The 24 angle measurement shows that the maximal error which could be expected is 12 percent. In a later series of experiments, detectors were placed further from the column to improve the ratios around the radial shells but bubble velocity distributions obtained with detectors further back, did not change. The RTD measured in this manner will give an accurate measurement averaged over the control volume since the gas hold-up flow is approximately axisymmetric (for example Yao et al., 1991; Hills, 1974).

A1.6 New Exhaust System

Originally the gas collection system consisted of a flexible hose connected to the top of the column which followed the ceiling and then redescended to enter the fume hood on the other side of the room. The secondary peaks were cause by this redescending portion of the hose which happened to be aligned with the faces of detectors in Positions 1, 2, 3, and 4 (through the column) and the back of detector in Position 5 (Figure 2.1). Since the detector at Position 5 was closest to the hose, the secondary peak was slightly more prominent on these signals. It was this slightly larger peak on the signal from the detector at Position 5 (i.e. slightly more intense than at Position 3; note that otherwise the signals at Positions 3 and 5 were the same) which finally lead to the diagnosis of the problem. The fact that literature data (see for example Kawagoe et al., 1989; Field and Davidson, 1980) also had secondary peaks meant that these secondary peaks were at first attributed to hydrodynamic phenomena. We assumed that the secondary peaks could be due to a recirculation of the gas phase bubbles. We checked the assumption qualitatively by injecting tracer into the upper portion of the column. Small peaks did appear and it was assumed that some of the gas was recirculated. Quite a bit of analytical effort went into trying to understand the hydrodynamic significance before the problem was finally diagnosed. Future students should be very careful that the exhaust system does not interfere with measurements.

Once the new exhaust system was installed, a few experiments were repeated to ensure that the secondary peaks were eliminated, and that results obtained with the data treatment procedure outlined in section 2.3.3 and specifically Equation 2.1 did not adversely affect the final results. Experiments at higher superficial gas velocity could possibly be the most affected, since the secondary peak were more closely attached to the primary peak (indicative column hydrodynamics). Figure A1.3 is Figure 2.8 with one of the repeated experiments. This figure shows that the results in Chapters II and III were not affected by the data treatment procedure.

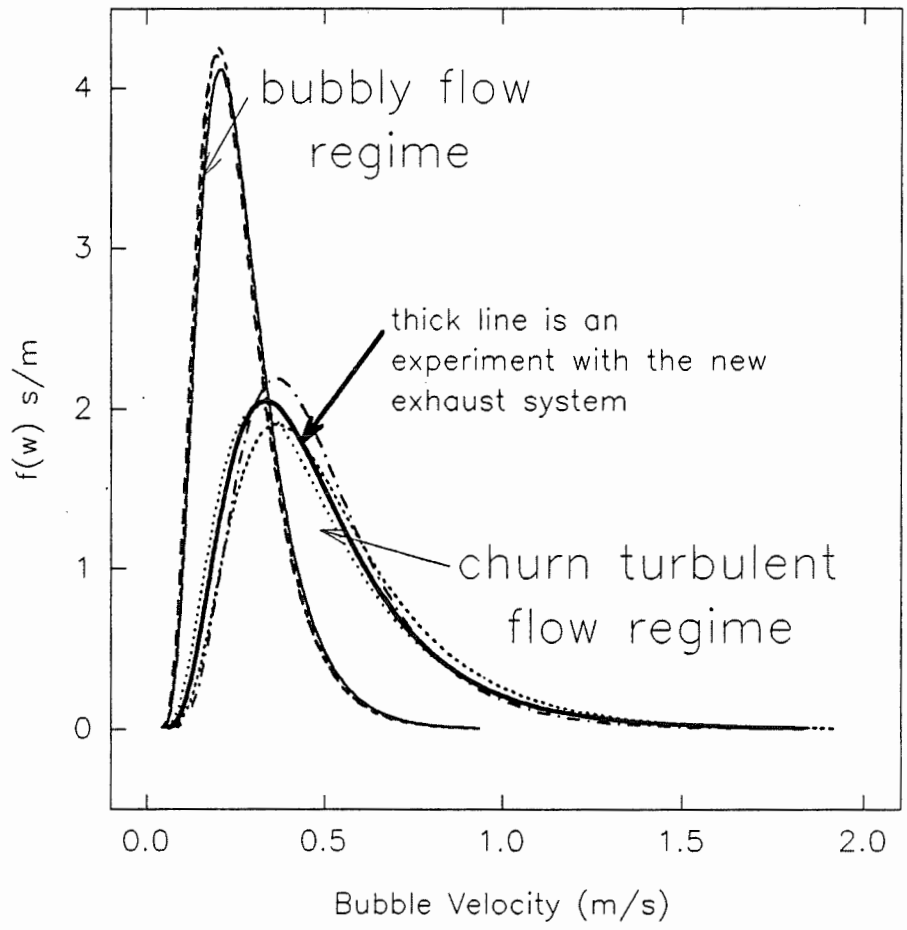

Figure A1.3: Figure 2.8 modified to show an experiment conducted with a new exhaust system.

A1.7 Objective Function for Optimization of Convective Model Parameters

The objective function reported in Chapter III (Equation 3.5 differs from that in Chapter II (Equation 2.10). Calculations were performed with Equation 2.10, but Equation 3.5 gives an equivalent final result. The change was made in Chapter III on the request of a reviewer because Equation 2.10 was considered to be a non-standard error function.

For the convective model at each iteration, after the optimization program chooses a new α and β, w_{min} and w_{max} are calculated and the log-normal distribution is discretized. Equation 3.5 can sometimes indicate that the optimization is finished when in fact all the points are just squeezed together at long times, t (i.e. the bubble velocity distribution is too slow). Equation 2.10 is a better objective function because of the normalizing effect of the denominator when the optimization routine is far from the result. With a good guess for α and β Equation 3.5 will give the same answer as Equation 2.10.

APPENDIX II

GAS HOLD-UP

A2.1 Gas Hold-up Measured with Manometers

For residence time distribution (RTD) experiments, gas hold-up was measured with manometers located at five axial locations to verify whether there was axial variation in gas hold-up and to establish the reliability of the newly installed pressure transducers. Within experimental error the gas hold-up was found not to vary with axial position.

A2.2 Pressure Transducer Calibration

Pressure transducers were calibrated in place with the column filled with water. Water level was reduced successively and readings taken until the upper inside edge of the pressure tap fitting was reached. The last measurement for each pressure transducer is its reference pressure, P_{ref}, and represents the extra head on the pressure transducer above what would be measured directly at the pressure tap. Calibrations were done before each series of experiments since the calibration can drift with time (i.e. calibrations were done before experiments when the transducer was dismantled and cleaned which was necessary if the equipment had not been used for a while).

A2.3 Gas Hold-up Calculation

Calculation of the gas hold-up for dynamic disengagement experiments is outlined in detail in Chapter IV (section 4.4 and Equation 4.1).

For residence time distribution experiments details of the calculation of gas hold-up are outline below (refer to Figure 2.1 or Figure 3.1 for experimental set-up). Data acquisition was conducted at a frequency of 10 Hz and continued for 200 s (it was triggered just before the RTD data acquisition which lasted 180 s). Pressures quoted below are the average values of the data collected over 200 s. Gas hold-up is calculated using the following equation:

$$\epsilon_g = \frac{(P_1 - P_{1,ref}) - (P_2 - P_{2,ref})}{(P_{1,nae} - P_{1,ref}) - (P_{2,nae} - P_{2,ref})} \qquad \text{(A1.1)}$$

Non-aerated pressures are measured at the end of a series of experiments or at the end of the day before emptying the column. Contrary to the method outlined by Equation 4.1, which is sensitive to exact clear liquid height, for Equation A1.1 measuring at the end of the day gives an accurate result. Reference pressures are measured as the column is being emptied (i.e. the column is emptied to the reference pressure and the measurement is taken).

APPENDIX III

DYNAMIC GAS DISENGAGEMENT

A3.1 Calibration of Pressure Transducers

The pressure transducer connected to the upper portion of the column is calibrated as outlined in Appendix II (section A2.2).

The pressure transducer connected to the distributor chamber which measures P_d needed to be calibrated filled with air at different pressures. Note that since the connection line is filled with air P_{ref} is negligible. For calibration purposes, the pressure transducer was connected to a "t" connection off the mercury manometer (instead of the distributor chamber; see Figure 4.1). Air was allowed to flow through the empty column at velocities which produced a back-pressure within the desired range of pressures for the calibration.

A3.2 Large Bubble Velocity

Large bubble velocity as a function of interstitial gas velocity is shown in Figure A3.1, the fourth order polynomial regression was done on all points except those encircled on the graph.

$$u_{bL} = 4.276(\frac{U_0}{\epsilon_O})^4 + 2.385(\frac{U_O}{\epsilon_O})^3 - 17.35(\frac{U_O}{\epsilon_O})^2 + 15.13(\frac{U_O}{\epsilon_O}) - 2.486 \qquad \text{(A3.1)}$$

These points were excluded because of the increased uncertainty near the transition point. This is the function $u_{bL}(\bar{v})$ used for kinetic model implementation.

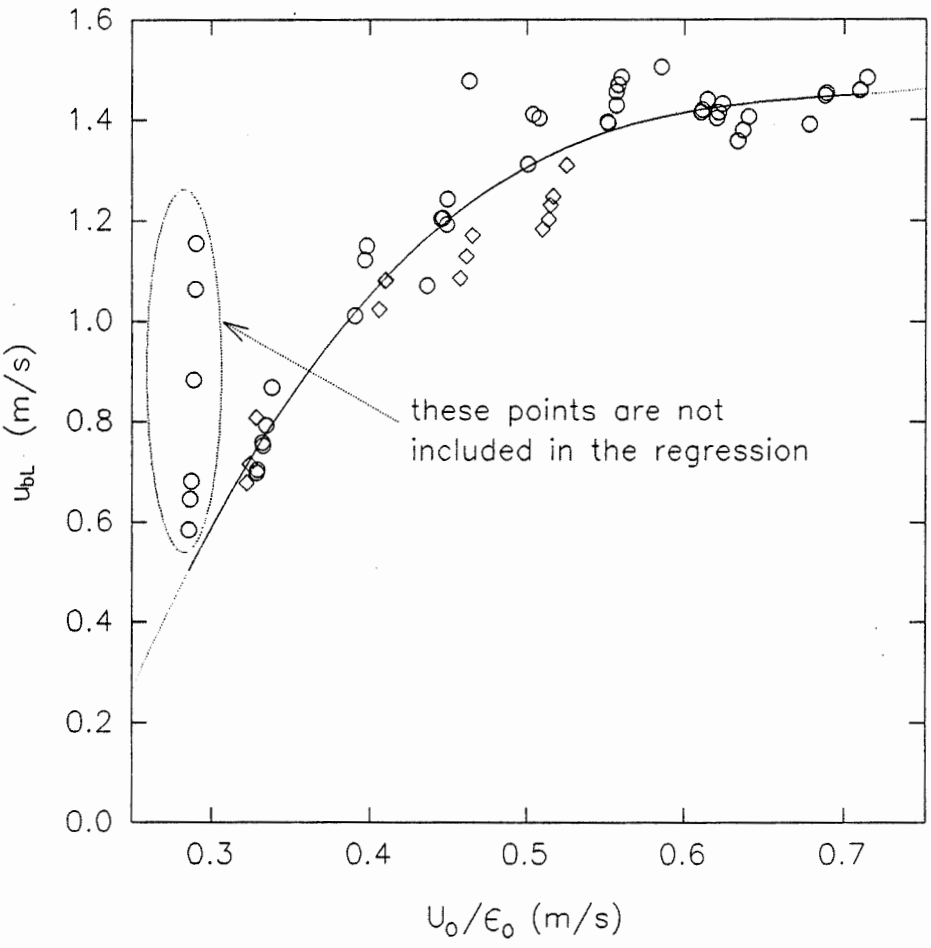

Figure A3.1: Large bubble velocity as a function of interstitial gas velocity (air ○; air/argon mixture ◇; regression ——).

APPENDIX IV

KINETIC MODEL

A4.1 Kinetic Model Derivation

The derivation of Equation 4.16 is based upon the model as it was presented by Iordache and Muntean (1981). Their model used a so called linear concentration. When dealing with bubble columns a more meaningful "concentration" of bubbles is the gas hold-up (or void fraction). The derivation presented here treats bubble-bubble interactions as volume interactions. The model is based upon an ideal bubble velocity distribution, $f^o(v,z,t)$, which would exist at a given operating condition in the absence of bubble-bubble interactions. Using the model an absolute bubble velocity distribution $f(v,z,t)$ is calculated.

Denote by $f_k(v_k,z,t)$ the velocity distribution function of bubbles located in the space $(z,z+\Delta z)$ at time t and moving with velocity v_k, $k = 1, \ldots, m$. Denote by $f^o(v_k,z,t)$ the corresponding ideal velocity distribution function. $a^o\Delta t$ is the probability that during Δt the bubble flow is ideal (i.e. no bubble-bubble interactions occur). Conversely, $1-a^o\Delta t$ represents the probability that interactions do occur during Δt. Denote by p_{ek} the probability for a bubble moving at velocity v_e to change to velocity v_k during Δt (i.e. bubble interaction occurs).

A population balance describing the evolution of the bubble velocity distribution, f_k, during Δt can be expressed as:

$$f_k(v_k,z,t+\Delta t) = a^o \Delta t f_k^o(v_k,z-v_k\Delta t,t) + (1-a^o\Delta t)\sum_{e=1}^{m} p_{ek}\, f_e(v_e,z-v_e\Delta t,t+\Delta t) \quad \text{(A4.1)}$$

According to Equation A4.1, a bubble arrives at location z with velocity v_k either by ideal flow (it started at velocity v_k before Δt), or by interactions with other bubbles (changing its velocity from v_e to v_k).

When two bubbles do interact, the slower bubble is accelerated to the velocity of the faster bubble.

$$v_e \oplus v_k \rightarrow \max(v_e,v_k) \quad \text{(A4.2)}$$

In other words, the fast bubble entrains the slower one. According to the above rule, the probabilities may be written as follows:

$$p_{ke} = a\, f_e(v_e,z,t)(v_e - v_k)\Delta t \qquad for\ v_e > v_k \quad \text{(A4.3)}$$

$$p_{ek} = a\, f_k(v_k,z,t)(v_k - v_e)\Delta t \qquad for\ v_k > v_e \quad \text{(A4.4)}$$

"a" is a proportionality constant. The bistochasticity principle states that transitions from velocities v_e to v_k equal transitions from v_k to v_e.

$$\sum_{e=1}^{m} p_{ke} = \sum_{e=1}^{m} p_{ek} \tag{A4.5}$$

As a result of Equation A4.5, the constant "a" is the same in Equation A4.3 and A4.4. The following statements presented by Iordache and Muntean (1981) still apply.

$$\sum_{e=1}^{m} p_{ek} = 1 \qquad for\ k = 1,\ldots,m \tag{A4.6}$$

$$p_{kk} = 1 - \sum_{\substack{e=1 \\ k \neq e}}^{m} p_{ke} \qquad for\ k = 1,\ldots,m \tag{A4.7}$$

Substituting Equation A4.7 into Equation A4.1 gives the following result.

$$\begin{aligned} f_k(v_k,z,t+\Delta t) &= a^o \Delta t f_k^o(v_k, z - v_k\Delta t, t) + \\ (1-a^o\Delta t)\ &[\sum_{\substack{e=1 \\ e\neq k}}^{m} p_{ek}\, f_e(v_e, z - v_e\Delta t, t+\Delta t) - (1 - \sum_{\substack{e=1 \\ e\neq k}}^{m} p_{ke})\, f_k(v_k, z - v_k\Delta t, t+\Delta t)] \end{aligned} \tag{A4.8}$$

The probability of interaction terms of the RHS of Equation A4.8 are examined in more detail (omitting the lengthy arguments shown in Equation A4.8). The interaction probabilities are written in terms of Equation A4.3 and A4.4.

$$I = a\Delta t\Big(\sum_{\substack{e=1 \\ e\neq k \\ v_k > v_e}}^{m} f_k(v_k - v_e) f_e - \sum_{\substack{e=1 \\ e\neq k \\ v_e > v_k}}^{m} f_e(v_e - v_k) f_k\Big) \tag{A4.9}$$

Simplifying Equation A4.9 becomes:

$$I = a\Delta t f_k \left(\sum_{\substack{e=1 \\ e \neq k}}^{m} (v_k - v_e) f_e \right) \tag{A4.10}$$

f_e is the volume distribution of bubble velocity. The area under the distribution curve is the gas hold-up, ϵ_O.

$$\sum_{e=1}^{m} f_e = \epsilon_O \tag{A4.11}$$

The area under the ideal distribution, f_e^o, is also ϵ_O.

$$\sum_{e=1}^{m} f_e^o = \epsilon_O \tag{A4.12}$$

While ideal distribution is different for each superficial gas velocity the normalized ideal bubble velocity distribution f_e^o/ϵ_O is independent of ϵ_O. The mean velocity is the first moment of the velocity distribution.

$$\bar{v} = \frac{1}{\epsilon_O} \sum_{e=1}^{m} f_e v_e \tag{A4.13}$$

In Equations A4.11, A4.12, A4.13 and 4.16, ϵ_O and $\bar{v}$ depend on z and t. Using these relations Equation A4.10 may be rewritten as follows.

$$I = a\Delta t \, f_k (v_k - \bar{v}) \epsilon_O \tag{A4.14}$$

A Taylor series expansion of the velocity distribution, f_k, around position z gives:

$$f_k(v_k,z-v_k\Delta t,t) = f_k(v_k,z,t) - v_k\Delta t\frac{\Delta f_k}{\Delta z} + \frac{1}{2}(v_k\Delta t)^2\frac{\Delta^2 f_k}{\Delta z^2} + \ldots \qquad \text{(A4.15)}$$

Combining Equations A4.8, A4.14 and A4.15 and taking the limit as $\Delta t \to 0$ gives the following result.

$$\frac{\partial f_k}{\partial t} + v_k\frac{\partial f_k}{\partial t} = -a^o(f_k - f_k^o) + a\epsilon_o(v_k - \bar{v})f_k \qquad \text{(A4.16)}$$

The continuous form of the kinetic model (Equation 4.16) is inferred from Equation A4.16 by replacing the discrete velocity (v_k) and distribution functions (f_k^o and f_k) by the continuous velocity (v) and distribution functions (f^o and f).